

Investigating important aspects of antimicrobial resistance in *Bacteroides* strains and a direct qPCR method as a promising tool for *Mycoplasma* detection

Ph.D. Thesis

By

Zain Baaity, Pharm.D., M.Sc.

Supervisors:

Dr. Ferenc Somogyvári Ph.D., Dr. József Sóki Ph.D.



Doctoral School of Interdisciplinary Medicine

Department of Medical Microbiology

Albert Szent-Györgyi Medical School

University of Szeged

Szeged

2022

PUBLICATIONS

• PUBLICATIONS RELATED TO THE TOPIC OF THE THESIS

This thesis is based on results published in the following papers:

- I. **Baaity, Z.**, Breunig, S., Önder, K. and Somogyvári, F. (2019) Direct qPCR is a sensitive approach to detect *Mycoplasma* contamination in U937 cell cultures. BMC Research Notes 12 (1), 720:
<https://doi.org/10.1186/s13104-019-4763-5>
(IF₂₀₁₉: 1.66), Rank: Q2 Citations: 1
- II. **Baaity, Z.**, Jamal, W., Rotimi, V.O., Burián, K., Leitsch, D., Somogyvári, F., Nagy, E. and Sóki, J. (2021) Molecular characterization of metronidazole resistant *Bacteroides* strains from Kuwait. Anaerobe 102357:
<https://doi.org/10.1016/j.anaerobe.2021.102357>
(IF₂₀₂₁: 3.331), Rank: Q2 Citations: 1
- III. **Baaity, Z.**, Loewenich, F., Nagy, E., Orosz, L., Burián, K., Somogyvári, F. and Sóki, J. (2022) Phenotypic and molecular characterization of carbapenem heteroresistant *Bacteroides fragilis* strains. Antibiotics (MDPI).
<https://doi.org/10.3390/antibiotics11050590>
(IF₂₀₂₂: 4.639), Rank: Q1 Citations: -
Cumulative Impact factor = 9.63

• PUBLICATIONS NOT RELATED TO THE TOPIC OF THE THESIS

- I. **Baaity, Z.**, Almahmoud, I. and Khamis, A. (2017) Prevalence of extended spectrum β lactamases (ESBL) in *E. coli* at Al-Assad Teaching Hospital. Research Journal of Pharmacy and Technology 10 (7), 2433-2436:
<http://dx.doi.org/10.5958/0974-360X.2017.00430.9>
(IF₂₀₁₇: 0.53), Rank: Q3 Citations: 12
- II. Ismail, R., **Baaity, Z.** and Csóka, I. (2021) Regulatory status quo and prospects for biosurfactants in pharmaceutical applications. Drug Discovery Today <https://doi.org/10.1016/j.drudis.2021.03.029>
(IF₂₀₂₁: 7.851), Rank: D1 Citations: 2
- III. Kincses, A.; Rácz, B.; **Baaity, Z.**; Vásárhelyi, O.; Kristóf, E.; Somogyvári, F.; Spengler, G. (2021) The Relationship between Antibiotic Susceptibility and pH in the Case of Uropathogenic Bacteria. Antibiotics (MDPI), 10, 1431.
<https://doi.org/10.3390/antibiotics10121431>
(IF₂₀₂₁: 4.639), Rank: Q1 Citations: -
- IV. Rutai, A., Zsikai, B., Tallósy, S., Ércses, D., Bizánc, L., Juhász, L., Poles, M., Sóki, J., **Baaity, Z.**, Fejes, R., Varga, G., Földesi, I., Burián, K., Szabó, A., Boros, M., and Kaszaki, J. (2022) A porcine sepsis model with numerical scoring for early prediction of severity. Frontiers in Medicine.
<https://doi.org/10.3389/fmed.2022.867796>
(IF₂₀₂₂: 5.091), Rank: Q1 Citations: -
Cumulative Impact factor = 18.111

Table of Contents

PUBLICATIONS	2
List of Abbreviations	5
1. INTRODUCTION	6
1.1. The current state of the antimicrobial resistance threat.....	6
1.2. Anaerobic bacteria and normal microbiota of the intestinal tract.....	7
1.3. <i>Bacteroides</i> spp. and their biology and clinical importance	7
1.3.1. <i>Bacteroides fragilis</i> and the virulence mechanisms of <i>Bacteroides</i>	9
1.3.2. Antibiotic resistance mechanisms in anaerobic bacteria (<i>B. fragilis</i>)	10
1.3.3. Beta lactams and carbapenems.....	12
1.3.4. Metronidazole.....	13
1.4. Bacterial tolerance, persistence, and heteroresistance	14
1.1.1. Bacterial Tolerance	14
1.1.2. Bacterial Persistence	14
1.1.3. Some relevant definitions	15
1.5. Bacterial Heteroresistance.....	16
1.6. Toxin-Antitoxin (TA) pairs.....	19
1.1.4. Toxin-antitoxin modules and persistence	20
1.7. <i>Mycoplasma</i> and its role in cell-culture studies	21
1.8. Realtime PCR.....	21
1.9. Detection of <i>Mycoplasma</i> contamination.....	22
2. AIMS AND OBJECTIVES.....	23
3. MATERIALS AND METHODS.....	24
3.1. Direct qPCR optimization for <i>Mycoplasma</i> detection	24
3.1.1. Cell culture.....	24
3.1.2. <i>Mycoplasma</i> elimination.....	24
3.1.3. DNA extraction and qPCR	24
3.2. Molecular characterization of metronidazole resistant <i>Bacteroides</i>	24
3.2.1. Bacterial strains, cultivation, identification and AST's.....	24
3.2.2. PCR experiments	25
3.2.3. Plasmid screening, Southern blotting and plasmid sequencing.....	25
3.3. Studying <i>B. fragilis</i> heterogeneous resistance to carbapenems	26
3.3.1. Bacterial Strains and Cultivation	26

3.3.2. MIC Determinations, Recording of Population Analysis Profiles and Time–Kill Curves	27
3.3.4. Imipenemase Activity and Induction of HR by Imipenem Treatment	27
3.3.5. Conventional PCR, Nucleotide Sequencing and qRT-PCR Experiments....	29
3.3.6. Curve Plotting, Curve Parameter Calculation, Statistical Evaluation and Bioinformatics.....	29
4. RESULTS	31
4.1. Direct qPCR optimization for <i>Mycoplasma</i> detection	31
4.2. Metronidazole resistant strains from Kuwait	33
4.3. Characterization of heteroresistance to imipenem in <i>Bacteroides fragilis</i>	37
5. DISCUSSION	42
5.1. Direct qPCR is a sensitive approach to detect <i>Mycoplasma</i> contamination in U937 cell cultures	42
5.2. Molecular characterization of metronidazole resistant <i>Bacteroides</i> strains from Kuwait.....	44
5.3. Characterization of heteroresistance to imipenem in <i>Bacteroides fragilis</i>	46
6. CONCLUSION	48
7. SUMMARY	49
8. NOVELTY (NEW FINDINGS).....	51
9. REFERENCES	52
10. ACKNOWLEDGMENTS.....	63
ANNEXES	64
I. Supplementary Materials.....	65
II. OTHER PUBLICATIONS	68
□ PRESENTATIONS AND ABSTRACTS RELATED TO THE TOPIC OF THE THESIS.....	68
□ PRESENTATIONS AND ABSTRACTS NOT RELATED TO THE TOPIC OF THE THESIS	69
RELATED ARTICLES	70

List of Abbreviations

AMR	Antimicrobial Resistance
AST	Antimicrobial Susceptibility Testing
AUC	Area Under Curve
BHIS	Supplemented Brain-Heart Infusion broth
BL-BLIC	Beta-lactam-beta-lactamase inhibitor combinations
CFU	Colony-forming unit
CLSI	Clinical and Laboratory Standards Institute
COVID-19	Coronavirus disease 2019
C _t	Threshold cycle
EDTA	Ethylenediaminetetraacetic acid
ERIC-PCR	Enterobacterial Repetitive Intergenic Consensus - polymerase chain reaction
ESBL	Extended spectrum beta-lactamase
EUCAST	European Committee on Antimicrobial Susceptibility Testing
HR	Heteroresistance
IS	Insertion Sequence
kb	Kilobase-pair
MALDI-TOF	Matrix-Assisted Laser Desorption/Ionization-Time of Flight
MDR	Multidrug resistance
MIC	Minimum inhibitory concentration
NGS	Next-generation sequencing
PAP	Population Analysis Profile
PBS	Phosphate-buffered Saline
PCR	Polymerase Chain Reaction
PSA	Polysaccharide A
qRT-PCR	Quantitative Real-Time PCR
RT-PCR	Reverse transcription polymerase chain reaction
TA	Toxin-Antitoxin
TF α	Thomsen-Friedenreich
TLR	Toll-like receptor
TNF	Tumor necrosis factor
WC	Wilkins-Chalgren agar

1. INTRODUCTION

1.1. The current state of the antimicrobial resistance threat

Millions of lives are spared by antibiotics. They provided many benefits, from curing common infections to allowing organ transplants and intensive care units; antibiotics have extended average life expectancy by decades. But have we gone too far in our intelligence? Antimicrobial resistance (AMR) is an international public health situation that intimidates our ability to treat bacterial infections successfully. Antimicrobial resistance was first recognized in the 1940s. Microbiologists have long identified the trouble. The inventor of penicillin, Sir Alexander Fleming himself, drew focus on the threat of underdosing resistance [1]. Resistant strains are the ones that defy therapy with antimicrobials, and they have been a significant and devastating healthcare issue. AMR has been involved in 1.8 million deaths in 2020, which is anticipated to be one-third as many people as COVID-19 has killed. AMR is estimated to cause 10 million worldwide deaths annually by 2050, surpassing the number of fatalities caused by cancer and adding US\$100 trillion to the world's healthcare expenses by that time [2-5].

Through Darwinian selection, bacteria treated with antimicrobial agents are subject to selection pressure, will enhance their fitness by acquiring and expressing resistance genes and then sharing those genes with other bacterial strains and species [6]. Other mechanisms, such as tolerance and persistence, have long been recognized as helping bacteria survive antibiotic exposure [7,8]. Resistance mechanisms can be divided into three major groups, which occasionally overlap: (i) intrinsic resistance, which includes bacterial mechanisms that limit the drug's activity, such as delayed absorption or ejection of the antibiotic through efflux pumps. (ii) acquired resistance, in which a resistance gene mutation or horizontal transfer confers resistance, often by modifying/degrading the antibiotic or modifying/protecting the target molecule. (iii) adaptive resistance, defined here as a brief rise in resistance caused by the antibiotic itself inducing a gene, i.e. the interaction with the antibiotic is the trigger of resistance to that antibiotic and possibly other antibiotics [9,10]. These "superbugs" are considered one of the most severe threats to human health since bacteria are quickly becoming resistant to all the antibiotics we use. By overusing this valuable clinical source, we take the chance of losing the effectiveness of antibiotics forever. Wherever antimicrobials are used, there will be reservoirs for resistance genes that will be used to render antibiotics ineffective [11].

Co-infections with AMR bacteria caused clinically significant deaths in previous pandemics. And now, the COVID-19 dilemma helps feed the stealth pandemic of AMR every day [12].

1.2. Anaerobic bacteria and normal microbiota of the intestinal tract

Anaerobes, the microorganisms that live and spread in settings lacking oxygen, play a considerable role in many processes in nature, such as the production of biological dinitrogen, methane and hydrogen sulfide, the destruction of wastes, fermentation of organic matter as well as CO₂ fixation. They also play a vital function in human health and wellness regarding causing infections and making up essential microflora inside humans and animals [13]. The human digestive tract microbiota is estimated to consist of 500 - 1000 various bacterial species (mostly anaerobes), in addition to fungi and viruses, with an estimation of 10¹⁸ CFU microorganisms, 10 times more than human cells. While the microbiome's genetic material is approximated to be one hundred times the human genome [14,15], anaerobes outnumber facultative organisms by 1000-fold [16].

The most abundant anaerobic genera of the intestinal flora are *Bifidobacterium*, *Clostridium*, *Bacteroides*, *Peptococcus*, *Peptostreptococcus*, *Ruminococcus* and *Eubacterium*, while the most common aerobics (facultative anaerobes) are *Escherichia*, *Enterobacter*, *Enterococcus*, *Klebsiella*, *Lactobacillus* and *Proteus* [17,18].

1.3. Bacteroides spp. and their biology and clinical importance

Bacteroides spp. is a genus of gram-negative, non-spore-forming, obligately anaerobic, rod-shaped, bile-resistant bacteria that occupy the digestive system and constitute roughly 25% to 30% of the intestinal microbiota. More than 30 species of *Bacteroides* have been recognized (**Table 1**). These commensal bacteria can interact with the immune system and modify its response [19,20]. Some *Bacteroides* spp. hold the ability to digest plant-derived polysaccharides in the intestines to be utilized later in energy production.

Bacteroides xylanisolvens has been proven to increase antibody (IgM) production against the Thomsen-Friedenreich (TF α) antigen, which will guide the host's immune response against the presence of tumorigenic cells. Oral administration of *B. uniformis* to mice with a high-fat diet has improved their lipid profile, leptin levels, and TNF- α production by dendritic cells [21]. *Bacteroides acidifaciens* has also been reported to have an antiobesity capability, as suggested by Yang, J-Y *et al.* [22].

Table 1. NCBI Taxonomy of *Bacteroides*, *Parabacteroides* and *Phocaeicola* [23-25]

<i>Bacteroides</i>		<i>Parabacteroides</i>	<i>Phocaeicola</i>
<i>Bacteroides acidifaciens</i>	<i>Bacteroides ilei</i>	<i>Parabacteroides acidifaciens</i>	<i>Phocaeicola abscessus</i>
<i>Bacteroides bouchedurhonensis</i>	<i>Bacteroides intestinalis</i>	<i>Parabacteroides bouchedurhonensis</i>	<i>Phocaeicola barnesiae</i>
<i>Bacteroides caccae</i>	<i>Bacteroides koreensis</i>	<i>Parabacteroides chartae</i>	<i>Phocaeicola coprocola</i>
<i>Bacteroides caecicola</i>	<i>Bacteroides kribbi</i>	<i>Parabacteroides chinchillae</i>	<i>Phocaeicola coprophilus</i>
<i>Bacteroides caecigallinarum</i>	<i>Bacteroides luti</i>	<i>Parabacteroides chongii</i>	<i>Phocaeicola dorei</i>
<i>Bacteroides caecimuri</i>	<i>Bacteroides mediterraneensis</i>	<i>Parabacteroides distasonis</i>	<i>Phocaeicola massiliensis</i>
<i>Bacteroides cellulosilyticus</i>	<i>Bacteroides ndongoniae</i>	<i>Parabacteroides faecis</i>	<i>Phocaeicola paurosaccharolyticus</i>
<i>Bacteroides clarus</i>	<i>Bacteroides neonati</i>	<i>Parabacteroides goldsteinii</i>	<i>Phocaeicola plebeius</i>
<i>Bacteroides congdonensis</i>	<i>Bacteroides nordii</i>	<i>Parabacteroides gordonii</i>	<i>Phocaeicola salanitronis</i>
<i>Bacteroides coprosuis</i>	<i>Bacteroides oleiciplenus</i>	<i>Parabacteroides johnsonii</i>	<i>Phocaeicola sartorii</i>
<i>Bacteroides cutis</i>	<i>Bacteroides ovatus</i>	<i>Parabacteroides massiliensis</i>	<i>Phocaeicola vulgatus</i>
<i>Bacteroides denticanum</i>	<i>Bacteroides propionificaciens</i>	<i>Parabacteroides merdae</i>	
<i>Bacteroides eggerthii</i>	<i>Bacteroides pyogenes</i>	<i>Parabacteroides pacaensis</i>	
<i>Bacteroides faecalis</i>	<i>Bacteroides reticulotermis</i>	<i>Parabacteroides provencensis</i>	
<i>Bacteroides faecichinchillae</i>	<i>Bacteroides rodentium</i>	<i>Parabacteroides timonensis</i>	
<i>Bacteroides faecis</i>	<i>Bacteroides salyersiae</i>		
<i>Bacteroides finegoldii</i>	<i>Bacteroides sedimenti</i>		
<i>Bacteroides fluxus</i>	<i>Bacteroides sp</i>		
<i>Bacteroides fragilis</i>	<i>Bacteroides stercorisoris</i>		
<i>Bacteroides galacturonicus</i>	<i>Bacteroides stercoris</i>		
<i>Bacteroides gallinaceum</i>	<i>Bacteroides thetaiotaomicron</i>		
<i>Bacteroides gallinarum</i>	<i>Bacteroides timonensis</i>		
<i>Bacteroides graminisolvens</i>	<i>Bacteroides togonis</i>		
<i>Bacteroides helcogenes</i>	<i>Bacteroides uniformis</i>		
<i>Bacteroides heparinolyticus</i>	<i>Bacteroides xylanisolvens</i>		
<i>Bacteroides ihuae</i>	<i>Bacteroides zoogloformans</i>		

1.3.1. *Bacteroides fragilis* and the virulence mechanisms of *Bacteroides*

Although *Bacteroides fragilis* is one of the least plentiful *Bacteroides* species, it is the most prevalent anaerobe associated with extraintestinal infections in humans [26]. Although *B. fragilis* comprises around 0.1 to 0.5% of total gut bacteria, it is the most frequently isolated anaerobe from peritoneal and abdominal abscesses and samples of bloodstream infections. Surprisingly, 50% of feces is composed of *Bacteroides fragilis* cells [20].

B. fragilis has also been linked to the production of fragilysin, which has been linked to the development of colon cancer [26,27] and produces polysaccharide A (PSA), known for its immunomodulatory roles activating the T cells. It also activates TLR-2 in a PSA-dependent manner, upgrading regulatory T cells for immune tolerance and maintenance of intestinal homeostasis [19,28]. *B. fragilis* may infiltrate tissues, pass barriers, and cause illness thanks to its virulence factors [29]. **Table 2** summarizes a collection of the most common anaerobe virulence factors.

Table 2. Selection of virulence factors in anaerobic bacteria [30]

<i>Virulence Factor</i>	<i>Organism</i>	<i>Activity</i>
Capsular polysaccharide	<i>Bacteroides fragilis</i>	Cell adherence
		Abscess formation
	<i>Prevotella melaninogenica</i>	Abscess formation
		Inhibition of phagocytosis
Fimbriae	<i>B. fragilis</i> group	Adherence to cells and mucus
	<i>Porphyromonas gingivalis</i>	
Lipopolysaccharide	<i>Bacteroides</i> spp.	Lacks classic lipid A– low endotoxicity
	<i>Fusobacterium</i>	Potent endotoxic action
Succinic acid enzymes	<i>Many species</i>	Inhibition of phagocytosis and intracellular killing
Hyaluronidase	<i>Bacteroides</i> spp.	attack the host extracellular matrix
Collagenase	<i>Bacteroides</i> spp.	Tissue damage
	<i>Prevotella melaninogenica</i>	Tissue damage
Phospholipase A	<i>Prevotella melaninogenica</i>	Cell membrane damage

1.3.2. Antibiotic resistance mechanisms in anaerobic bacteria (*B. fragilis*)

The most effective and commonly used antibiotics against anaerobes include aminopenicillins, penicillins, beta-lactam-beta-lactamase inhibitor combinations (BL-BLIC), cephalosporins (cefoxitin), metronidazole, clindamycin, moxifloxacin, carbapenems and tigecycline [31]. Vancomycin and fidaxomicin are only active against *Clostridioides difficile*. AMR in anaerobes is complicated and facilitated by several mechanisms such as drug inactivation by enzymes, modification of target molecule through mutations, efflux pumps and porin alterations, as shown in **Figure 1**. The primary genetic mutations are summarized in **Table 3** [32]. Notably, the mechanisms underlying high-level resistance to certain antimicrobials, including metronidazole, are not yet fully clarified, and harboring these genes does not necessarily result in phenotypic resistance [33].

Key anti-anaerobic agents are now compromised; metronidazole and carbapenem resistance is still low. However, they are increasingly becoming less efficient. In addition to losing two effective agents, clindamycin and moxifloxacin have reached a level where they can no longer be used for empiric treatment of major infections [34].

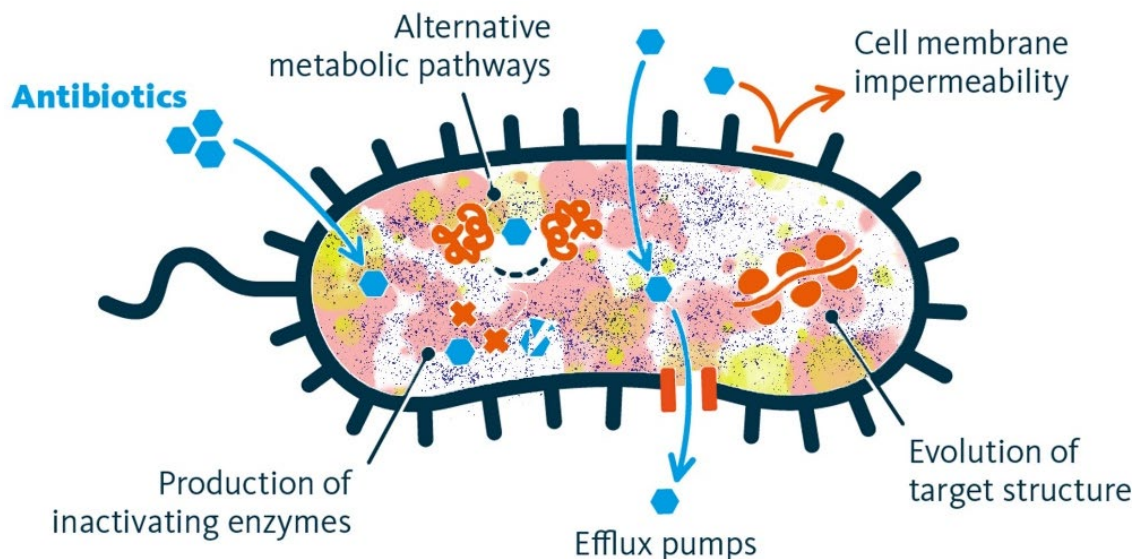


Figure 1. Mechanisms of antimicrobial resistance (AMR) in bacteria

Table 3. Examples for AMR mechanisms exhibited by anaerobes [32,35]

Antibiotic class	Mechanism of resistance	Genes or enzymes involved	Examples of microorganisms
Aminoglycosides	Lack of O-based or N-based electron transport systems; unable to reach target ribosomal subunit (30S)		All anaerobes
β-Lactams	Penicillinases	<i>FUS-1 (OXA-85)</i>	<i>Clostridium</i> spp., <i>Fusobacterium</i> spp., <i>Prevotella</i> spp., <i>Porphyromonas</i> spp.
	Cephalosporinases	<i>cepA</i> , <i>cfxA</i>	<i>B. fragilis</i> sp.
	Metallo- β -lactamases	<i>cfiA (ccrA)</i>	<i>B. fragilis</i> sp.
	Reduced affinity to target molecule	PBP1–2 alterations	Anaerobic Gram-positive cocci, <i>B. fragilis</i> sp.
		PBP-3 (aztreonam)	All anaerobes
	Loss of porin channels	-	<i>B. fragilis</i> sp.
Chloramphenicol	Acetylation	<i>cat</i>	<i>B. fragilis</i> sp.
	Nitro-reduction	-	<i>B. fragilis</i> sp.
Clindamycin	Methylation of the 23S rRNA	<i>ermF</i> , <i>ermG</i> , <i>ermS</i>	<i>B. fragilis</i> sp.
		<i>ermB</i> , <i>ermF</i> , <i>ermG</i> , <i>ermFG</i>	<i>Prevotella</i> spp.
		<i>ermF</i>	<i>Porphyromonas</i> spp.
		<i>ermB</i> , <i>ermQ</i>	<i>Clostridium difficile</i>
		<i>ermP</i> , <i>ermQ</i>	<i>Clostridium perfringens</i>
	Inactivation	-	<i>B. fragilis</i> sp.
Macrolides	Methylation of the 23S rRNA	<i>ermA</i> , <i>ermB</i> , <i>ermF</i> , <i>ermG</i> , <i>ermQ</i> , <i>ermTM</i>	<i>Finegoldia magna</i> , <i>Peptostreptococcus tetradius</i> , <i>Peptostreptococcus anaerobius</i>
Metronidazole	Intrinsic	-	Gram-positive anaerobic bacteria
	Reduction of the drug by nitroimidazole reductase	<i>nimA–H</i>	<i>B. fragilis</i> sp., <i>Veillonella</i> spp.
	-	<i>nimI</i>	<i>Prevotella</i> spp.
	Reduced uptake of the drug	-	<i>B. fragilis</i> sp.
	Increase in LDH activity	-	<i>B. fragilis</i> sp.
Quinolones	DNA gyrase (topoisomerase II)	<i>gyrA</i> , <i>gyrB</i>	<i>B. fragilis</i> , <i>C. perfringens</i> , <i>C. difficile</i>
	Topoisomerase IV	<i>parC</i>	<i>C. difficile</i>
Tetracyclines	Ribosomal protein	<i>tet(Q)</i>	<i>B. fragilis</i> sp.
		<i>tet(M)</i> , <i>tet(W)</i>	<i>Fusobacterium</i> spp.
		<i>tet(M)</i> , <i>tet(Q)</i> , <i>tet(W)</i>	<i>Prevotella</i> spp.
	Ribosomal modification	<i>tetA(P)</i> , <i>tetB(P)</i>	<i>Clostridium</i> spp.
	Efflux pumps	<i>tetA–E</i>	<i>B. fragilis</i> sp.
	Enzyme degradation (oxidative)	<i>tetK–L</i>	<i>Peptostreptococcus</i> spp., <i>Veillonella</i> spp.
		<i>tetX</i>	<i>B. fragilis</i> sp.

1.3.3. Beta lactams and carbapenems

The *B. fragilis* ‘group’ is ordinarily resistant to benzylpenicillin, other penicillins, and except for cephamycins such as cefoxitin, many cephalosporins. Carbapenems such as imipenem and meropenem are active, but some monobactams are inactive as they lack the affinity for the penicillin-binding proteins of *B. fragilis* [20]. A small group of *B. fragilis* strains produces metallo- β -lactamase of Ambler class B, which needs zinc and is involved in resistance to carbapenems and cephamycins. Classic β -lactam inhibitors (clavulanic acid, sulbactam and tazobactam) have no effect on this enzyme, but EDTA, which chelates zinc, may render it inactive [36]. The proposed mechanism for the hydrolysis of the C-N bond involves an initial interaction of the nucleophile zinc hydroxide in the enzyme's active site. This polarizes the carbonyl (C=O) group of the β -lactam; second, zinc interacts with the nitrogen, resulting in bond cleavage. The chromosomally encoded gene *cfiA* (or *ccrA*) has

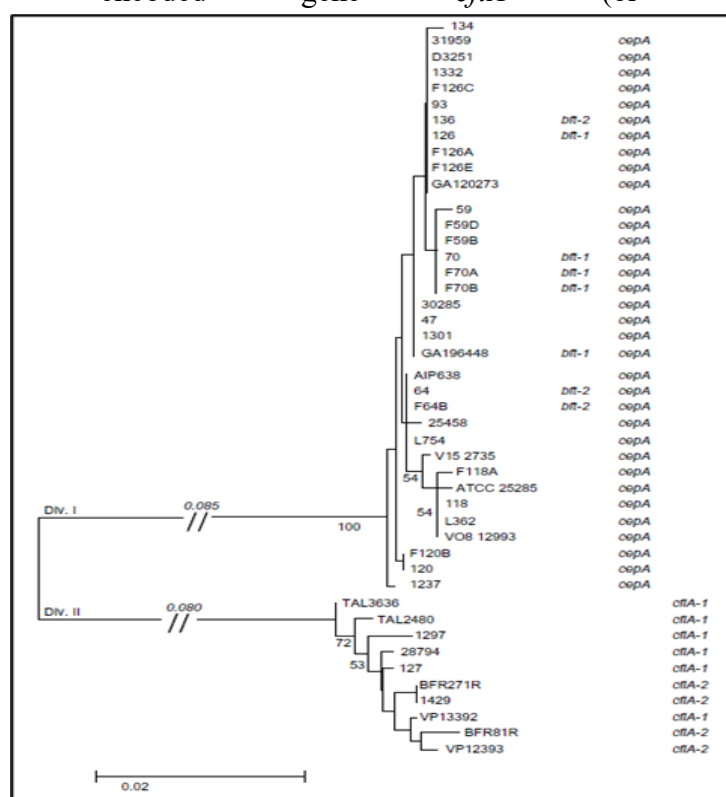


Figure 2. Genetic divisions of *B. fragilis*:
Division I (*cepA*⁺, *cfiA*⁺), Division II (*cepA*⁻, *cfiA*⁺) [37]

been identified as the carbapenem resistance factors. Using the *cfiA* gene as a probe, the gene was identified in 3% of *B. fragilis* clinical isolates, which relates to the *B. fragilis* DNA homology group II. These strains lacked the *cepA* gene that encodes the more

common β -lactamase of *B. fragilis* found in the DNA homology group I, as shown in **Figure 2**.

Differences in the composition of the outer-membrane proteins and lipopolysaccharides of the two groups have also been noted. The *cfiA* gene-positive group as well carried one or more of the three IS elements: *IS4351*, *IS1186* or *IS942*. These are involved in the regulation of gene expression. Potentially, alteration of penicillin-binding proteins can confer resistance to β -lactams in *Bacteroides* spp. However, the importance of this mechanism in the context of β -lactamase production and efflux pump action has not yet been fully proven [20,38]. Several studies have already examined and described this configuration. However, the carbapenem resistance of *B. fragilis* is more complicated: (i) strains without an IS element have a silent *cfiA* gene and have low carbapenem MIC (<1 $\mu\text{g/mL}$), (ii) IS-activated *cfiA*-positive strains have high carbapenem minimal inhibitory concentrations (MICs, ≥ 16 $\mu\text{g/mL}$) and (iii) *cfiA*-positive strains with an inactive IS element have elevated carbapenem MICs (>2 $\mu\text{g/mL}$). These latter strains also show heterogeneous carbapenem resistance phenotypes usually identified through Etest antimicrobial susceptibility test (AST) experiments [39-42].

1.3.4. Metronidazole

The antibiotic metronidazole is the most prescribed antibiotic for both prevention and treatment of Gram-negative anaerobic infections. It is a 5-nitroimidazole antimicrobial with a 5-nitro group on the heterocyclic imidazole ring. However, well-characterized metronidazole-resistant *Bacteroides* isolates have reached a significant number too [20]. The best-known and most extensively examined resistance mechanism of *Bacteroides* against metronidazole is mediated by *nim* genes [43]. These were first described between 1980 and 1990 and have since continued to gain more members. Now we have 11 representatives (*nimA-K*) that bear approximately 50-70% amino acid homology among each other. They are suspected of acting by reducing the nitro moiety of 5-nitroimidazoles into hydroxylamine groups without producing the toxic radical intermediate that mediates metronidazole's antimicrobial effect. After a more thorough investigation, *nim* genes were found to be preceded by insertion sequence (IS) elements whose function is to drive high expression of those same *nim* genes. This is the case for other *Bacteroides* resistance genes, e.g., the carbapenem resistance *cfiA* gene [38].

However, strains with *nim* genes do not usually have high or stable MIC values for metronidazole. Moreover, the metronidazole MIC value of some *nimA*-positive strains does not correlate to the expression of *nimA* genes. This latter finding brings the resistance mechanism mentioned above into question, yet most identified metronidazole-resistant *Bacteroides* strains harbor *nim* genes. They can be carried in small plasmids or the chromosome - the association of chromosomal copies with *cfiA* genes has been described earlier. The *cfiA* gene also accompanied the chromosomal *nimB* genes in an international cluster of multidrug-resistant *B. fragilis* strains.

Additionally, it is an intriguing and not fully understood phenomenon that *cfiA*-positive *B. fragilis* strains form a genetically well-separated group (Division II), clearly distinguishable with molecular typing methods, from *cfiA*-negative ones (Division I). Some former *Bacteroides* species, like *B. dorei*, *massiliensis*, *salanitronis* and *vulgatus*, were reclassified into the genus *Phocaeicola* (first established for *Phocaeicola abscessus*) based on genomic similarity assessments [44].

Despite the excellent action of metronidazole on clinical *Bacteroides* isolates, overuse can significantly affect resistance rates. Regular antibiotic susceptibility surveys conducted in Europe demonstrated a north-south division in metronidazole resistance, in which the north showed lower resistance rates, perhaps due to more prudent use of metronidazole. Some reports have also demonstrated some extreme metronidazole resistance values [33,45,46].

1.4. Bacterial tolerance, persistence, and heteroresistance

1.1.1. Bacterial Tolerance

By slowing down critical bacterial functions, tolerant bacterial populations (tolerance phenotype) can outlast exposure to higher antibiotic doses without changing the MIC. Tolerance to bactericidal compounds can be acquired through exposure to stress conditions in the environment [47].

1.1.2. Bacterial Persistence

Over 70 years ago, it was reported that antibiotics that were bactericidal and killed bacteria, according to Hobby and Bigger, do not sterilize cultures. Bigger discovered that the tiny number of bacteria that survive antibiotic treatments form a separate subpopulation of bacteria he dubbed "persisters" [48,49].

Persistence is non-heritable, but the frequency of persister cells in a population is a heritable trait. Being heritable, it likely evolved as a 'bet hedging' strategy to be better prepared for unpredictable environmental perturbations, such as encountering antibiotics [8].

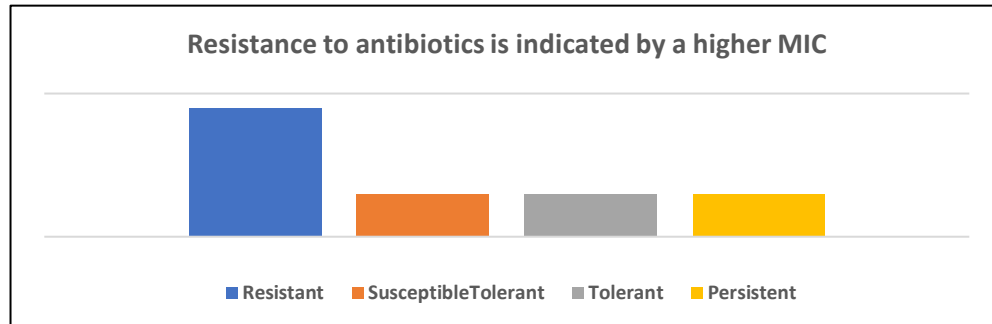


Figure 3. To stop resistant bacteria from growing, the antibiotic's minimum inhibitory concentration (MIC) must be much greater than for susceptible bacteria. *In contrast to susceptible individuals, persistence and tolerance do not result in an increase in the MIC*

1.1.3. Some relevant definitions

i. Antibiotic-resistant cell

An antibiotic-resistant cell has a resistance component by which it survives antibiotic treatment (for example, changes in cell-wall/membrane permeability). Resistance factors allow resistant bacteria to flourish at antibiotic doses that would stop more susceptible bacteria from growing [49].

ii. Antibiotic-tolerant cell

An antibiotic-tolerant cell survives antibiotic treatment without developing resistance and can regenerate once the drug is removed. Tolerant cells are frequently, but not always, non-growing prior to antibiotic administration. Tolerance factors allow bacteria to withstand treatments that would kill more susceptible bacteria for more extended periods of time. Environmental or genetic factors may also contribute to tolerance [49].

iii. Antibiotic persistence

Antibiotic persistence is a population-level phenomenon that has traditionally been drawn from the observation of biphasic killing curves, which indicates the presence of two subpopulations, one of which is killed quickly by the antibiotic and the other of which may survive. Antibiotic persistence is always associated with a heterogeneous population, in which only a portion of the population is made up of tolerant cells [49].

iv. Tolerance

Tolerance is a population-level phenomenon that allows bacterial cells to withstand a temporary antibiotic treatment multiple times longer than the minimum inhibitory concentration (MIC) without developing resistance. **Figure 3.** indicates the MIC levels in the different phases of microbial survival [49].

v. Dormancy

Dormancy describes the state of a bacterial cell that does not grow and has diminished activity compared to developing cells or even standard stationary phase cells. Single cells that are viable but do not proliferate despite favorable environmental conditions are also referred to as "dormant cells." Because their growth has slowed or their metabolism has slowed, dormant bacteria are generally resistant to numerous antibiotics. Nevertheless, without dormancy, tolerance and persistence may emerge [49]. **Figure 4.** demonstrates the characteristic drug responses of resistance, tolerance, and persistence.

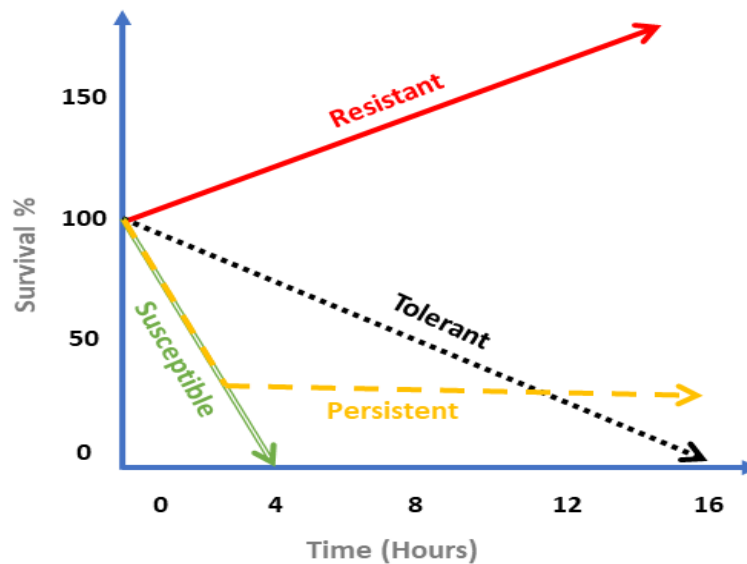


Figure 4. Four types of response to the presence of antibiotics in the media

1.5. Bacterial Heteroresistance

Heteroresistance (HR) is a phenomenon that describes variable responses of seemingly homogenous bacterial subpopulations to a specific antibacterial agent that is generally regarded as entirely susceptible, intermediate, or even completely resistant to [50]. **Figure 5.** presents the differences between heteroresistant and homogeneous responses to antibiotics.

In 1970, the first reported use of the term “heteroresistance” took place when the subinhibitory levels of cephalexin resulted in an expression of HR against some strains of *S. aureus* [51]. However, heterogeneous antibiotic resistance was first described in 1947 against *Haemophilus influenzae* [52]. Since then, quite a few bacteria have been listed as heteroresistant, although this anomalous observation is common across many bacterial species and remains a rather poorly defined concept [53,54]. Even though it has been known for a long time, HR is still a vague concept that lacks the precise definitions and guidelines to characterize or readily detect its presence [55].

HR has been proved to significantly impact the efficacy of antibiotic treatment *in vitro* and *in vivo* [56,57]. However, the molecular background of HR is still fairly mysterious though some papers reported that unstable tandem gene amplification generates HR [58,59].

In the clinical field, HR subpopulations may cause fatal outcomes due to misleading susceptibility results of bacterial species in hemocultures. Hence, inappropriate antibiotic therapy eventually leads to treatment failure and inability to eliminate the infection [57,60].

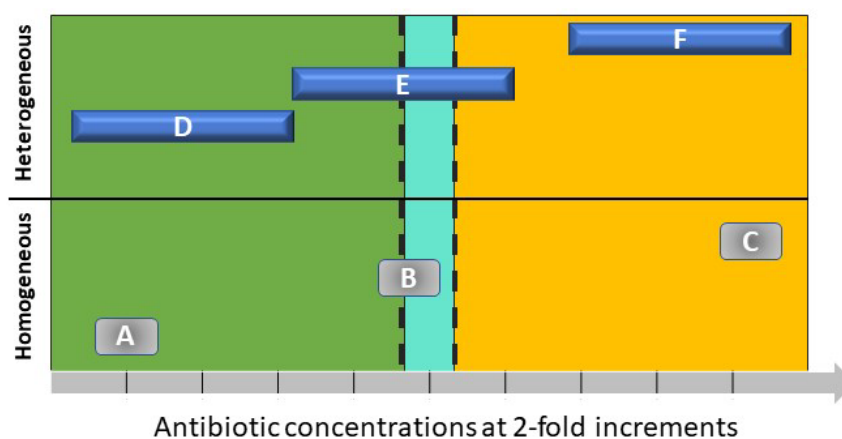


Figure 5. Heteroresistant versus homogeneous antimicrobial reaction.

Dashed lines represent resistance breakpoints. Homogeneous cultures of bacteria can be either susceptible (A) of intermediate susceptibility (B), or resistant (C) to an antibiotic according to classic *in vitro* susceptibility testing. Bacteria that are heteroresistant can be any of the following. (D) Bacteria are totally susceptible to an antibiotic, with various subpopulations responding to antibiotic concentrations below the breakpoints. This type is less likely to be found and has the least clinical significance (until antimicrobial resistance develops in the least sensitive subpopulations). (E) Bacteria exhibit the more classical form of heteroresistance, in which most of the bacterial population is susceptible to an antibiotic, with a highly resistant minority. Antibiotic treatment based on conventional susceptibility testing breakpoints would favor resistant individuals, resulting in therapeutic failure. (F) The whole bacterial population, even the least resistant subpopulations, is resistant to the antibiotic. The main problem of such bacterial communities is the chemical communication of antibiotic resistance from the more resistant cells of the community shielding less resistant ones [50].

Figure 6. exhibits an example where HR is a cause of unexplained antibiotic treatment failure in which the antibiotic selective pressure selects for heteroresistant cells to thrive and grow. However, those heteroresistant cells (also called monoclonal heteroresistant cells) are unsettled and may turn back to the antibiotic-susceptible state when the selective pressure is gone [59,60].

HR detection in the clinical laboratory is still not standardized and usually observed by using disc diffusion methods such as Etest strips and considered positive when there are some colonies inside the inhibition zone. At the same time, in research approaches, the population analysis profile method (PAP) is considered the gold standard method for identifying HR. Briefly, this method involves quantifying the proportion of resistant cells existing within a culture at a variety of antibiotic concentrations and then comparing it to the growth in the absence of the antibiotic [50,59,61].

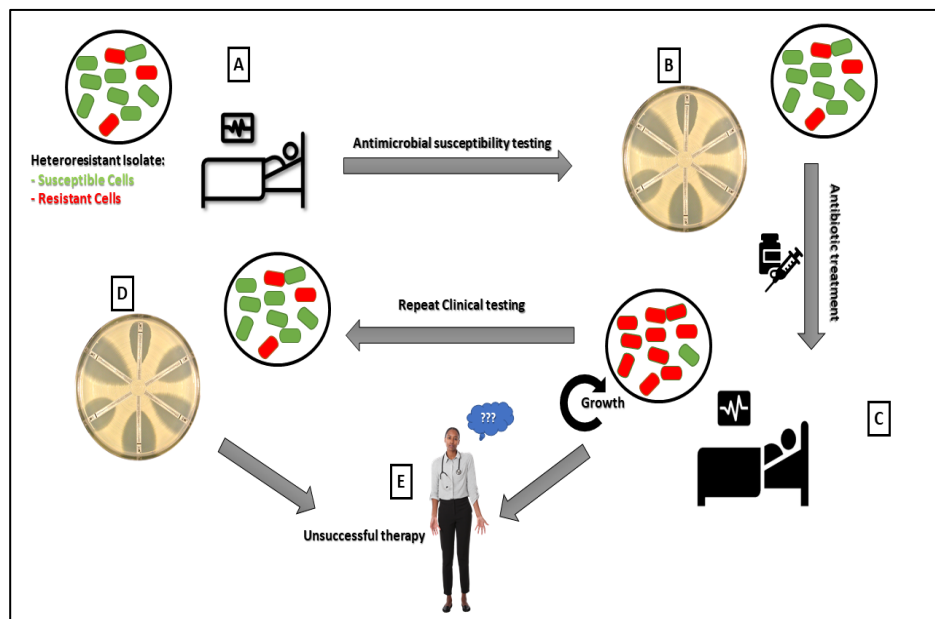


Figure 6. The impact of heteroresistance in the clinical settings

Although PAP is the most reproducible and reliable method for detecting HR, unfortunately, it cannot be easily implemented into the clinical setting because it is a tedious and time-consuming approach. However, there is no feasible and reliable alternative method available at present [50,62,63].

HR is gaining recognition, but its biological and clinical relevance must be better understood to accomplish a more achievable yet reliable standardization of its methodology. HR detection is difficult, and there are few studies on it. HR's clinical and therapeutic implications are still unknown. Data from relevant in vitro and clinical studies are urgently needed [59,64].

1.6. Toxin-Antitoxin (TA) pairs

Most bacteria and archaea have genes whose expression limits cell growth and, if overproduced, can lead to cell death. The presence of at least 33 TA systems in *Escherichia coli* shows that TA systems are involved not only in normal bacterial physiology but also in bacterial pathogenicity [65]. The first TA system discovered was on a plasmid, and it was revealed to be involved in plasmid maintenance [66].

When a plasmid encoding the TA system is removed from a cell, the toxin is unleashed from the existing TA complex, bearing in mind that the antitoxin is more volatile than the toxin. This inhibits cell development and eventually leads to cell death. Since this finding, a variety of TA systems encoded from bacterial genomes have been identified. Toxins from these TA systems are thought to be involved in a variety of cellular activities such as gene expression regulation, bacterial population control, and programmed cell death [65].

TA systems are classified to six types. Type II system is fairly understood, where a labile proteic antitoxin binds to a stable toxin and blocks its function. Type II systems are organized in operons, with the antitoxin protein generally placed upstream of the toxin, preventing the toxin from being expressed without the antitoxin [67].

Thousands of TA operons have been detected since their discovery, not only in plasmids and phages, but also, rather unexpectedly, on the chromosomes of most free-living bacteria [68].

Antitoxins are either RNA or proteins that counteract the toxin or the RNA that encodes it, whereas toxins are nearly exclusively proteins that inhibit metabolism (but do not kill bacteria). While TA systems obviously stabilize mobile genetic elements, the physiological function of chromosomal TA systems are less evident after four decades of research [69].

In normally developing cells, these toxins are usually co-expressed and neutralized by their corresponding antitoxins via a TA operon [65].

A TA (addiction) system, **Figure 7**, is made up of two or more closely connected genes that code for both toxin and antitoxin proteins [70].

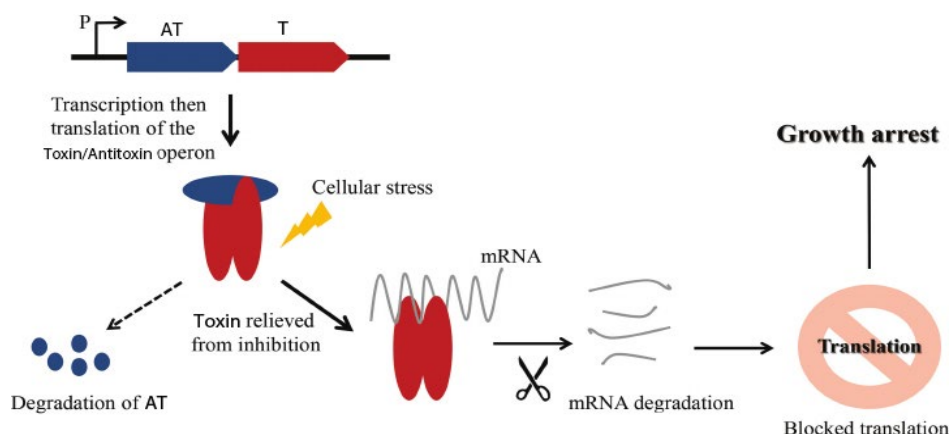


Figure 7. Mechanism of a Type II Toxin/Antitoxin pair [71]

1.1.4. Toxin-antitoxin modules and persistence

TA modules are gene loci that play a key role in the persister state, according to recent research [68]. Bacterial persistence can be triggered through several factors, e.g., starvation. However, several studies have revealed that persistence is triggered by various mechanisms, including the inherent bimodal distribution of TA proteins, resulting in non-uniform bacterial populations in which those cells contain high levels of toxin stop growing for long periods [9]. The *cfiA* operon in *B. fragilis* harbors two acetyltransferase (TA pair) genes: GNAT (toxin), XAT (antitoxin), and the IS element as shown in **Figure 8**. [9,72].

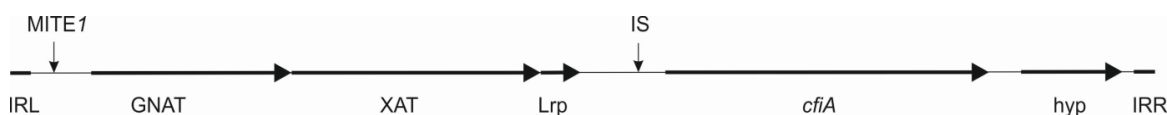


Figure 8. An updated scheme of the *cfiA* 'element'.

IRL and *IRR* inverted repeats bordering the element; 'GNAT'—ORF coding a Gcn5-like acetylase protein; 'XAT'—another acetylase protein; *Lrp*—a short ORF coding for a lysine-rich peptide; *hyp*—an ORF coding for a hypothetical protein; MITE1 with arrow—possible insertion of miniature transposable element 1; IS with arrow—possible insertion of a *cfiA*-activating IS element. [72,73].

TA gene pairs, with their toxic and labile neutralizing antitoxin activities, can kill post-segregational plasmid-less daughter cells (if harbored by plasmids) or halt cell division by stopping vital cellular functions (in the case of chromosomal localization). In this latter case, antibiotic persistence can emerge, meaning that during the replication stop, a small

fraction of bacterial cells withstands the action of bactericidal antibiotics and, after their removal, the cells start dividing again [74].

1.7. Mycoplasma and its role in cell-culture studies

Mycoplasma is a small cell-wall free prokaryotic bacterium with a remarkable diversity at the species level. Besides causing human respiratory and urogenital tract infections, *Mycoplasma* contamination of cell cultures is a frequent phenomenon. According to the DSMZ-German Collection of Microorganisms and Cell Cultures survey, the prevalence of *Mycoplasma* contamination of cell lines was 28% including *Mycoplasma* species *M. orale*, *M. hyorhinae*, *M. arginini*, *M. fermentans*, *M. hominis* and *Acholeplasma laidlawii* [75]. *Mycoplasma* contamination may be introduced by cross-infection with a *Mycoplasma* positive cell line, laboratory personnel (e.g., *M. orale*) or by contaminated cell-culture reagents such as fetal bovine serum. Indeed, bovine *Mycoplasma* species *M. arginini* and *A. laidlawii* are frequent contaminating agents. *Mycoplasma* contamination is hard to prevent/eradicate since the bacterium is less sensitive to antibiotics commonly applied in cell cultures. Its small size (0.3-1 μm) and non-rigid cell wall make it also hard to remove by filtration. *Mycoplasma* infection has a pleiotropic effect on cellular physiology, including altered metabolism, DNA, RNA and protein synthesis and pro- and anti-inflammatory effects [75-77]. U937 human monocytic cells respond to the *Mycoplasma* infection by producing monocyte chemotactic protein-1, matrix metalloproteinase-12 [78] and interleukin-1 β [79].

1.8. Realtime PCR

In traditional PCR, an end-point analysis is used to detect the amplified DNA product, or amplicon. The accumulation of amplification product is measured in real time as the reaction proceeds, with product measurement after each cycle in RT-PCR. As indicated in **Figure 9.**, a PCR has four phases: ground, exponential, linear, and plateau. Real-time PCR is considered one of the most sensitive and reliable quantitative approaches for gene expression analysis. C_t is the point where the amplification curve and the threshold line meet and is a C_t is a concentration-related measure of the target in PCR reactions. Real-time PCR is used in microarray verification, pathogen quantification, cancer quantification, and other research and procedures [80,81].

The fundamental advantage of real-time PCR over PCR is that it allows you to identify the starting number of copies of template DNA (the amplification target sequence) accurately and sensitively over a large dynamic range. Real-time PCR takes advantage of the fact that, under ideal conditions, the quantity of PCR products in exponential phase is proportional to the quantity of original template [80,82].

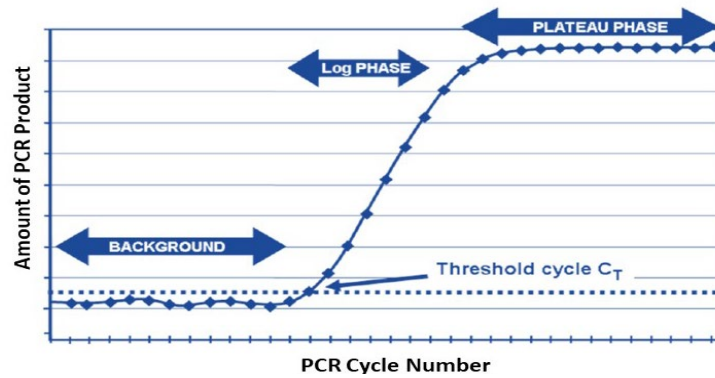


Figure 9. PCR cycle number plotted versus product amount

The results of RT-PCR might be qualitative (the presence or absence of a sequence) or quantitative (the number of copies of a sequence) (copy number). Thus, qPCR analysis is also known as quantitative real-time PCR [81,83].

1.9. Detection of Mycoplasma contamination

The high probability of introducing novel *Mycoplasma* infections into cell cultures means it is necessary to monitor cell culture ingredients and cell lines for *Mycoplasma* contamination. A wide variety of detection methods are available, including metabolism detection and *Mycoplasma* genome detection by PCR and qPCR. Regular PCR has high sensitivity and specificity, but most cases require nucleic acid purification and gel electrophoresis. qPCR eliminates the gel electrophoresis step, but regular qPCR protocols also include nucleic acid purification. DNA purification can be a long and laborious procedure, especially if there are several samples to be purified. Also, most column-based purification methods are not able to preserve all the nucleic acid content of the original sample. With direct PCR and direct qPCR, we eliminate the purification step and significantly shorten the protocol time required, but the inhibitory effect of the direct sample is always present. Previously direct qPCR methods were successfully applied to monitor *Chlamydia* and herpes simplex virus-2 growth and the effects of antimicrobial compounds on these pathogens and simplify these traditional microscopy-based experiments [84-89].

2. AIMS AND OBJECTIVES

The overall goals of this work were to:

- Examine several antibiotic resistance elements in *Bacteroides* clinical isolates and to further characterize imipenem HR and investigate using phenotypical and molecular methods.
- Exploit the Direct qPCR as a rapid method to detect bacterial presence in cell lines.

The specific goals of the study were the following:

- **Directly detect *Mycoplasma* DNA in a U937 suspension cell culture without using DNA purification:**
 - To make *Mycoplasma* contamination monitoring easier.
 - To leave out the DNA purification step and develop a direct qPCR detection method that is suitable to detect *Mycoplasma* contamination within U937 cell cultures.
- **Molecular characterization of metronidazole resistant *Bacteroides* strains from Kuwait:**
 - To investigate the prevalence and function of *nim* genes that provide metronidazole resistance among clinical *Bacteroides* isolates and related upstream regulatory elements known as insertion sequences (*IS*).
 - Isolation of plasmids from the metronidazole-resistant strains and analysis of them by PCR, Southern blotting and sequencing.
 - Conduct genetic typing of the *nimE*-positive *B. fragilis* strains by means of ERIC PCR.
- **Examine and characterize the carbapenem heteroresistance of *B. fragilis* by phenotypic and molecular methods and correlate them:**
 - To characterize HR and investigate diagnostic issues in the set of *cfiA*-positive *B. fragilis* using phenotypic and molecular methods, AST's and the gold standard method PAP (Population analysis profile).
 - To induce *B. fragilis* isolates using imipenem pressure, conduct PAP testing and compare the outcomes with the other strains.
 - To trace the changes of RNA expression of the TA pair using qRT-PCR in clinical and induced strains

- Analyse and correlate a set of phenotypic and molecular traits of HR strains in order to have a clearer picture of HR detection methods and mechanisms.

3. MATERIALS AND METHODS

3.1. *Direct qPCR optimization for Mycoplasma detection*

3.1.1. *Cell culture*

Mycoplasma infected U937 human monocytic cells were grown in an RPMI 1640 medium containing 10% heat- inactivated FBS (Sigma, St. Louis, MO, USA), and 50 µg/ mL gentamicin at 37 °C in 5% CO₂, all within a 25 cm² cell culture flask (Greiner Bio-One Hungary, Mosonmagyaróvár, Hungary).

3.1.2. *Mycoplasma elimination*

Mycoplasma elimination was performed using *Mycoplasma* Elimination Reagent (Bio-Rad, Hercules, USA). The reagent was added to the RPMI 1640 medium at a 0.5 µg/ml final concentration and the U937 cells were then cultured in this medium for 7 days.

3.1.3. *DNA extraction and qPCR*

According to the manufacturer's instructions, DNA was extracted from *Mycoplasma* infected U937 cell supernatants using the Qiagen QIAamp DNA Mini Kit (Qiagen, Hilden, Germany). PhoenixDx® *Mycoplasma* Mix (Procomcure Biotech, Thalgau, Austria) was used in the qPCR experiments. qPCRs with 20 µl final volume were performed using the Bio-Rad CFX Connect qPCR real-time system. A statistical comparison of qPCR cycle threshold (Ct) values was performed with Student's t-test, as described previously [80,96].

3.2. *Molecular characterization of metronidazole resistant Bacteroides*

3.2.1. *Bacterial strains, cultivation, identification and AST's*

Twelve metronidazole-resistant strains (Table 4) were selected from the 421 clinical *Bacteroides/Phocaeicola* isolates collected from 2006-2018 in an antibiotic resistance survey in Kuwait [90].

The long-term storage and transfer of these strains from Kuwait to Hungary was done by lyophilization. The strains were revitalized in chopped-meat bouillon and long-term storage in Hungary was made in a 20% glycerol-containing Brain-Heart Infusion (BHI) broth at -70 °C. The species identification and determination of *B. fragilis* strains' genetic

divisions were carried out by MALDI-TOF MS as described earlier [91]. Regular cultivation of the strains involved solid (Columbia agar supplemented with 10% defibrinated and 5% laked sheep blood, 0.3 g/l cysteine and 1 mg/l vitamin K₁) or liquid media (Brain-Heart Infusion broth supplemented with 0.5% yeast extract, 10 mg/l hemin and 1 mg/l vitamin K₁, BHIS) in anaerobiosis (85% N₂, 10% H₂ and 5% CO₂ in an anaerobic cabinet, Concept, Ruskinn, UK) at 37 °C. In Hungary, antimicrobial susceptibilities for metronidazole and imipenem were recorded by Etests as recommended by the supplier (bioMeriux) [33].

3.2.2. PCR experiments

PCR template DNA was prepared by the boiling method. The *nim*, *cfiA* PCR reactions and the upstream region examination of both of *nim* and *cfiA* genes were assessed as described previously [3]. The types of *nim* genes were determined by capillary sequencing using the DTCS kit (Beckman Coulter) and the capillary sequencing instrument (GenomeLab GeXP Genetic Analysis System, Beckman Coulter) as recommended by the suppliers. Enterobacterial repetitive intergenic consensus PCR (ERIC-PCR) typing, phylogenetic analysis (complete linkage, band-based clustering with Jaccard coefficients) was done with Fingerprinting II software (Bio-Rad) for the ERIC banding profiles of a total of 42 *Bacteroides* strains containing non-*fragilis Bacteroides*, *cfiA*-negative and *cfiA*-positive *B. fragilis* strains in addition to the strains from Kuwait. and evaluation were carried out as described earlier [72].

3.2.3. Plasmid screening, Southern blotting and plasmid sequencing

The plasmid profiles of the test *Bacteroides* and *P. doeri* strains were determined by the alkaline-SDS lysis procedure as described earlier [92]. Their analysis was done in 0.7% agarose gels containing 0.5 µg/ml ethidium bromide in 0.5 TBE buffer using a 12 V/cm voltage gradient. For large-scale plasmid isolation, we used the QIAGEN Plasmid Midi Kit (Qiagen, Hilden, Germany).

When Southern blotting, the plasmid DNA was transferred by capillary action to Hybond+ nylon membranes [92]. The probe labeling, hybridization, and detection were carried out by North2South Labeling and Hybridization kits (Thermo Fisher Scientific).

Permanent records of the gels and blots were done by the PXi gel documentation system (Syngene, UK). The nucleotide sequences of the plasmids of *nim*-positive strains were

determined on an Illumina platform and de novo assembly of plasmid sequences from preparations was done by the Lasergene 16 suite (DNASTar, Madison, USA).

The sequences of *nim* gene-containing plasmids were deposited in GenBank under the following accession numbers: MW388914 (pPDQ1c), MW388913 (pBFQ6d), MW388915 (pBFQ8b), MW448185 (pBFQ10c) and MW448186 (pBFQ11c). The plasmid sequences were aligned using Mauve software [33,93].

Table 4. Antibiofilms and isolation of the test strains

No.	Organism	SPECIMEN	XL	CM	MP	MZ	PG	PP	PTC	FOX	TGC	HOSPITAL
1	<i>P. dorei</i>	Wound swab	>256	>256	1	>256	>256	>256	32	16	-	MAK
2	<i>B. thetaiotaomicron</i>	Wound swab	>256	>256	0.125	16	64	>256	16	32	-	MAK
3	<i>B. fragilis</i>	Wound swab	0.5	0.5	0.5	>256	>256	>256	-	128	-	MAK
4	<i>B. fragilis</i>	Pus swab	0.25	>256	0.25	16	32	32	-	4	-	MAK
5	<i>B. fragilis</i>	Swab	32	2	8	>256	>256	>256	-	64	-	AMIRI
6	<i>B. fragilis</i>	Pus swab	8	>256	1	>256	>256	>256	-	8	8	MAK
7	<i>B. fragilis</i>	Perianal tissue	32	>256	8	64	>256	>256	-	32	4	AMIRI
8	<i>B. fragilis</i>	Pus swab	16	>256	8	32	>256	>256	-	32	4	AMIRI
9	<i>B. fragilis</i>	Peritoneal fluid	2	>256	4	>256	>256	>256	-	64	16	MAK
10	<i>B. fragilis</i>	Pus swab	>256	>256	>32	>256	>256	>256	-	>256	2	MAK
11	<i>B. fragilis</i>	Pus fluid	>256	>256	>32	>256	>256	>256	-	32	8	MAK
12	<i>B. fragilis</i>	Blood	16	>256	0.5	>256	>256	>256	-	8	4	AMIRI

XL amoxicillin/clavulanic acid, PTC piperacillin/tazobactam, CM clindamycin, FOX cefoxitin, MP meropenem, TGC tigecycline, MZ metronidazole, PP piperacillin, MAK Mubarak hospital, AMIRI Amiri Hospital
 - Resistant values, according to EUCAST [94] or CLSI [95], are in bold.

3.3. Studying *B. fragilis* heterogeneous resistance to carbapenems

3.3.1. Bacterial Strains and Cultivation

The test strains used in this study are listed in **Table 5**. The strains were selected from our collection stored at -70°C in brain–heart infusion broth (BHI) containing 20% glycerol. Their cultivation was performed on anaerobic Columbia blood agar plates (Columbia agar supplemented with 2.5% defibrinated sheep blood, 1.25% laked sheep blood, 300 mg/L L-cysteine and 1 mg/L vitamin K1), on Wilkins–Chalgren (WC) agar or in supplemented BHI broth (BHIS, with the addition of 0.5% yeast extract, 5 mg/L hemin and 1 mg/L vitamin K1) at 37°C under anaerobiosis (85% N_2 , 10% H_2 and 5% CO_2) in an anaerobic cabinet (Concept400, Ruskinn, UK). Isolates were confirmed to be *B. fragilis* via the MALDI-TOF MS method (Microflex LP instrument and Biotyper 3.1 software package, Bruker Daltonics, Bremen, Germany) following the MALDI Biotyper CA System instructions.

3.3.2. MIC Determinations, Recording of Population Analysis Profiles and Time–Kill Curves

Gradient tests (E-test, bioMérieux, France) were conducted on supplemented Columbia blood agar plates. Agar dilution was carried out as recommended by CLSI [97] on supplemented Columbia blood agar plates. Agar dilution was also performed on WC plates as the PAP records were also determined on this media.

In PAP experiments, we used the following cell suspensions/cultures: (1) 0.5 McFarland phosphate-buffered saline (PBS, 137 mM NaCl/2.7 mM KCl/1.8mM KH₂PO₄/10 Na₂HPO₄ pH 7.2) cell suspensions taken after 48 h cultivations on Columbia blood agar plates or (2) overnight incubated BHIS broth culture. Optical density (at 600 nm) was measured by spectrophotometer (Thermo Scientific, Budapest, Hungary) for later normalization. Ten-fold dilutions were composed in PBS and 100 µL inocula were spread on Wilkins-Chalgren agar plates with an appropriate concentration of imipenem (from the 0.008–1024 µg/mL range), which was determined by trials to yield 50–500 countable colonies per plate. Two independent experiments (biological replicates) were carried out using two–three parallels (technical replicates) for each concentration. The inoculated WC plates were then incubated anaerobically for 48 h and, afterwards, colony counts were determined by a gel documentation system (PXi, SYNGENE, Oxford, UK).

Time–kill curves were recorded by plating after 0h, 2h, 4h, 10h and 24h of incubation on antibiotic-free WC agar plates, 100 µL aliquots of serial 10-fold dilutions of PBS suspensions with a turbidity of 0.5 McFarland. These also contained 32-fold higher imipenem concentrations than the original imipenem MICs. The WC plates were incubated in an-aerobiosis for 48 h. Colonies were counted as described above.

3.3.4. Imipenemase Activity and Induction of HR by Imipenem Treatment

In total, 8 mL of overnight BHIS cultures was centrifuged (at 4 °C, 8000 rpm, 10 min), washed 3 times with cold PBS and sonicated. The crude cell extracts were then used for imipenemase activity determination in 1 mL UV-transparent plastic cuvettes in an Assay buffer (50 mM HEPES, 25 µM ZnSO₄, pH 7) using 0.1 mM imipenem concentration and an adjusted enzyme volume to obtain a linear decay of imipenem followed at 299 nm. The results were expressed by 1 pmole imipenem hydrolyzed per 1 min (U) and standardized by the protein content of the extracts (U/mg). Protein concentrations were determined by the Qubit Protein Assay Kit (Thermo Fisher Scientific, Hungary).

Table 5. List of strains, recorded data on imipenem susceptibilities, PAP profiles, imipenemase production and molecular data.

<i>B. fragilis</i>	Ref.	Phenotypic Parameters ^a											Molecular Parameters									
														<i>cfiA</i> and IS		qRT-PCR ^b				Lrp ^c		
		x ₀ PBS	x ₀ BHIS	bS PBS	bS HIS	d PBS	d ^d BHIS	AUC PBS	AUC BHIS	MIC B	MIC WC	IP HRI	Ipase	<i>cfiA</i>	<i>cfiA</i> -IS	<i>cfiA</i>	‘GNAT’	‘XAT’	‘GNAT/XAT’	K no.	K%	
Susceptible controls																						
NCTC 9343	-	-4.8142	-4.3392	-0.2092	-0.3902	2	2	1	1	0.125	0.064	0	0	-	n.a.	0	0	0	n.a.	n.a.	n.a.	
638R	-	-4.4449	-4.9148	-0.2721	-1.0111	2	2	1.4757	1.4046	0.125	0.064	0	0	-	n.a.	0	0	0	n.a.	n.a.	n.a.	
D39	[98]	-4.4350	-5.7965	-0.1012	-0.2192	2	2	1.4886	0.7642	0.5	0.064	0	0	-	n.a.	0	0	0	n.a.	n.a.	n.a.	
Silent/HR ^d																						
7979	This study	-3.0103	-3.5941	-0.4000	-0.8885	3	4	1.8045	1.5884	0.125	0.032	0	5.1	+	-	16.35	6.91	5.56	1.2428	7	26.9	
3130	This study	-2.7685	-3.0168	-0.6269	-0.0451	3	6	1.8785	1.5532	8	8	0	2.6	+	-	1	1	1	1	5	13.5	
3035	[39]	-2.8450	-2.7613	-0.3141	-0.3887	3	3	1.7810	1.4387	1	2	5	9.7	+	-	166.3	0.02	0.993	0.0201	9	25.0	
SY69	[98]	-2.2774	-3.4300	-0.2062	-1.5269	5	6	2.0114	1.7008	4	4	5	10.1	+	-	92.0	17.7	32.6	0.5429	5	13.5	
CZE65	[99]	-2.6235	0.9301	-0.9546	-1.1148	5	5	2.6027	2.3992	16	8	2	25.5	+	-	2.46	1.93	0.16	12.0625	7	26.9	
CZE60	[99]	0.0886	-0.7637	-1.4586	-0.6320	3	4	2.7013	1.8329	16	16	5	33.3	+	-	12.91	7.78	0.49	15.8775	7	26.9	
SLO8	[41]	1.8171	-4.0275	-0.6387	-1.1367	3	8	2.7294	2.2562	128	128	3	133	+	-	76.06	182.94	255.47	0.7161	8	25.0	
HR-ind ^d																						
3130i5	This study	-0.3129	-2.1373	-1.2807	-0.5161	4	8	2.9720	2.4650	4	4	5	28	+	-	5.91	52.18	18.67	2.80	5	13.5	
CZE60i2	This study	3.1618	-2.7092	-0.4220	-2.0045	3	5	3.0608	2.4110	128	64	6	36.8	+	-	22.93	8.78	0.33	26.6061	7	26.9	
With IS ^d																						
De248514/19	This study	0.2977		-0.5716	-3.9655	3	4	2.4364	2.1085	16	64	3	134	+	IS614B	509.8	460.1	3.7	124.3514	8	25.0	
1672	[40]		2.1815	-7.1023	-0.8173	2	3	2.6174	2.5047	256	256	4	189	+	IS1168	2.02	10.49	185.59	0.0565	7	26.9	
TAL3636	[100]	3.5263	3.3190	-0.6621	-0.4304	2	4	2.8433	2.7366	128	256	0	354	+	IS942	97.5	0.024	0.697	0.0343	8	25.0	

^a Abbreviations as follows: bS PBS—b parameter from PBS suspensions; bS BHIS—b parameter from BHIS broth cultures; d PBS—fold/dilution increase in PBS PAPs; d BHIS—fold/dilution increase in BHIS PAPs; Ipase—specific imipenemase production (u/mg cell extract). ^b Q-RT-PCR expressions and the relative expression (ratio of expressions) of ‘GNAT-XAT’. ^c K no.—number of lysines in Lrp; K %—the lysine content in Lrp in percentages. ^d Types of *cfiA*-positive strains: silent without IS elements but showing some HR, induced HR and strains with IS activated *cfiA* genes

Imipenem and imipenem heteroresistance were increased through 10 mL anaerobic BHIS cultures of *B. fragilis* 3130 and CZE60 being exposed to stepwise increments (0, 2, 8, 32 and 128 µg/mL for *B. fragilis* 33130 and 0, 32 and 128 µg/mL for *B. fragilis* CZE60) of imipenem concentrations. This was achieved by subculturing the lower imipenem concentration, containing stationary phase cultures, to the next level of imipenem-concentrated BHIS broth, to obtain an OD₆₀₀ of 0.05–0.1. We let it propagate to a stationary phase (OD₆₀₀ of 0.7–1.5) which took more time, from 1 to 4 days, as the imipenem concentrations increased.

3.3.5. Conventional PCR, Nucleotide Sequencing and qRT-PCR Experiments

Conventional PCRs and the nucleotide sequencing of some of its PCR products were carried out as described previously. PCR primer sequences and cycling conditions are contained in **Table 6**.

To examine the ‘*cfiA* element’ constant gene (‘GNAT’, ‘XAT’ and *cfiA*) expression levels, total RNA was isolated (HighPure RNA Isolation Kit, Roche) from the *cfiA*-positive test strains and we performed subsequent qRT-PCR in an RT-PCR instrument (StepOne, Life Technologies). The 10 µL final volume PCR reactions contained 5 µL SYBR Green mastermix (Verso 1-Step RT-PCR Mastermix with ROX, Thermo Fisher Scientific, Budapest, Hungary), 0.7 µM primers and 1 µL RNA sample.

3.3.6. Curve Plotting, Curve Parameter Calculation, Statistical Evaluation and Bioinformatics

Means and standard deviations were calculated after normalization of the OD₆₀₀ values in MS Excel. The highest colony counts for each type of measurement were then regarded as 1, and smaller colony counts were expressed as a fraction of that. The values of growth fraction for each imipenem concentration obtained this way were then plotted (Sigma plot 12) by direct axes (quasi hyperbolic curves), logarithmic x axis of imipenem concentrations and direct y axis of growth fraction (‘saturation curves’) and with both axes logarithmic (classical PAP curves). For the saturation curves, the following equation (3-parameter sigmoid models) was used to assess the slope (b parameters) of the HR growth:

$$y = a / (1 + \exp(-(x - x_0)/b)) \quad (1)$$

In estimating HR by calculating the ≥ 3 dilution decreases (dilution change) in the PAP curves, we started to count once the difference in the number of colonies was in the ten-fold range (since there were minimal differences in colony counts in the low-concentration ranges). For PAP curves, the extensions in imipenem concentrations and area under curve (AUC) ratios were calculated after all cell content was normalized to 10^{10} CFU. PAP AUCs were calculated by Sigmaplot 12 and divided by the value of *B. fragilis* NCTC 9343 PAPs (from PBS suspensions and BHIS cultures). We also included the HR index of gradient tests (HRI), which expressed the number of step differences in 2-fold increments between the full growth and full inhibition values (**Table 5**).

To estimate the congruence between the test strains various phenotypic and molecular parameters, 1-way ANOVA with different HR grouping parameters ((i) ≥ 3 -fold changes in PBS PAP dilutions, (ii) ≥ 3 -fold changes in BHIS PAP dilutions and (iii) $HRI > 0$) was used. The Holm–Sidak method (normal distributions) or Dunn’s methods were used (Sigmaplot 12) between group differentiations. In addition, Spearman rank correlation calculations were performed to estimate congruences between recorded parameters (Sigmaplot 12). Alignments of nucleotide and amino acid sequences were performed by Lasergene 17 (DNASar Inc., Madison, Wisconsin, USA) using the Clustal Ω algorithm.

Table 6. PCR experiment parameters

Primer	PCR type	Sequence 5'-3'	PCR cycling ^a	Ref.
<i>cfiA1</i>	conv. ^b	TCCATGCTTTTCCCTGTCGAGTTAT	94 °C 30 s, 50 °C 1 min, 72 °C 1 min, 35x	[40]
<i>cfiA2</i>		GGGCTATGGCTTTGAAGTGC		
Up2	conv.	TACGCTTTTCTGTGCCATAACTGC	94 °C 30 s, 52 °C 1 min, 72 °C 3 min, 35x	[39]
G		CGCCAAGCTTTGCCTGCCATTA		
gap-F	qRT-PCR	AGCCATTGTAGCAGCTTTTT		[101]
gap-R		GAAGACGGGATGATGTTTT		
<i>cfiA</i> -RT1	qRT-PCR	AATCGAAGGATGGGGTATGG		
<i>cfiA</i> -RT2		CGGTCAGTGAATCGGTGAAT	94 °C 15 s, 55 °C 30 s, 72 °C 30s, 35x	
GNAT-F	qRT-PCR	ACAGAAATGGTGAAGAAAT		This study
GNAT-R		GTTGACGGTAATCGTCTCTG		
XAT-F	qRT-PCR	CTGATAATCGGCAAGTTTTG		
XAT-R		CTTCGTAACCGATCCATACA		
Lrp-F	conv.	GAGGGGCTTGCGGCTGTG	94 °C 30 s, 50 °C 30 s, 72 °C 30 s, 35x	This study
Lrp-R		ATCTTATGGTTGTTTTCCG		

^a For conventional PCR, we used starting denaturation and final elongation with the following parameters 94 °C for 5 min and 72 °C for 10 min, respectively. For qRT-PCR the values recommended by the supplier were used. ^b Conventional PCR.

4. RESULTS

4.1. Direct qPCR optimization for *Mycoplasma* detection

To achieve optimal sensitivity and the shortest possible reaction time of direct qPCR, we followed a step-wise optimization of the PhoenixDx *Mycoplasma* Mix (Procomcure Biotech, Thalgau, Austria) protocol that was originally designed to amplify purified DNA samples. First, we tested the optimal annealing/extension temperature for detecting unpurified *Mycoplasma* DNA in *Mycoplasma*-infected U937 cell culture supernatants (**Figure 12A**).

The results indicated that reactions with 50–52 °C annealing/extension temperature produced the lowest Ct values (26.84 ± 0.14 – 27.06 ± 0.26). We chose the 52 °C annealing/extension temperature for further tests. Next, we tested to see whether reducing the annealing/extension time might influence qPCR performance (**Figure 10B**).

Our findings showed that the 60 s annealing/extension time provided the lowest Ct values (23.56 ± 0.47), but the 20 and 40 s annealing/ extension times led to only slightly higher Ct values (24.20 ± 0.23 , 24.11 ± 0.27 , respectively), which suggested that reducing the annealing/extension time from 60 to 20 s had a minimal influence on qPCR sensitivity. 20 s annealing/extension time was used for further qPCRs.

Next, we tested the effect of sample volume on qPCR performance (**Figure 10C**). The Ct levels of samples with 6 µl, 8 µl and 10 µl volumes of supernatants were similar (21.92–22.13 Ct value range), indicating that qPCR sensitivity is influenced by higher *Mycoplasma* DNA content and also by a higher level of qPCR inhibition in the 8 and 10 µl samples. In further experiments, we opted for the 6 µl sample volume.

Finally, we compared the performance of direct qPCR and regular qPCR with purified DNA samples (**Figure 10D**). The QIAamp DNA purification kit was used to isolate Myco-plasma DNA from U937 cell cultures (medium + cells).

The elution volume was 100 μl . A comparison of the 6 μl direct sample volume and 6 μl purified sample was not possible as just 6 μl of the 100 μl total elution volume could be used during regular qPCR. Therefore, we also decreased the 6 μl direct sample volume by a factor of 6/100 (0.36 μl). In a comparison of these samples, we found that the 6 μl purified sample produced lower C_t values (~ 2 cycles) than the 0.36 μl direct sample, suggesting a low level of qPCR inhibition of the supernatant. However, when we

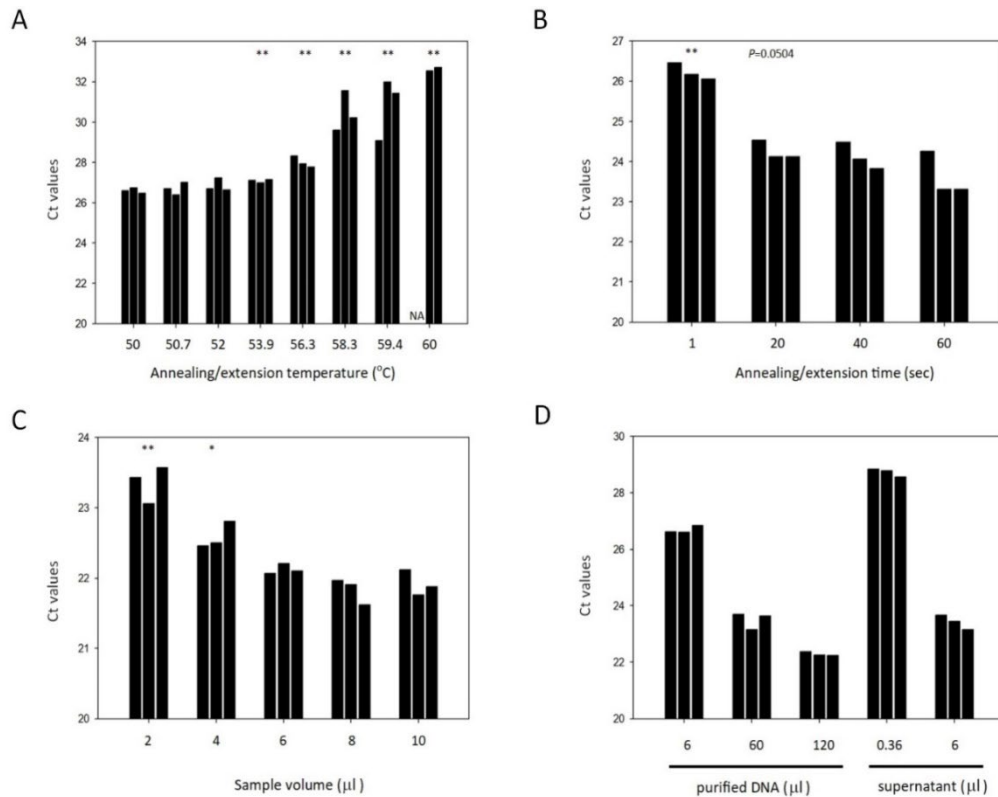


Figure 10. Optimization of *Mycoplasma* genus-specific direct qPCR and comparison of its performance with regular qPCR using purified DNA templates.

A, effect of the qPCR annealing/extension temperature on the direct qPCR performance. Student's *t*-test was applied to compare the C_t values of samples with various annealing/extension temperatures to those samples with a 50 $^{\circ}\text{C}$ annealing/extension temperature ($n=3$). **B**, effect of the annealing/extension time on direct qPCR performance. Student's *t*-test was applied to compare the C_t values of the samples with various annealing/extension times to those samples with a 60 sec annealing/extension time ($n=4$).

C, effect of sample volume on direct qPCR performance. Student's *t*-test was applied to compare the C_t values of various template volume samples with samples having a 10 μl template volume ($n=3$). **D**, comparison of direct qPCR performance with regular qPCR using a purified DNA template ($n=3$). The DNA was purified from a 6, 60 and 120 μl cell culture supernatant via the QIAamp protocol and eluted in a 100 μl elution buffer. 6 μl of eluted DNA was used in the qPCR procedure. As a comparison, 6 μl of the cell culture supernatant was used in direct qPCR. NA: no amplification was detected. *: $P<0.05$, **: $P<0.01$.

compared the Ct levels of samples with 6 μ l supernatant to the Ct levels of samples with purified DNAs we noticed that the Ct values produced with 6 μ l supernatants were almost identical to those of the purified 60 μ l supernatant (23.42 ± 0.26 , 23.49 ± 0.30 , respectively) indicating an altogether higher sensitivity of the direct qPCR. As an application of optimized direct qPCR, we monitored *Mycoplasma* elimination from the infected U937 cell culture. Our results showed that the supernatants ($n = 4$) containing removal agent or free from removal agent both resulted in nearly the same Ct levels (27.04 ± 0.24 and 26.94 ± 0.45 , respectively) (**Figure 11A**). This indicated that the presence of removal agent did not influence qPCR performance. *Mycoplasma* DNA dropped rapidly (by $\sim 80\%$) after a 24-hour treatment (**Figure 11B**).

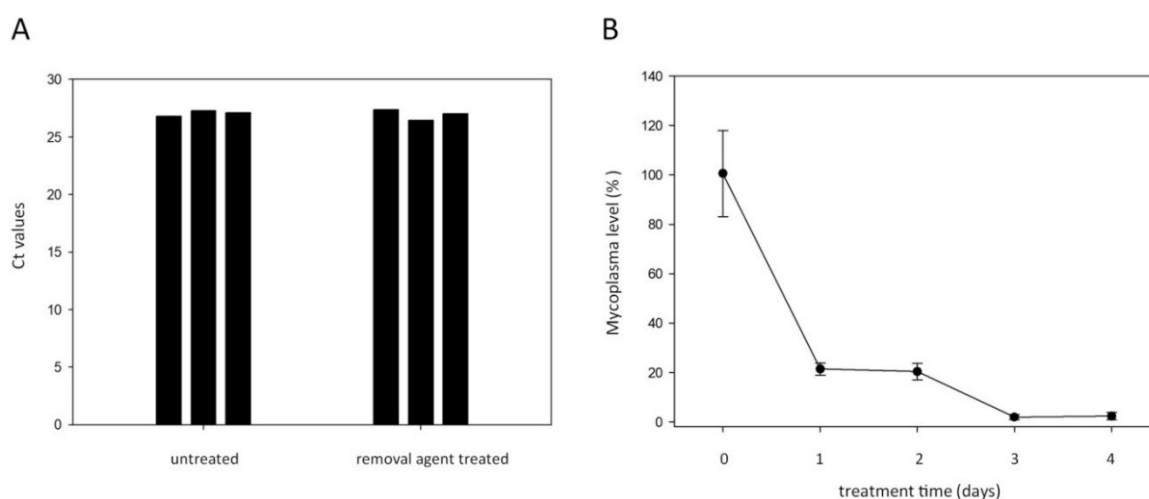


Figure 11. Monitoring *Mycoplasma* elimination by direct qPCR.

Mycoplasma contaminated U937 cells were treated with Bio-Rad *Mycoplasma* Removal Agent at 0.5 μ g/ml concentration. A, A comparison of qPCR Ct values in the absence and presence of *Mycoplasma* Removal Agent in the medium of contaminated U937 cells. Student's t-test was applied to compare the Ct values of removal agent containing samples with those of removal agent free samples ($n=3$). B, The first four days of treatment monitored by direct qPCR is shown ($n=4$ at each time point). The *Mycoplasma* genome concentration on day 0 was defined as 100%.

On the fourth day, *Mycoplasma* concentration was 2.3% of the original concentration. By the sixth day of treatment, *Mycoplasma* DNA was no longer detectable (data not shown). Overall, direct qPCR method proved to be a quick and effective method for monitoring the decrease in *Mycoplasma* DNA during the elimination process.

4.2. Metronidazole resistant strains from Kuwait

The strains were identified by MALDI-TOF MS, metronidazole and imipenem resistance values were determined by Etest (**Table 7**). The molecular resistance mechanisms and

the possible emergence of the strains showed that all but one strain were *nim* gene-positive and nucleotide sequencing revealed that these to be the *nimE* type. Since *nimE* has been described as associated with the *ISBf6* insertion sequence element [46,92,102].

We carried out PCR detection and PCR mapping of *ISBf6* in the *nimE* genes. Among the 11 *nimE*-positive strains, 10 carried *ISBf6* that could be mapped to the upstream region of the *nimE* genes. Subsequent sequencing of *nimE-ISBf6* via PCR-mapping showed that the distance between these elements was a constant 26 bp.

We determined the plasmid profiles of the *nimE*-positive strains, and by Southern blotting, the *nimE* carrying plasmids were detected (data not shown). Although only one *nimE* plasmid type has been described to date, in our Southern blots, we detected 5 different *nimE* plasmids. One representative of each of the different sized plasmids was also sequenced by high-throughput sequencing. The exact sizes of these plasmids were: 5364 bp (pPDQ1d), 10711 bp (pBFQ6d), 8331 bp (pBFQ8b), 9322 bp (pBFQ10c), and 9932 bp (pBFQ11c) (see also **Table 7**).

All proved to harbor one copy of the *nimE* gene and using Mauve alignment, all were shown to be related (**Figure 12**), implying a common origin. From the plasmid sequences obtained, we could also deduce that *ISBf6* is present in pPDQ1d in truncated form and in pBFQ11c with an internal insertion of *IS612B*.

A high prevalence of *cfiA* (n=6, 60%), by PCR and MALDI-TOF MS typing, was encountered among the *B. fragilis* strains. Among these, one was resistant to imipenem and in its upstream region of the *cfiA* gene, an insertion sequence element (*IS613*) was detected. All the other *cfiA*-positive strains were 'silent' (**Table 7**).

Because of the similarities of the 5 *nimE* plasmids with different sizes and the high prevalence of *cfiA*-positive strains among the *nimE*-positives, we also carried out genetic typing of the 10 *nimE*-positive *B. fragilis* strains by ERIC PCR. This showed that the *cfiA*-negative ones belonged to Division I and all the *cfiA*-positives belonged to Division II (**Figure 13**).

However, in this latter case, they were different from the earlier described *nimB-cfiA*-positive '*B. fragilis* BF8 MDR cluster' (**Figure 13**) [72].

Table 7. Characterization of the metronidazole resistant strains from Kuwait

No.	Species	MTZ MIC ₁ ^a (µg/ml)	MTZ MIC ₂ ^a (µg/ml)	<i>nim</i> gene	<i>nim</i> upstream IS ^b - IS <i>Bf6</i>	plasmids (kb) ^c	IP MIC ^d (µg/ml)	DivI I ^e	<i>cfiA</i>	<i>cfiA</i> -up ^f
1	<i>Phocaicola (Bacteroides) dorei</i>	>256	0.5	<i>nimE</i>	ΔIS <i>Bf6</i> 26bp	4.1, 5.3 (pPDQ1d), 51	0.25	n.a.	-	n.a.
2	<i>Bacteroides thetaiotaomicron</i>	16	0.25	-	n.a.	n.t. ^e	0.125	n.a.	-	n.a.
3	<i>Bacteroides fragilis</i>	>256	2	<i>nimE</i>	IS <i>Bf6</i> 26bp	5.6, 8.3	0.064	-	-	n.a.
4	<i>Bacteroides fragilis</i>	16	2	<i>nimE</i>	IS <i>Bf6</i> 26bp	5.6, 8.3 , 66	0.125-(2) ^g	-	-	n.a.
5	<i>Bacteroides fragilis</i>	>256	128-(>256) ^g	<i>nimE</i>	IS <i>Bf6</i> 26bp	2.7, 4.1, 5.6, 10.7 , 41	0.125	+	+	282 bp
6	<i>Bacteroides fragilis</i>	>256	128-(>256)	<i>nimE</i>	IS <i>Bf6</i> 26bp	2.7, 4.1, 5.6, 10.7 (pBFQ6d), 46	0.5	-	-	n.a.
7	<i>Bacteroides fragilis</i>	64	2	<i>nimE</i>	IS <i>Bf6</i> 26bp	5.6, 8.3 , ~60	0.25	+	+	282 bp
8	<i>Bacteroides fragilis</i>	32	2	<i>nimE</i>	IS <i>Bf6</i> 26bp	5.6, 8.3 (pBFQ8b), ~60	0.25	+	+	282 bp
9	<i>Bacteroides fragilis</i>	>256	8	<i>nimE</i>	IS <i>Bf6</i> 26bp	4.1, 5.6, 8.3 , 11.0	0.5	+	+	282 bp
10	<i>Bacteroides fragilis</i>	>256	16	<i>nimE</i>	IS <i>Bf6</i> 26bp	2.7, 5.6, 9.3 (pBFQ10c)	> 32	+	+	1.5 kb (IS613)
11	<i>Bacteroides fragilis</i>	>256	256	<i>nimE</i>	IS612C (IS <i>Bf6</i>)	2.6, 5.6, 9.9 (pBFQ11c)	0.25-(8) ^g	+	+	282 bp
12	<i>Bacteroides fragilis</i>	>256	2	<i>nimE</i>	IS <i>Bf6</i> 26bp	5.6, 8.3	0.125	-	-	n.a.

^a Metronidazole MICs measured in Kuwait (MTZ MIC₁) and in Hungary (MTZ MIC₂). ^b IS elements detected upstream of the *nimE* genes by PCR mapping or sequencing. ^c Plasmid profiles of the strains. Sizes are in kilobase pairs (kb). Plasmid hybridizing with the *nimE* probes are shown in bold, sequenced plasmid are in brackets. ^d Imipenem MICs. ^e MALDI-TOF MS typing results (n.a. – not applicable, n.t. – not tested). ^f The sizes of the *cfiA* upstream regions (IS613 was detected in *B. fragilis* Q10) ^g When heterogeneous resistance phenotype was experienced, the full inhibition zone is indicated, and the disappearance of individual resistance colonies is indicated in parenthesis

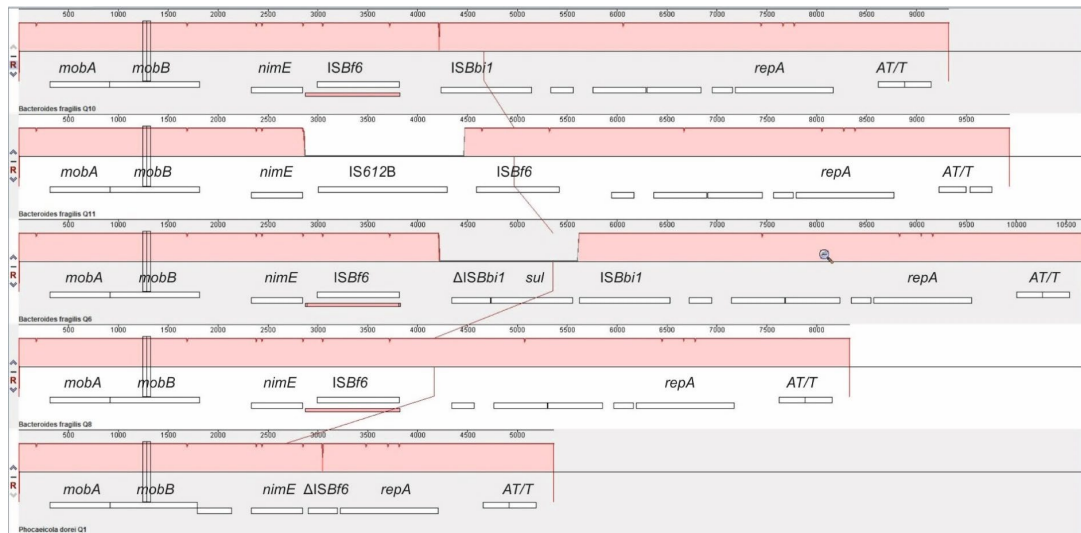


Figure 12. The full backbone alignment of the five different *nimE* plasmids

the harboring strains are indicated in the lower-left corners and the homology rates (>0-100 %) are marked in pink. Rectangles on the bottoms mark the ORFs of the different plasmids: *mobA* and *mobB* – mobilization protein genes, *nimE* – *nimE* metronidazole resistance gene, Δ ISBf6 – truncated ISBf6, Δ ISBb1 – truncated ISBb1 (*Bifidobacterium bifidum* IS), *sul* – Sulfonamide resistance gene, *repA* – replication initiation protein, *TA/T* – antitoxin-toxin addiction system/plasmid stability antitoxin toxin pairs (hypothetical ORFs are not marked with gene names)

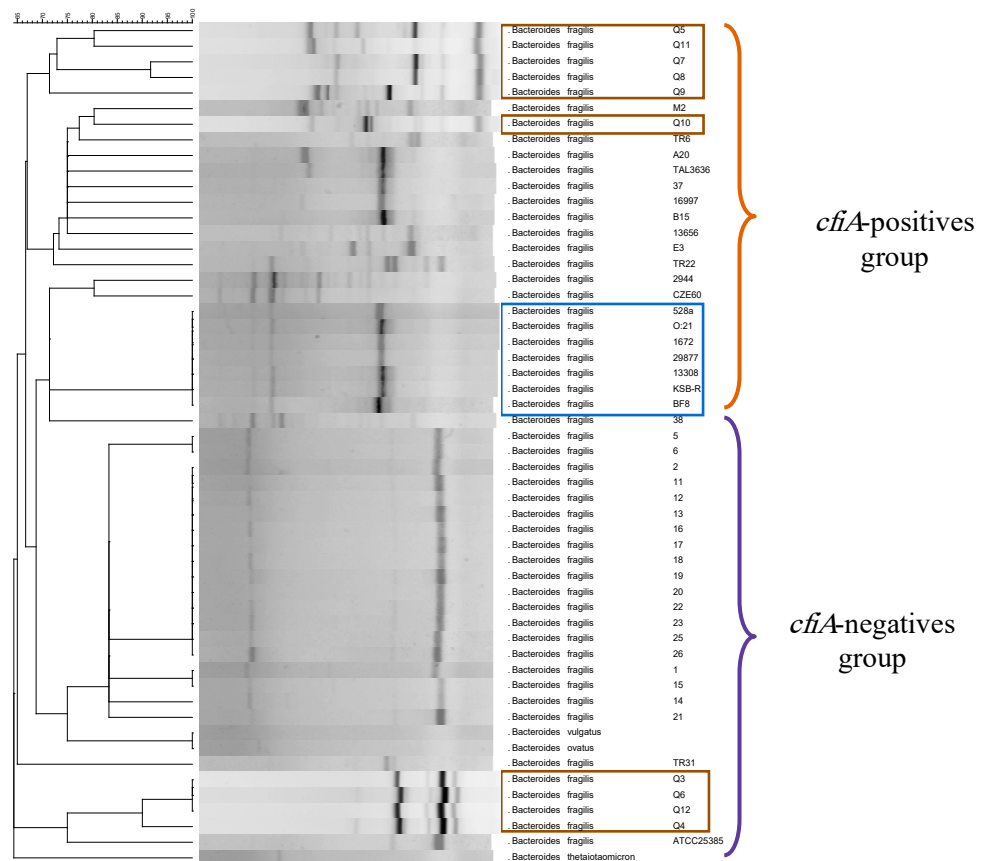


Figure 13. ERIC PCR typing of *B. fragilis* strains from different sources

The *cflA*-negative and positive *B. fragilis* groups are indicated on the right. The strains from Kuwait are shown in brown boxes and the '*B. fragilis* BF8 multidrug-resistant cluster' is boxed in blue.

4.3.Characterization of heteroresistance to imipenem in *Bacteroides fragilis*

4.3.1. Phenotypic Characterization and PAP Experiments

As our main aim was to further characterize imipenem HR, we chose the following test strains (**Table 5.**): three imipenem-susceptible *cfiA*-negative, nine *cfiA*-positive but ‘silent’ or heterogeneously imipenem-resistant in gradient tests and three imipenem-resistant, *cfiA*-positive, IS element-activated *B. fragilis* strains. A typical imipenem gradient test example showing HR is displayed in **Figure 14A.**, marking the start of the inhibition zone to the total disappearance of resistant colonies. The expression of imipenem HR phenotypes, as determined by gradient tests, varied from low to high (**Table 5.**). We analyzed the HR behavior of colonies in the partial inhibition zone. For strains displaying low-grade HR phenotypes, the direct use of the cells in further gradient tests did not result in partial inhibition. However, if we allowed a ‘recovery’ period for those cells, incubating them on supplemented Columbia blood agar, the original HR phenotype recovered (without increased HR; **Figure 14B–D.**), which demonstrated a monoclonal HR[103]. However, for strains showing a highly expressed HR phenotype, such as *B. fragilis* CZE60, some induction was observed as HR increased in these cases (data not shown).

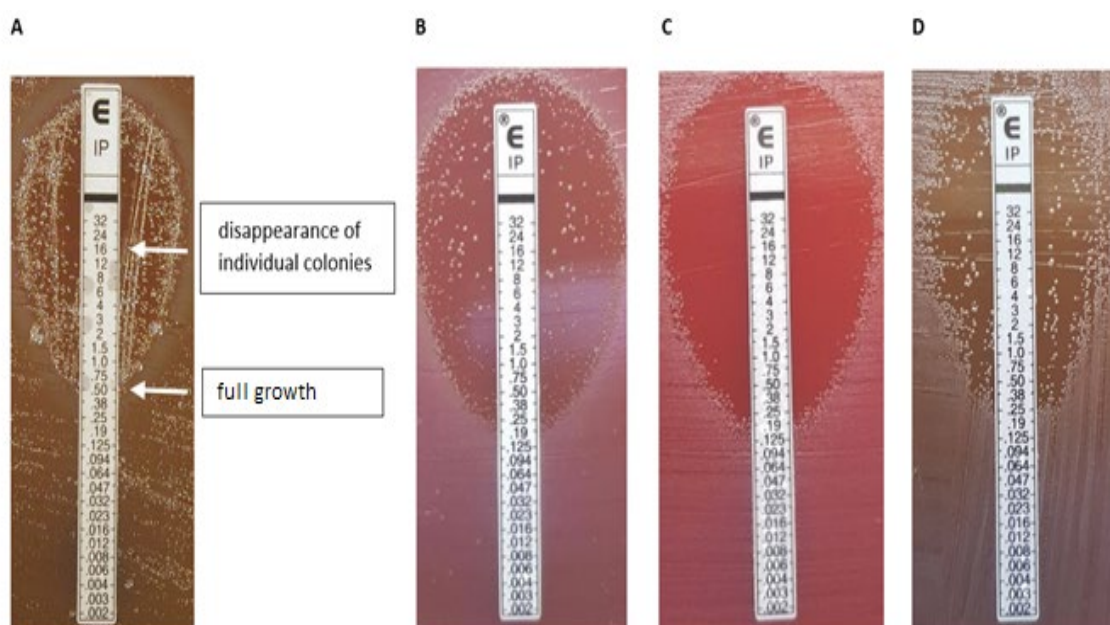


Figure 14. Etest HR phenotypes

A typical Etest phenotype (*B. fragilis* 16997) [8] showing the reading annotation; in this example 0.5–(16), the first value expresses the inhibition of full growth, then after a dash, the value indicates in parenthesis where the inside colonies disappeared. (A). The ‘inheritance’ of the Etest HR phenotype (**B–D**). Original appearance (**B**); an inner colony direct Etest (**C**); an Etest result of an inner colony after an intermediate cultivation on a Columbia blood agar (**D**).

4.3.2. PAP Curves, Assessment and Correlation of the Phenotypic Heteroresistance Parameters

In addition to PAP plots, plots without logarithmic axes (x and y axis direct—hyperbolic curves, x axis logarithmic and y axis direct—saturation curves) were also examined (**Figure 17A–F**), allowing more insight into the nature of HR. The saturation curves displayed some meaningful properties: it was interesting that, sometimes, at the lowest imipenem concentrations, we obtained fewer colony-forming units (CFU) than on the next higher-concentration plate (**Figure 17B, E**). We explained this by presuming that some dormant cells were present in the inoculating cell preparations (cultures suspended in PBS or BHIS) and that the higher, but non-selective, imipenem concentration, induced the cells to exit dormancy.

The starting imipenem concentrations caused a smoothly decreasing curve, validating our sigmoid hypothesis, and the decrease in CFUs caused by increasing imipenem concentrations also tended to be somewhat continuous (**Figure 17B, E**). The saturation curves widened as the HR increased (**Table 5**, bS PBS and BHIS) and also produced the x_0 value (**Equation (1)**), which was the inflection point or the maximum value of their derivative, the density function. In addition to these parameters, the PAP curves widened (the maximum being ≥ 3 times the minimum values, dil PBS and BHIS; **Table 5**).

To evaluate this curve's widening in conjunction with other possible HR parameters, agar dilution MICs, HRI and imipenemase production were measured and compared for all strains (**Table 5**). We also recorded imipenem MICs on WC agar plates, since the latter was also used for PAP measurements. The PAP AUC ratios were also calculated, curves for which can be seen in **Figure 16** and values in **Table 5**. All the phenotypic parameters are summarized and shown in **Table 5**.

To analyze the data, the first variance analysis was performed according to HR categorization values (as PAP dilution increased by ≥ 3 or HRI was >0 , **Table 8**). Almost all test parameters showed some potential for HR (**Table 8**).

These parameters were also cross-correlated to see the connections between them, which was a cumulative assessment of relatedness (**Appendix 1**, where cells marked with different colors show differing degrees of correlation). Instead of examining the connection of only two parameters, it was a much more complete analysis. Through the cross-correlations, we also wanted to assess which had the best predictive and explanatory values for HR. We obtained a quite good rate of relatedness between the following

parameters: (i) the x_0 PBS and BHIS values correlated well with almost all the phenotypic parameters, (ii) the AUC PBS and BHIS and MIC Brucella and MIC WC also demonstrated a very high correlation and (iii) imipenemase production also correlated well with the other phenotypic parameters.

This implied that (i) the AUC calculation best predicted HR, (ii) agar dilution predicted the resistance level quite well and (iii) an increased imipenemase production could be a cause of the HR phenotype.

4.3.3. HR Induction by Imipenem and Correlation of the Molecular Characteristics of Heteroresistance

A chromosomal segment ('*cfiA* element') containing the *cfiA* gene and a proposed TA gene pair with some insertional elements (MITE1, IS elements) were identified earlier as being characteristic of Division II *B. fragilis* strains (**Figure 8.**). Additionally, during examination of the upstream regions of *cfiA* genes in *B. fragilis* strains, we identified a lysine-rich peptide (Lrp) in the '*cfiA* element' (Figure 1). The 'GNAT' toxin gene showed a high homology to the elongation protein 3 ($e = 1.03 \times 10^{-40}$) [104] or to the AtaT-TacT-ItaT TA toxins ($e = 3.4 \times 10^{-5}$, classical members of acetylating toxin members of bacterial TA systems) [105] in protein BLAST conserved domain searches (**Figure 18**). Since a proposed TA gene pair resided on the '*cfiA* element' and imipenem stirred the HR strain cells from dormancy, we attempted to induce or increase HR by imipenem treatment. The same phenotypic parameters for two strains (*B. fragilis* 3130i5 and CZE60i2) after serial imipenem inductions (five steps for 3130i5 and two steps for CZE60i2) were also recorded (**Table 5**). The detailed data for the *B. fragilis* 3130i5 HR induction process is shown in **Figure 15**.

As imipenem concentration increased, HR, measured by E-tests and *cfiA* expression, 'GNAT' and 'XAT' genes and the 'GNAT-XAT' expression ratio, also showed increases. The increased HR in *B. fragilis* 3130i5 through induction with imipenem could also be clearly seen (**Figure 17G**), where the detected PAP curve widened and showed an increased resistance span. No growth was obtained when we exposed *B. fragilis* 3130 to a 128 mg/L imipenem concentration directly.

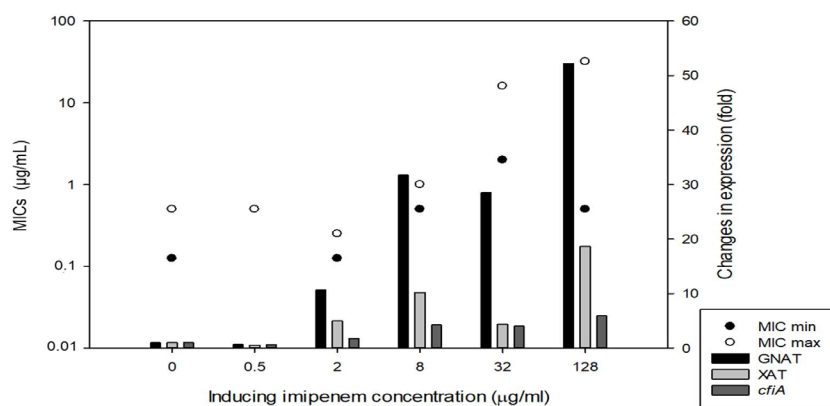


Figure 15. Induction of HR in *B. fragilis* 3130 with increasing imipenem concentration in the culture media (BHIS). The left-hand y axis denotes the Etest AST values (full and partial inhibition marked as minimal and maximal MICs) and right-hand y axis shows the gene expression changes for the strains in the induction experiments, respectively.

Table 8. Variance analysis of the examined traits of the test *B. fragilis* strains.

Trait															
Grouping Category	x ₀ PBS	x ₀ BHIS	bS PBS ^a	bS BHIS	d PBS	d BHIS	AUC PBS	AUC BHIS	MIC B	MIC WC	IP HRI	Ipase	cfiA	'GNAT'	'XAT'
Dilution change in PBS (p) ^b	0.003	0.018	0.031	n.s. ^c	p.d.^d (0.004)	0.015	0.005	0.002	0.017	0.017	n.s.	0.007	0.033	0.029	0.031
Differences between groups ^e	1-2, 1-3	1-3	1-3			1-2	1-2, 1-3	1-2, 1-3, 2-3	1-3	1-3		1-3	1-2	1-2	
Dilution change in BHIS (p)	0.01	0.03	0.021	n.s.	0.02	p.d. (0.011)	0.002	0.002	0.019	0.029	0.031	0.009	0.009	0.009	0.009
HRI (p)	0.001	n.s.	n.s.	n.s.	n.s.	n.s.	<0.001	<0.001	0.019	0.017	p.d. (<0.001)	0.005	0.028	0.024	n.s.
Differences between groups	1-2, 1-3						1-2, 1-3	1-2, 1-3			1-2, 2-3	1-3, 1-2		1-2	

^a Abbreviations are the same as Table 5. ^b P—significance values; ^c n.s.—non-significant; ^d Classifier traits (in bold, p.d.—per definition). ^e Numbers mean the following groups: 1—homogeneously susceptible; 2—heterogeneous resistance; 3—homogeneously resistant.

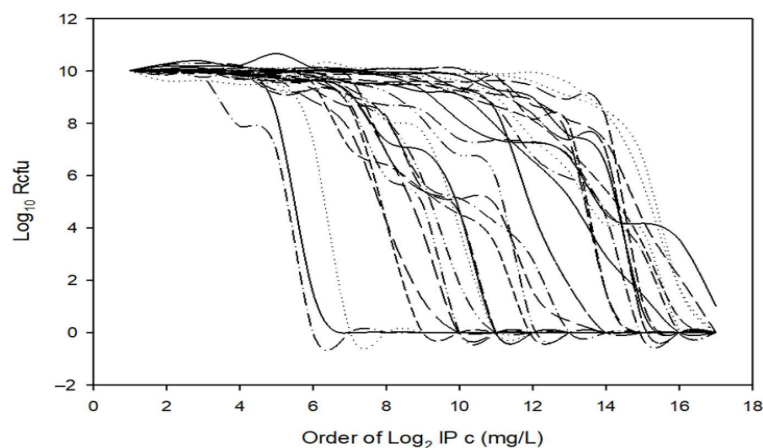


Figure 16. Cumulative PAP plots used in AUC calculations of our 15 *B. fragilis* test strains (Table 5) cultured on solid (supplemented Columbia blood agar) or in liquid (BHIS) media.

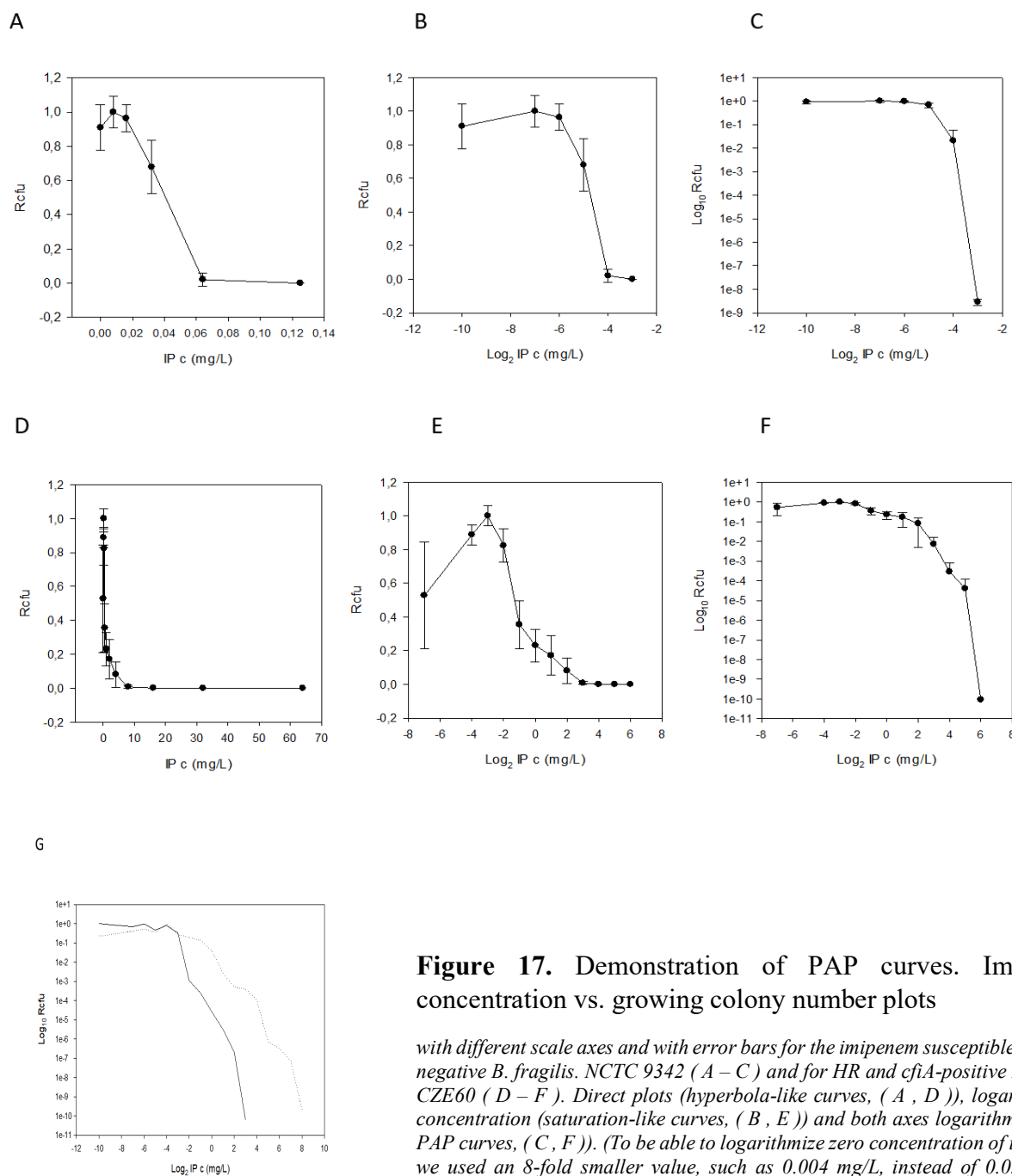


Figure 17. Demonstration of PAP curves. Imipenem concentration vs. growing colony number plots

with different scale axes and with error bars for the imipenem susceptible and *cfiA*-negative *B. fragilis* NCTC 9342 (A – C) and for HR and *cfiA*-positive *B. fragilis* CZE60 (D – F). Direct plots (hyperbola-like curves, (A, D)), logarithmic IP concentration (saturation-like curves, (B, E)) and both axes logarithmic (classic PAP curves, (C, F)). (To be able to logarithmize zero concentration of imipenem, we used an 8-fold smaller value, such as 0.004 mg/L, instead of 0.032 mg/L). Comparison of the PAP curves of imipenem uninduced (solid line) and imipenem-induced (dashed line) *B. fragilis* 3130 (G)

Since we hypothesized that ‘GNAT-XAT’ formed a TA pair that may also cause persister phenotypes, we performed some time–kill experiments to obtain further data (**Appendix 4**). However, the curves were straight, reminiscent of antibiotic tolerance [106] even for the *B. fragilis* 638R control strain. Additionally, if a strain is tolerant to one antibiotic, it can also display tolerance to others through slow growth [106].

This was not the case for our strains, as shown in **Appendix 5**. Nonetheless, we assumed that the tolerance to imipenem was mediated by other mechanisms in *B. fragilis* 638R and our other *cfiA*-positive test strains. This was reinforced, as imipenem induction did not cause alterations in the curves of imipenem-induced and non-induced strains (**Appendix 4**).

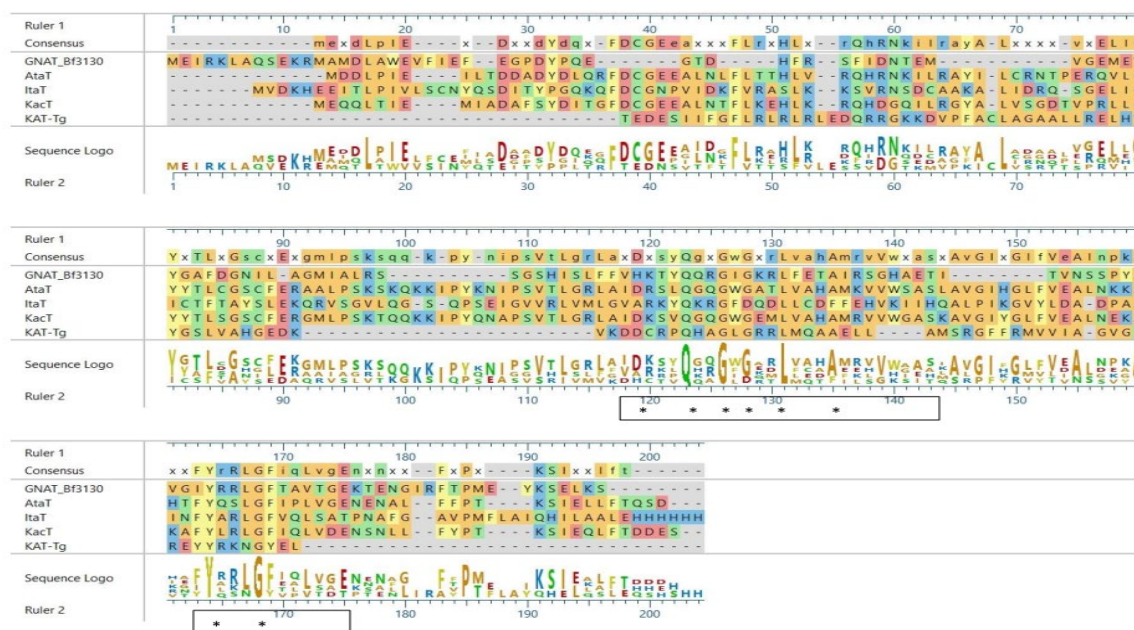


Figure 18. Alignment of amino acid sequences of GNAT acetylating toxin homologs.

GNAT_Bf3130 – the ‘GNAT’ protein of the ‘*cfiA* element’ in *B. fragilis* 3130; *AtaT* – TA toxin of *Escherichia coli* (acc. no. WP_142447164); *ItaT* – TA toxin of *Escherichia coli* (acc. no. 7BYJ_D); *KacT* – TA toxin of *Klebsiella pneumoniae* (acc. no. QXW56992); *KAT-Tg* – the lysine acetylase domain in *Toxoplasma gondii* Elongation protein 3 (acc. no. PUA86011, residues 617-721) Conserved active centre residues are marked with asterisks.

5. DISCUSSION

5.1. Direct qPCR is a sensitive approach to detect *Mycoplasma* contamination in U937 cell cultures

While various methods exist for the detection of *Mycoplasma* contamination [114,115], probably the most frequently used ones are biochemical detection of *Mycoplasma* metabolism and PCR-based detection of *Mycoplasma* DNA. Though the biochemical detection of *Mycoplasma* ATP generation (Mycoalert, Lonza, Basel, Switzerland) is a quick protocol, it has certain disadvantages that should be mentioned, including requiring that reagents be reconstituted and brought to 22 °C before each measurement and

requiring a luminometer for ATP detection. Aspecificity due to ATP generated by other cells may lead to a high background and eventually false negative measurements.

The *Ureaplasma* species which are also a common contaminant in a cell culture [116] cannot be detected by Mycoalert as their own ATP production relies on the hydrolysis of urea [117]. Finally, the sensitivity of biochemical detection has been shown to be lower than that for PCR or qPCR methods [118,119].

There are a variety of kits on offer based on regular PCR, followed by gel electrophoresis. The major advantage of these kits is the wide availability of regular PCR and electrophoresis equipment. However, decreased specificity compared to probe-based qPCR, the additional electrophoresis step, and the inability to quantitatively monitor the decrease in *Mycoplasma* genome concentration during treatment are clear drawbacks. Intercalation-based (e.g. SYBR Green) qPCR kits such as MycoSEQ *Mycoplasma* Detection Assay (Thermo Fisher, Waltham, MA, USA) eliminate the electrophoresis step and provide quantitative information about *Mycoplasma* genome concentration. The disadvantages of intercalation-based qPCR kits compared to probe-based kits are a lower specificity, lack of internal control and the potential effect of cell culture composition, ionic composition and ionic strength to change the melting temperature of the qPCR product [120-122]. Since this melting temperature is the basis for evaluating specificity in intercalation-based qPCRs, changing it can be problematic. Probe-based qPCRs such as PhoenixDx (Procomcure Biotech, Thalgau, Austria), Microsart RESEARCH *Mycoplasma* (Sartorius, Göttingen, Germany) and qPCR Detection Kit (XpressBio, Frederick, MD, USA) avoid these problems and due the additional requirement of the binding of the probe sequence, these kits provide a higher specificity than regular PCRs and intercalation-based qPCRs.

Noting the advantages of probe-based qPCRs, we optimized the Procomcure PhoenixDx kit to perform a direct qPCR with a *Mycoplasma* infected U937 cell culture. Our results indicates that the optimal temperature was the same as that in the original protocol, so the primer + probe binding was not affected by the presence of the direct template. The fact that the optimal template volume was 6 µl (30% of the total qPCR volume) meant that the direct sample did not have a significant inhibitory effect on the qPCR. A major optimization step that we performed was decreasing the annealing/extension time from

60 s to 20 s, thus saving 40 s in each cycle. Interestingly, this decrease led to only a minor decrease in the sensitivity (~ 0.6 Ct level increase). In addition, decreasing the number of cycles from 50 to 40, reduced the total qPCR time required to 65 min. When we used the optimized qPCR protocol with direct and purified cell culture templates, we found that Ct levels of a 6 μ l direct template was almost identical to that of purified DNA from a 60 μ l cell culture. The reason for this is mainly due to a dilution of the original DNA content during the elution step at the end of DNA purification. Overall, in our case, direct qPCR sensitivity was higher than qPCR with a purified template, with a saving in the cost/time of DNA purification. We monitored the elimination of *Mycoplasma* contamination from the U937 cell culture using the optimized direct qPCR protocol. One of the concerns using pathogen DNA detection is that the non-viable pathogen's DNA can also be detected and lead to a false positive signal. In our case however, the *Mycoplasma* DNA content dropped to $\sim 20\%$ of the original concentration after 1 day of treatment, and though days 1 and 2 contained a similar level of DNA, this decrease continued on day 3. In summary, with direct qPCR we were able to monitor the elimination of *Mycoplasma* over the treatment period.

5.2. Molecular characterization of metronidazole resistant Bacteroides strains from Kuwait

This study characterized 12 metronidazole resistant *Bacteroides* and *P. dorei* strains from Kuwait, in which the initial antibiotic susceptibility survey detected a 4% prevalence of metronidazole resistance across the country [90]. This figure is high compared to the resistance prevalent in northern countries but is in the described range for countries south of Europe [107-110]. Essentially, non-prudent use of metronidazole can be held responsible for this phenomenon.

However, further phenotypic and molecular characterization of these strains at the Szeged laboratory showed that metronidazole MICs were lower than those detected in most strains in Kuwait. In our view, this is not unexpected as it has been experienced before, that in other strains MICs can change through metronidazole induction or withdrawal [111], or the same *nimB* or *nimE* genes with the same IS elements with constant distances give rise to different metronidazole MICs as it has also been described earlier by S3ki *et al.* [72] or what we encountered in this study. We reported in an earlier study that

sometimes the metronidazole MIC of *nim*-positive *Bacteroides* strains does not correlate with *nim* gene expression [101]. This phenomenon is under further investigation in our laboratories. However, since almost all strains that had resistance in Kuwait were *nim* gene-positive, we still expect a functional role for *nim* genes in metronidazole resistance. We also found a highly imipenem resistant strain (*B. fragilis* Q10) for which we have a good explanation – an IS element, IS613, was carried in the upstream region also found for other highly imipenem resistant strains [38]. So, for the regulation of *cfiA* and *nim* genes, variations can be suspected.

The *nim* gene typing by sequencing also showed that the 11 *nim* positive strains harbored the *nimE* type, which is also characteristic of strains in southern countries. The *nimE* gene was found predominantly in metronidazole resistant *Bacteroides* strains in India [107,110], Afghanistan [112], and in an earlier report for Kuwait [46].

All these 11 *nimE* genes were located on plasmids, six with the same characteristic size (8.3 kb) described earlier for *nimE* plasmids [46,102,112]. Of the other five, one was much smaller in size (5.3 kb), and the other four (three variants) larger (9.3, 9.9 and 10.7 kb), than the prototypic 8.3 kb. Of the 11 *nimE* genes, 9 harbored IS*Bf6* in their upstream region, while the other two had a truncated IS*Bf6* or IS612B in their upstream regions, proving the necessity of an IS for the expression of *nimE* genes. Additionally, the plasmid backbones seemed to share large segments of common DNA sequences (**Figure 12**, pink bars). Where we could PCR-map the IS*Bf6* element to the *nimE* genes (using the PCR mapping or the full plasmid sequences), their distances were constant (26 bp). This implied to us that there was no independent insertion of IS*Bf6* in the different plasmids, but rather a preformed *nimE*-IS*Bf6* configuration inserted into a plasmid, and that then mutated and spread later as suggested in S6ki *et al.* [46].

This is also supported by the fact that these *nimE* plasmids had a common backbone despite some variance. Of these, the most notable are pPDQ1c and pBFQ11c where only a sub-segment of IS*Bf6* and IS612B respectively were in the upstream regions of the *nimE* genes. This origin hypothesis can be discussed together with earlier findings: (i) that chromosomal *nim* gene carrying strains tend to also harbor the *cfiA* gene [113]. and (ii) that some such strains (*nimB*, *cfiA*, IS1186 and IS4351 coincidentally positive, '*B. fragilis* BF8 multidrug-resistant cluster') are genetically related [72]. In our case, the *cfiA* positivity was very high (60%) among the *nimE* positive *B. fragilis* strains. ERIC PCR

typing confirmed that our *cfiA*-negative strains belonged to Division I and *cfiA*-positive strains belonged to Division II. The strains did not have a common origin to indicate the mobility and horizontal transfer of these plasmids. The *nimE* and *cfiA*-positive strains were different from the '*B. fragilis* BF8 multidrug-resistant cluster' as shown by ERIC typing (**Figure 13**), indicating that they emerged from a different background. Additionally, the association between *nim* and *cfiA* genes invites further investigation, crucially in terms of multidrug-resistance phenotypes. One of our *nimE* and *cfiA*-positive strains was highly imipenem resistant, and all our strains can be regarded as multidrug resistant (**Table 4**) to at least three groups of antibiotics (most β -lactams, clindamycin and metronidazole).

5.3. Characterization of heteroresistance to imipenem in *Bacteroides fragilis*

This study revealed that carbapenem heteroresistance is a characteristic phenotype of some *cfiA*-positive *B. fragilis* strains. The phenotypic parameters studied as the saturation curve x_0 and b , the PAP curve dilution and AUC, the imipenem MIC and HRI values and the specific imipenemase activities of the strains were interconnected and predicted HR well. The most important and central parameter was the imipenemase production, which could mediate the resistance and affect the other phenotypic parameters as it was proportional to the other parameters observed: agar dilution MICs, PAP AUC ratios and the saturation curve (simpler PAP curve) extension in PAPs of agar plate-grown cells. In our opinion, all the studied parameters could predict HR, but PAP AUC was the best. However, since most of these parameters were continuous in form from low to high imipenem MICs and HR parameters, continuing to use PAP curve extensions could also be regarded as a very good method. The PAP AUC method was also suggested as a good prediction parameter for the reduced glycopeptide susceptibility of *staphylococci* [123].

We related the HR phenotype to stochastic processes. According to our hypothesis, this was due to the action of a proposed toxin ('GNAT') that may stop growth, but also allows viability under antibiotic-exposed circumstances. The primary finding supporting this was the widening of the PAP saturation curve parameter, b , which could be regarded as a standard deviation parameter. To improve the discussion of HR and persistence, Brauner and Balaban suggested the term heterotolerance for HR [124]. In more thoroughly investigated tolerance and persistence mechanisms, it has also been suggested that wider distributions, and those above a certain persistence factor threshold, yield more persisters [24]. We believe this is true for the carbapenem heteroresistance of *B. fragilis*,

as we also detected a widening of our saturation curves. Imipenemase activity values, as an effector mechanism, also correlated with most of the phenotypic parameters of HR [125].

We propose an HR mechanism of *cfiA*-positive *B. fragilis* strains as follows: (i) *cfiA* is expressed proportionally to HR, and (ii) the parallel expression of ‘GNAT-XAT’ allows reduced cellular activities. We conclude the same from experiments in which we induced imipenem HR by imipenem; however, to obtain a more detailed picture about this, experiments are under way in our laboratory to determine the promoters of *cfiA* and ‘GNAT-XAT’, how they act individually and in conjunction with other promoters, what is the biochemical nature of ‘GNAT’ and ‘XAT’, do they form a TA pair and what is the role of the lysine-rich peptide in the ‘*cfiA* element’. It is conceivable through the above that ‘GNAT’ acts through the acetylation of a lysine in a ribosomal protein or in tRNA-Lys molecules and Lrp may modify these actions.

At present, no particular common mechanism was found to explain HR in other bacteria. However, in some cases, regulatory proteins were involved as well [126-130], which we believe may also produce stochastic regulation. Additionally, monoclonal heteroresistance could also emerge by the tandem duplication of DNA segments of the effector genes of *Acinetobacter baumannii* [131], *Escherichia coli* [132], *Klebsiella pneumoniae* [133], *Pseudomonas aeruginosa* [134], *Salmonella typhimurium* [58] or *Streptococcus pneumoniae* [135]. However, this latter mechanism can result in a variable number of repeats in the cells of a given population, which can be both stochastic and difficult to detect. Recently, for the aminoglycoside HR of *A. baumannii* in a *recA*-negative background, a modest copy number variation of the *aadB* gene-containing integron was linked to HR. The step causing the copy number increase was hypothesized as a stochastic process [131]. In earlier experiments, we did not observe that *cfiA* or the ‘*cfiA* element’ had copy number variations or that the *cfiA* promoter was invertible (data not shown), as CPS promoters usually are in *B. fragilis*. The role of global regulatory systems ((p)ppGpp, *relA*, *spoT*) in bacterial persistence was proven, something which we would like to examine regarding the HR of *B. fragilis* [125].

For TA systems, the prominent role of governing persistence was attributed, but some parallels between HR and persister phenotypes could also be drawn, HR can be regarded as concentration-dependent, while persistence can be regarded as a time-dependent

survival phenomenon. In our opinion, the stochastic hypothesis of carbapenem HR of *B. fragilis* may facilitate research into this being the case in other HR systems as well.

6. CONCLUSION

We optimized a probe-based qPCR to detect *Mycoplasma* contamination in a user-friendly manner. This direct qPCR method does not require a purification step, maintains sensitivity and offers a shorter 65 min protocol.

In Kuwait, similarly other southern countries, there is a considerable resistance rate to metronidazole and the resistance mechanism is plasmid-carried *nimE* genes preceded by IS-provided promoters, the *nimE* genes are carried on differently sized plasmids of common origin where the *nimE*-IS*Bf6* configuration emerged first, and the majority of the *nimE*-positive strains also carry the *cfiA* gene together causing severe issues linked to multidrug-resistance.

We analyzed extensively the phenotypic parameters of control and HR *B. fragilis* strains, which yielded scattered but statistically evaluable data enabling novel description by saturation curves. In summary, these investigations into the various HR traits revealed that while the AUC PAP method was the best predictor/classifier for HR, other traits could also be considered suitable. Among the phenotypic traits examined, the saturation curve, PAP AUC, agar dilution and imipenemase activities correlated well. This indicated that they were also good predictors and were linked to the HR mechanism, for which imipenemase production could be the primary contributor. The two parameters that most correlate with the others are imipenemase production and ‘GNAT’ expression, which prompted us to suspect that carbapenem heteroresistance of the *B. fragilis* strains is stochastically regulated and is mediated by the altered imipenemase production. The calculation of the widening of the saturation and PAP curves, for the PBS suspensions, showed a good correlation with the PAP AUCs, agar dilution MICs and imipenemase production. Therefore, we saw our stochastic explanation of the nature of HR as compelling. This latter point was also supported by the fact that imipenem HR could be induced by imipenem and that the expression of the ‘*cfiA* element’ genes (‘GNAT’, ‘XAT’, and *cfiA*) correlated. ‘GNAT’ can act as a toxin causing dormancy, and these genes may form a complex interaction.

7. SUMMARY

Antimicrobial resistance (AMR) is an international public health concern that intimidates our ability to treat bacterial infections successfully. AMR has been involved in 1.8 million deaths in 2020, anticipated to be one-third as many people as COVID-19 has killed. Anaerobes are microorganisms that live and spread in settings lacking oxygen. They play a vital function in human health and wellness regarding causing infections and making up essential microflora. *Bacteroides* spp. is a genus of gram-negative, non-spore-forming, obligately anaerobic, rod-shaped, bile-resistant bacteria. These commensal bacteria can interact with the immune system and modify its response. *Bacteroides fragilis* is the most frequently isolated anaerobe from peritoneal and abdominal abscesses and samples of bloodstream infections.

- *Mycoplasma* is a small cell-wall free prokaryotic bacterium with a remarkable diversity at the species level. It causes human respiratory and urogenital tract infections and can also cause bovine cell-culture contamination. Mycoplasmosis is hard to prevent/eradicate since it is less sensitive to antibiotics commonly applied in cell cultures. We want to skip the DNA purification step in this study and develop a direct qPCR detection method for *Mycoplasma* contamination in U937 cell cultures.

In summary, direct qPCR allowed us to track *Mycoplasma* elimination during treatment. We optimized a probe-based qPCR to detect *Mycoplasma* contamination. This direct qPCR method eliminates purification, maintains sensitivity, and is only 65 minutes long.

- Eleven metronidazole resistant *Bacteroides* and one newly classified *Phocaeicola dorei* strain from Kuwait were investigated for their resistance mechanisms and the emergence of their resistant plasmids. All but one strain harbored *nimE* genes on differently sized plasmids. Of the 11 *nimE* genes, 9 were preceded by full copies of the prototype *ISBf6* insertion sequence element, one carried a truncated *ISBf6* and one was activated by an additional copy of *IS612B*. Nucleotide sequencing results showed that the *nimE* *ISBf6* distances were constant and all five different plasmids shared a common region, suggesting that (i) the *nimE*-*ISBf6* configuration was inserted into an undisclosed common genetic element, (ii) over time, this common element was mutated by insertions and deletions, spreading the resultant plasmids. Of the 10 *B. fragilis* strains in this

collection, 6 were also *cfiA*-positive, one with full imipenem resistance, indicating a tendency for multidrug resistance (MDR) among such isolates. The significant number of metronidazole resistant *Bacteroides* spp. and *P. dorei* strains with the MDR phenotype warns of difficulties in treatment and suggests promoting adherence to antibiotic stewardship recommendations in Kuwait.

- Carbapenem-resistant *Bacteroides fragilis* strains usually emerge by an insertion sequence (IS) jump into the upstream region of the *cfiA* carbapenemase gene. However, intermediate or fully resistant *cfiA*-positive strains also exist. These do not have such IS element activations, but usually have heterogeneous resistance (HR) phenotypes, as detected by a disc diffusion or gradient tests. Heteroresistance is a serious antibiotic resistance problem, whose molecular mechanisms are not fully understood. We aim to characterize HR and investigate diagnostic issues in the set of *cfiA*-positive *B. fragilis* strains using phenotypic and molecular methods. Of the phenotypic methods used, the population analysis profile (PAP) and area under curve (AUC) measurements were the best prognostic markers for HR. PAP AUC, imipenem agar dilution and imipenemase production corresponded well with each other. We also identified a saturation curve parameter (quasi-PAP curves), which correlated well with these phenotypic traits, implying that HR is a stochastic process. The genes, on a previously defined ‘*cfiA* element’, act in a complex manner to produce the HR phenotype, including a lysine-acetylating toxin and a lysine-rich peptide. Furthermore, imipenem HR is triggered by imipenem. The two parameters that most correlate with the others are imipenemase production and ‘GNAT’ expression, which prompted us to suspect that carbapenem heteroresistance of the *B. fragilis* strains is stochastically regulated and is mediated by the altered imipenemase production.

8. NOVELTY (NEW FINDINGS)

- A novel user-friendly probe-based qPCR was developed to detect *Mycoplasma* contamination method.
- The developed direct qPCR method eliminates purification, maintains sensitivity, and is 65 minutes long.
- The developed direct qPCR method could be implemented to detect the presence of other microorganisms.
- In Kuwait, majority of metronidazole resistance in *B. fragilis* is due to plasmid-carried *nimE* genes preceded by IS-provided promoters.
- The prevalence of metronidazole resistant *Bacteroides* strains is around 4% in Kuwait.
- *nimE*-positive strains also carry the *cfiA* gene, causing severe issues linked to multidrug-resistance, particularly in sub-Saharan Africa.
- This is the first work to investigate HR in anaerobes and successfully determined some of the main factors involved in this phenomenon in *B. fragilis*.
- The study shows that the saturation curve, PAP AUC, agar dilution and imipenemase activities are good predictors of HR.
- The expression of the '*cfiA* element' genes ('GNAT', 'XAT', and *cfiA*) can act as a toxin causing dormancy.
- Imipenem HR could be induced by exposure to imipenem.
- Carbapenem heteroresistance of the *B. fragilis* strains is stochastically regulated and is mediated by the altered imipenemase production.
- The proposed factors causing HR in *B. fragilis* could provide a strong basis to conduct more research and establish a better understanding of this ambiguous phenomenon.

9. REFERENCES

- 1 McEwen, S.A. and Collignon, P.J. (2018) Antimicrobial Resistance: a One Health Perspective. In *Antimicrobial Resistance in Bacteria from Livestock and Companion Animals*, pp. 521-547
- 2 Coers, J., Band, V.I. and Weiss, D.S. (2019) Heteroresistance: A cause of unexplained antibiotic treatment failure? *PLOS Pathogens* 15 (6)<https://doi.org/10.1371/journal.ppat.1007726>
- 3 Ventola, C.L. (2015) The antibiotic resistance crisis: part 1: causes and threats. *P t* 40 (4), 277-283:
- 4 Murray, C.J.L., Ikuta, K.S., Sharara, F., Swetschinski, L., Robles Aguilar, G., Gray, A., Han, C., Bisignano, C., Rao, P., Wool, E., Johnson, S.C., Browne, A.J., Chipeta, M.G., Fell, F., Hackett, S., Haines-Woodhouse, G., Kashef Hamadani, B.H. and Naghavi, M. (2022) Global burden of bacterial antimicrobial resistance in 2019: a systematic analysis. *The Lancet* 399 (10325), 629-655: [https://doi.org/10.1016/S0140-6736\(21\)02724-0](https://doi.org/10.1016/S0140-6736(21)02724-0)
- 5 Knight, G.M., Glover, R.E., McQuaid, C.F., Olaru, I.D., Gallandat, K., Leclerc, Q.J., Fuller, N.M., Willcocks, S.J., Hasan, R., van Kleef, E. and Chandler, C.I.R. (2021) Antimicrobial resistance and COVID-19: Intersections and implications. *eLife* 10, e64139: <https://doi.org/10.7554/eLife.64139>
- 6 Holmes, A.H., Moore, L.S.P., Sundsfjord, A., Steinbakk, M., Regmi, S., Karkey, A., Guerin, P.J. and Piddock, L.J.V. (2016) Understanding the mechanisms and drivers of antimicrobial resistance. *The Lancet* 387 (10014), 176-187: [https://doi.org/10.1016/s0140-6736\(15\)00473-0](https://doi.org/10.1016/s0140-6736(15)00473-0)
- 7 Levin-Reisman, I., Ronin, I., Gefen, O., Braniss, I., Shores, N. and Balaban, N.Q. (2017) Antibiotic tolerance facilitates the evolution of resistance. *Science* 355 (6327), 826-830: <https://doi.org/10.1126/science.aaj2191>
- 8 Urbaniec, J., Xu, Y., Hu, Y., Hingley-Wilson, S. and McFadden, J. (2021) Phenotypic heterogeneity in persisters: a novel 'hunker' theory of persistence. *FEMS Microbiology Reviews* 46 (1)<https://doi.org/10.1093/femsre/fuab042>
- 9 Corona, F. and Martinez, J.L. (2013) Phenotypic Resistance to Antibiotics. *Antibiotics (Basel)* 2 (2), 237-255: <https://doi.org/10.3390/antibiotics2020237>
- 10 Hughes, D. and Andersson, D.I. (2017) Environmental and genetic modulation of the phenotypic expression of antibiotic resistance. *FEMS microbiology reviews* 41 (3), 374-391: <https://doi.org/10.1093/femsre/fux004>
- 11 Huijbers, P.M.C., Blaak, H., de Jong, M.C.M., Graat, E.A.M., Vandenbroucke-Grauls, C.M.J.E. and de Roda Husman, A.M. (2015) Role of the Environment in the Transmission of Antimicrobial Resistance to Humans: A Review. *Environmental Science & Technology* 49 (20), 11993-12004: <https://doi.org/10.1021/acs.est.5b02566>
- 12 Ukuhor, H.O. (2021) The interrelationships between antimicrobial resistance, COVID-19, past, and future pandemics. *J Infect Public Health* 14 (1), 53-60: <https://doi.org/10.1016/j.jiph.2020.10.018>
- 13 Hatti-Kaul, R., Mamo, G., Mattiasson, B. and Springer International Publishing, A.G. (2018) Anaerobes in Biotechnology. <https://doi.org/10.1007/s12223-018-0658-4>
- 14 Mentella, M.C., Scaldaferri, F., Pizzoferrato, M., Gasbarrini, A. and Miggiano, G.A.D. (2020) Nutrition, IBD and Gut Microbiota: A Review. *Nutrients* 12 (4)<https://doi.org/10.3390/nu12040944>

- 15 Salvado, R., Santos-Minguez, S., Agudo-Conde, C., Lugones-Sanchez, C., Cabo-Laso, A., J, M.H.-S., Benito, R., Rodriguez-Sanchez, E., Gomez-Marcos, M.A., Hernandez-Rivas, J.M., Guimarães Cunha, P., Garcia-Ortiz, L. and Investigators, M. (2021) Gut microbiota composition and arterial stiffness measured by pulse wave velocity: case-control study protocol (MIVAS study). *BMJ Open* 11 (2), e038933: <https://doi.org/10.1136/bmjopen-2020-038933>
- 16 Riedel, S., Hobden, J.A., Miller, S., Morse, S.A., Mietzner, T.A., Detrick, B., Mitchell, T.G., Sakanari, J.A., Hotez, P. and Mejia, R. (2019) *Jawetz, Melnick, & Adelberg's Medical Microbiology*, McGraw-Hill Education LLC.
- 17 O'Hara, A.M. and Shanahan, F. (2006) The gut flora as a forgotten organ. *EMBO Rep* 7 (7), 688-693: <https://doi.org/10.1038/sj.embor.7400731>
- 18 Guarner, F. and Malagelada, J.-R. (2003) Gut flora in health and disease. *The Lancet* 361 (9356), 512-519: [https://doi.org/10.1016/s0140-6736\(03\)12489-0](https://doi.org/10.1016/s0140-6736(03)12489-0)
- 19 Dahiya, D.K., Renuka, Dangi, A.K., Shandilya, U.K., Puniya, A.K. and Shukla, P. (2019) Chapter 44 - New-Generation Probiotics: Perspectives and Applications. In *Microbiome and Metabolome in Diagnosis, Therapy, and other Strategic Applications* (Faintuch, J. and Faintuch, S., eds.), pp. 417-424, Academic Press
- 20 Patrick, S. (2015) Chapter 51 - Bacteroides. In *Molecular Medical Microbiology (Second Edition)* (Tang, Y.-W. Sussman, M. Liu, D. Poxton, I. and Schwartzman, J., eds.), pp. 917-944, Academic Press
- 21 Gauffin Cano, P., Santacruz, A., Moya, Á. and Sanz, Y. (2012) Bacteroides uniformis CECT 7771 Ameliorates Metabolic and Immunological Dysfunction in Mice with High-Fat-Diet Induced Obesity. *PLOS ONE* 7 (7), e41079: <https://doi.org/10.1371/journal.pone.0041079>
- 22 Yang, J.Y., Lee, Y.S., Kim, Y., Lee, S.H., Ryu, S., Fukuda, S., Hase, K., Yang, C.S., Lim, H.S., Kim, M.S., Kim, H.M., Ahn, S.H., Kwon, B.E., Ko, H.J. and Kweon, M.N. (2017) Gut commensal Bacteroides acidifaciens prevents obesity and improves insulin sensitivity in mice. *Mucosal Immunol* 10 (1), 104-116: <https://doi.org/10.1038/mi.2016.42>
- 23 Schoch, C.L., Ciufo, S., Domrachev, M., Hotton, C.L., Kannan, S., Khovanskaya, R., Leipe, D., McVeigh, R., O'Neill, K., Robbertse, B., Sharma, S., Soussov, V., Sullivan, J.P., Sun, L., Turner, S. and Karsch-Mizrachi, I. (2020) NCBI Taxonomy: a comprehensive update on curation, resources and tools. *Database (Oxford)* 2020 <https://doi.org/10.1093/database/baaa062>
- 24 NCBI. (2020) The NCBI taxonomy database - Bacteroidales. (Vol. 2021), NCBI
- 25 NCBI. (2020) The NCBI taxonomy database - Bacteroides. (Vol. 2021), NCBI
- 26 Valguarnera, E. and Wardenburg, J.B. (2020) Good Gone Bad: One Toxin Away From Disease for Bacteroides fragilis. *Journal of Molecular Biology* 432 (4), 765-785: <https://doi.org/https://doi.org/10.1016/j.jmb.2019.12.003>
- 27 Actor, J.K. (2012) 12 - Clinical Bacteriology. In *Elsevier's Integrated Review Immunology and Microbiology (Second Edition)* (Actor, J.K., ed.), pp. 105-120, W.B. Saunders
- 28 Deng, H., Li, Z., Tan, Y., Guo, Z., Liu, Y., Wang, Y., Yuan, Y., Yang, R., Bi, Y., Bai, Y. and Zhi, F. (2016) A novel strain of Bacteroides fragilis enhances phagocytosis and polarises M1 macrophages. *Scientific Reports* 6 (1), 29401: <https://doi.org/10.1038/srep29401>

- 29 Finegold, S.M. and Sussman, M. (2002) 88 - Anaerobic Infections: A Clinical Overview. In *Molecular Medical Microbiology* (Sussman, M., ed.), pp. 1867-1874, Academic Press
- 30 Wexler, H.M. (2015) Anaerobic Infections. In *Molecular Medical Microbiology*, pp. 875-897
- 31 Reygaert, W.C. (2018) An overview of the antimicrobial resistance mechanisms of bacteria. *AIMS Microbiol* 4 (3), 482-501:
<https://doi.org/10.3934/microbiol.2018.3.482>
- 32 Gajdács, M., Spengler, G. and Urbán, E. (2017) Identification and Antimicrobial Susceptibility Testing of Anaerobic Bacteria: Rubik's Cube of Clinical Microbiology? *Antibiotics* 6 (4)<https://doi.org/10.3390/antibiotics6040025>
- 33 Baaity, Z., Jamal, W., Rotimi, V.O., Burián, K., Leitsch, D., Somogyvári, F., Nagy, E. and Sóki, J. (2021) Molecular characterization of metronidazole resistant *Bacteroides* strains from Kuwait. *Anaerobe*, 102357:
<https://doi.org/https://doi.org/10.1016/j.anaerobe.2021.102357>
- 34 Meletis, G. (2016) Carbapenem resistance: overview of the problem and future perspectives. *Ther Adv Infect Dis* 3 (1), 15-21:
<https://doi.org/10.1177/2049936115621709>
- 35 Voha, C., Docquier, J.D., Rossolini, G.M. and Fosse, T. (2006) Genetic and biochemical characterization of FUS-1 (OXA-85), a narrow-spectrum class D beta-lactamase from *Fusobacterium nucleatum* subsp. polymorphum. *Antimicrob Agents Chemother* 50 (8), 2673-2679:
<https://doi.org/10.1128/aac.00058-06>
- 36 Wang, Z., Fast, W. and Benkovic, S.J. (1999) On the Mechanism of the Metallo- β -lactamase from *Bacteroides fragilis*†. *Biochemistry* 38 (31), 10013-10023:
<https://doi.org/10.1021/bi990356r>
- 37 Gutacker, M., Valsangiacomo, C., Bernasconi, M.V. and Piffaretti, J.-C. (2002) *recA* and *glnA* sequences separate the *Bacteroides fragilis* population into two genetic divisions associated with the antibiotic resistance genotypes *cepA* and *cfiA*. *Journal of Medical Microbiology* 51 (2), 123-130:
<https://doi.org/10.1099/0022-1317-51-2-123>
- 38 Sóki, J. (2013) Extended role for insertion sequence elements in the antibiotic resistance of *Bacteroides*. *World Journal of Clinical Infectious Diseases* 3 (1), 1-12:
- 39 Sóki, J., Edwards, R., Urbán, E., Fodor, E., Beer, Z. and Nagy, E. (2004) Screening of isolates from faeces for carbapenem-resistant *Bacteroides* strains; existence of strains with novel types of resistance mechanisms. *International Journal of Antimicrobial Agents* 24 (5), 450-454:
<https://doi.org/https://doi.org/10.1016/j.ijantimicag.2004.06.017>
- 40 Sóki, J., Fodor, E., Hecht, D.W., Edwards, R., Rotimi, V.O., Kerekes, I., Urbán, E. and Nagy, E. (2004) Molecular characterization of imipenem-resistant, *cfiA*-positive *Bacteroides fragilis* isolates from the USA, Hungary and Kuwait. *Journal of Medical Microbiology* 53 (5), 413-419:
<https://doi.org/10.1099/jmm.0.05452-0>
- 41 Jeverica, S., Sóki, J., Premru, M.M., Nagy, E. and Papst, L. (2019) High prevalence of division II (*cfiA* positive) isolates among blood stream *Bacteroides fragilis* in Slovenia as determined by MALDI-TOF MS. *Anaerobe* 58, 30-34: <https://doi.org/https://doi.org/10.1016/j.anaerobe.2019.01.011>
- 42 Sóki, J., Eitel, Z., Urbán, E. and Nagy, E. (2013) Molecular analysis of the carbapenem and metronidazole resistance mechanisms of *Bacteroides* strains

- reported in a Europe-wide antibiotic resistance survey. *International Journal of Antimicrobial Agents* 41 (2), 122-125:
<https://doi.org/https://doi.org/10.1016/j.ijantimicag.2012.10.001>
- 43 Alauzet, C., Berger, S., Jean-Pierre, H., Dubreuil, L., Jumas-Bilak, E., Lozniewski, A. and Marchandin, H. (2017) nimH, a novel nitroimidazole resistance gene contributing to metronidazole resistance in *Bacteroides fragilis*. *Journal of Antimicrobial Chemotherapy* 72 (9), 2673-2675:
<https://doi.org/10.1093/jac/dkx160>
- 44 García-López, M., Meier-Kolthoff, J.P., Tindall, B.J., Gronow, S., Woyke, T., Kyrpides, N.C., Hahnke, R.L. and Göker, M. (2019) Analysis of 1,000 Type-Strain Genomes Improves Taxonomic Classification of Bacteroidetes. *Frontiers in Microbiology* 10<https://doi.org/10.3389/fmicb.2019.02083>
- 45 Freeman, C.D., Klutman, N.E. and Lamp, K.C. (1997) Metronidazole. *Drugs* 54 (5), 679-708: <https://doi.org/10.2165/00003495-199754050-00003>
- 46 Sóki, J., Gal, M., Brazier, J.S., Rotimi, V.O., Urbán, E., Nagy, E. and Duerden, B.I. (2006) Molecular investigation of genetic elements contributing to metronidazole resistance in *Bacteroides* strains. *Journal of Antimicrobial Chemotherapy* 57 (2), 212-220: <https://doi.org/10.1093/jac/dki443>
- 47 Trastoy, R., Manso, T., Fernández-García, L., Blasco, L., Ambroa, A., Pérez Del Molino, M.L., Bou, G., García-Contreras, R., Wood, T.K. and Tomás, M. (2018) Mechanisms of Bacterial Tolerance and Persistence in the Gastrointestinal and Respiratory Environments. *Clin Microbiol Rev* 31 (4)<https://doi.org/10.1128/cmr.00023-18>
- 48 Hobby, G.L., Meyer, K. and Chaffee, E. (1942) Observations on the Mechanism of Action of Penicillin. *Experimental Biology and Medicine* 50 (2), 281-285:
<https://doi.org/10.3181/00379727-50-13773>
- 49 Balaban, N.Q., Helaine, S., Lewis, K., Ackermann, M., Aldridge, B., Andersson, D.I., Brynildsen, M.P., Bumann, D., Camilli, A., Collins, J.J., Dehio, C., Fortune, S., Ghigo, J.-M., Hardt, W.-D., Harms, A., Heinemann, M., Hung, D.T., Jenal, U., Levin, B.R., Michiels, J., Storz, G., Tan, M.-W., Tenson, T., Van Melderen, L. and Zinkernagel, A. (2019) Definitions and guidelines for research on antibiotic persistence. *Nature Reviews Microbiology* 17 (7), 441-448: <https://doi.org/10.1038/s41579-019-0196-3>
- 50 El-Halfawy, O.M. and Valvano, M.A. (2015) Antimicrobial Heteroresistance: an Emerging Field in Need of Clarity. 28 (1), 191-207:
<https://doi.org/10.1128/CMR.00058-14> %J Clinical Microbiology Reviews
- 51 Kayser, F.H., Benner, E.J. and Hoeprich, P.D. (1970) Acquired and native resistance of *Staphylococcus aureus* to cephalixin and other beta-lactam antibiotics. *Appl Microbiol* 20 (1), 1-5:
- 52 Alexander, H.E. and Leidy, G. (1947) MODE OF ACTION OF STREPTOMYCIN ON TYPE b HEMOPHILUS INFLUENZAE : II. NATURE OF RESISTANT VARIANTS. *J Exp Med* 85 (6), 607-621:
<https://doi.org/10.1084/jem.85.6.607>
- 53 Rizvanov, A.A., Haertlé, T., Bogomolnaya, L. and Talebi Bezmin Abadi, A. (2019) *Helicobacter pylori* and Its Antibiotic Heteroresistance: A Neglected Issue in Published Guidelines. *Frontiers in microbiology* 10, 1796-1796:
<https://doi.org/10.3389/fmicb.2019.01796>
- 54 Andersson, D.I., Nicoloff, H. and Hjort, K. (2019) Mechanisms and clinical relevance of bacterial heteroresistance. *Nature Reviews Microbiology* 17 (8), 479-496: <https://doi.org/10.1038/s41579-019-0218-1>

- 55 He, J., Jia, X., Yang, S., Xu, X., Sun, K., Li, C., Yang, T. and Zhang, L. (2018) Heteroresistance to carbapenems in invasive *Pseudomonas aeruginosa* infections. *International Journal of Antimicrobial Agents* 51 (3), 413-421: <https://doi.org/https://doi.org/10.1016/j.ijantimicag.2017.10.014>
- 56 Band, V.I., Satola, S.W., Burd, E.M., Farley, M.M., Jacob, J.T. and Weiss, D.S. (2018) Carbapenem-Resistant *Klebsiella pneumoniae* Exhibiting Clinically Undetected Colistin Heteroresistance Leads to Treatment Failure in a Murine Model of Infection. *MBio* 9 (2) <https://doi.org/10.1128/mBio.02448-17>
- 57 Band, V.I., Crispell, E.K., Napier, B.A., Herrera, C.M., Tharp, G.K., Vavikolanu, K., Pohl, J., Read, T.D., Bosinger, S.E., Trent, M.S., Burd, E.M. and Weiss, D.S. (2016) Antibiotic failure mediated by a resistant subpopulation in *Enterobacter cloacae*. *Nature Microbiology* 1 (6), 16053: <https://doi.org/10.1038/nmicrobiol.2016.53>
- 58 Hjort, K., Nicoloff, H. and Andersson, D.I. (2016) Unstable tandem gene amplification generates heteroresistance (variation in resistance within a population) to colistin in *Salmonella enterica*. *102* (2), 274-289: <https://doi.org/10.1111/mmi.13459>
- 59 Dewachter, L., Fauvart, M. and Michiels, J. (2019) Bacterial Heterogeneity and Antibiotic Survival: Understanding and Combatting Persistence and Heteroresistance. *Molecular Cell* 76 (2), 255-267: <https://doi.org/10.1016/j.molcel.2019.09.028>
- 60 Band, V.I. and Weiss, D.S. (2019) Heteroresistance: A cause of unexplained antibiotic treatment failure? *PLOS Pathogens* 15 (6), e1007726: <https://doi.org/10.1371/journal.ppat.1007726>
- 61 Sherman, E.X., Wozniak, J.E. and Weiss, D.S. (2019) Methods to Evaluate Colistin Heteroresistance in *Acinetobacter baumannii*. *Methods in molecular biology (Clifton, N.J.)* 1946, 39-50: https://doi.org/10.1007/978-1-4939-9118-1_4
- 62 El-Halfawy, O.M. and Valvano, M.A. (2015) Antimicrobial Heteroresistance: an Emerging Field in Need of Clarity. *Clinical Microbiology Reviews* 28 (1), 191-207: <https://doi.org/10.1128/cmr.00058-14>
- 63 Földes, A., Székely, E., Voidăzan, S.T. and Dobreanu, M. (2022) Comparison of Six Phenotypic Assays with Reference Methods for Assessing Colistin Resistance in Clinical Isolates of Carbapenemase-Producing Enterobacterales: Challenges and Opportunities. *Antibiotics* 11 (3), 377:
- 64 Rossi, E., La Rosa, R., Bartell, J.A., Marvig, R.L., Haagensen, J.A.J., Sommer, L.M., Molin, S. and Johansen, H.K. (2021) *Pseudomonas aeruginosa* adaptation and evolution in patients with cystic fibrosis. *Nature Reviews Microbiology* 19 (5), 331-342: <https://doi.org/10.1038/s41579-020-00477-5>
- 65 Yamaguchi, Y., Park, J.-H. and Inouye, M. (2011) Toxin-Antitoxin Systems in Bacteria and Archaea. *Annual Review of Genetics* 45 (1), 61-79: <https://doi.org/10.1146/annurev-genet-110410-132412>
- 66 Thisted, T., Sørensen, N.S., Wagner, E.G. and Gerdes, K. (1994) Mechanism of post-segregational killing: Sok antisense RNA interacts with Hok mRNA via its 5'-end single-stranded leader and competes with the 3'-end of Hok mRNA for binding to the mok translational initiation region. *Embo j* 13 (8), 1960-1968:
- 67 Deter, H., Jensen, R., Mather, W. and Butzin, N. (2017) Mechanisms for Differential Protein Production in Toxin–Antitoxin Systems. *Toxins* 9 (7) <https://doi.org/10.3390/toxins9070211>

- 68 Page, R. and Peti, W. (2016) Toxin-antitoxin systems in bacterial growth arrest and persistence. *Nature Chemical Biology* 12 (4), 208-214: <https://doi.org/10.1038/nchembio.2044>
- 69 Song, S. and Wood, T.K. (2020) A Primary Physiological Role of Toxin/Antitoxin Systems Is Phage Inhibition. *Frontiers in Microbiology* 11 <https://doi.org/10.3389/fmicb.2020.01895>
- 70 Fozo, E.M., Makarova, K.S., Shabalina, S.A., Yutin, N., Koonin, E.V. and Storz, G. (2010) Abundance of type I toxin-antitoxin systems in bacteria: searches for new candidates and discovery of novel families. *Nucleic Acids Res* 38 (11), 3743-3759: <https://doi.org/10.1093/nar/gkq054>
- 71 Al-Hinai, M.A., Fast, A.G. and Papoutsakis, E.T. (2012) Novel System for Efficient Isolation of Clostridium Double-Crossover Allelic Exchange Mutants Enabling Markerless Chromosomal Gene Deletions and DNA Integration. *Applied and Environmental Microbiology* 78 (22), 8112-8121: <https://doi.org/doi:10.1128/AEM.02214-12>
- 72 Sóki, J., Hedberg, M., Patrick, S., Bálint, B., Herczeg, R., Nagy, I., Hecht, D.W., Nagy, E. and Urbán, E. (2016) Emergence and evolution of an international cluster of MDR Bacteroides fragilis isolates. *Journal of Antimicrobial Chemotherapy* 71 (9), 2441-2448: <https://doi.org/10.1093/jac/dkw175>
- 73 Baaity, Z., von Loewenich, F.D., Nagy, E., Orosz, L., Burián, K., Somogyvári, F. and Sóki, J. (2022) Phenotypic and Molecular Characterization of Carbapenem-Heteroresistant Bacteroides fragilis Strains. *Antibiotics* 11 (5), 590:
- 74 Unterholzner, S.J., Poppenberger, B. and Rozhon, W. (2013) Toxin-antitoxin systems. *Mobile Genetic Elements* 3 (5), e26219: <https://doi.org/10.4161/mge.26219>
- 75 Drexler, H.G. and Uphoff, C.C. (2002) Mycoplasma contamination of cell cultures: Incidence, sources, effects, detection, elimination, prevention. *Cytotechnology* 39 (2), 75-90: <https://doi.org/10.1023/a:1022913015916>
- 76 Feng, N., Huang, X. and Jia, Y. (2019) Mycoplasma contamination affects cell characteristics and decreases the sensitivity of BV2 microglia to LPS stimulation. *Cytotechnology* 71 (2), 623-634: <https://doi.org/10.1007/s10616-019-00311-8>
- 77 Hoff, F.W., Hu, C.W., Qutub, A.A., Qiu, Y., Graver, E., Hoang, G., Chauhan, M., de Bont, E.S.J.M. and Kornblau, S.M. (2018) Mycoplasma contamination of leukemic cell lines alters protein expression determined by reverse phase protein arrays. *Cytotechnology* 70 (6), 1529-1535: <https://doi.org/10.1007/s10616-018-0244-2>
- 78 Benedetti, F., Davinelli, S., Krishnan, S., Gallo, R.C., Scapagnini, G., Zella, D. and Curreli, S. (2014) Sulfur compounds block MCP-1 production by Mycoplasma fermentans-infected macrophages through NF-κB inhibition. *Journal of Translational Medicine* 12 (1), 145: <https://doi.org/10.1186/1479-5876-12-145>
- 79 Yang, J., Craig Hooper, W., Phillips, D.J. and Talkington, D.F. (2003) Interleukin-1β responses to Mycoplasma pneumoniae infection are cell-type specific. *Microbial Pathogenesis* 34 (1), 17-25: [https://doi.org/https://doi.org/10.1016/S0882-4010\(02\)00190-0](https://doi.org/https://doi.org/10.1016/S0882-4010(02)00190-0)
- 80 Yuan, J.S., Reed, A., Chen, F. and Stewart, C.N. (2006) Statistical analysis of real-time PCR data. *BMC Bioinformatics* 7 (1), 85: <https://doi.org/10.1186/1471-2105-7-85>

- 81 Boggy, G.J. and Woolf, P.J. (2010) A mechanistic model of PCR for accurate quantification of quantitative PCR data. *PLoS One* 5 (8), e12355: <https://doi.org/10.1371/journal.pone.0012355>
- 82 Gibson, U.E., Heid, C.A. and Williams, P.M. (1996) A novel method for real time quantitative RT-PCR. *Genome Res* 6 (10), 995-1001: <https://doi.org/10.1101/gr.6.10.995>
- 83 Wong, M.L. and Medrano, J.F. (2005) Real-time PCR for mRNA quantitation. *BioTechniques* 39 (1), 75-85: <https://doi.org/10.2144/05391rv01>
- 84 Eszik, I., Lantos, I., Önder, K., Somogyvári, F., Burián, K., Endrész, V. and Virok, D.P. (2016) High dynamic range detection of Chlamydia trachomatis growth by direct quantitative PCR of the infected cells. *Journal of Microbiological Methods* 120, 15-22: <https://doi.org/https://doi.org/10.1016/j.mimet.2015.11.010>
- 85 Bogdanov, A., Janovák, L., Lantos, I., Endrész, V., Sebők, D., Szabó, T., Dékány, I., Deák, J., Rázga, Z., Burián, K. and Virok, D.P. (2017) Nonactivated titanium-dioxide nanoparticles promote the growth of Chlamydia trachomatis and decrease the antimicrobial activity of silver nanoparticles. *Journal of Applied Microbiology* 123 (5), 1335-1345: <https://doi.org/https://doi.org/10.1111/jam.13560>
- 86 Lantos, I., Virok, D.P., Mosolygó, T., Rázga, Z., Burián, K. and Endrész, V. (2018) Growth characteristics of Chlamydia trachomatis in human intestinal epithelial Caco-2 cells. *Pathogens and Disease* 76 (3) <https://doi.org/10.1093/femspd/fty024>
- 87 Párducz, L., Eszik, I., Wagner, G., Burián, K., Endrész, V. and Virok, D.P. (2016) Impact of antiseptics on Chlamydia trachomatis growth. *Letters in Applied Microbiology* 63 (4), 260-267: <https://doi.org/https://doi.org/10.1111/lam.12625>
- 88 Raffai, T., Burián, K., Janovák, L., Bogdanov, A., Hegemann, J.H., Endrész, V. and Virok, D.P. (2019) Vaginal Gel Component Hydroxyethyl Cellulose Significantly Enhances the Infectivity of Chlamydia trachomatis Serovars D and E. *Antimicrob Agents Chemother* 63 (1) <https://doi.org/10.1128/aac.02034-18>
- 89 Virok, D.P., Eszik, I., Mosolygó, T., Önder, K., Endrész, V. and Burián, K. (2017) A direct quantitative PCR-based measurement of herpes simplex virus susceptibility to antiviral drugs and neutralizing antibodies. *Journal of Virological Methods* 242, 46-52: <https://doi.org/https://doi.org/10.1016/j.jviromet.2017.01.007>
- 90 Jamal, W., Khodakhast, F.B., AlAzmi, A., Sóki, J., AlHashem, G. and Rotimi, V.O. (2020) Prevalence and antimicrobial susceptibility of enterotoxigenic extra-intestinal Bacteroides fragilis among 13-year collection of isolates in Kuwait. *BMC Microbiology* 20 (1), 14: <https://doi.org/10.1186/s12866-020-1703-4>
- 91 Fenyvesi, V.S., Urbán, E., Bartha, N., Abrók, M., Kostrzewa, M., Nagy, E., Minárovits, J. and Sóki, J. (2014) Use of MALDI-TOF/MS for routine detection of cfiA gene-positive Bacteroides fragilis strains. *Int J Antimicrob Agents* 44 (5), 474-475: <https://doi.org/10.1016/j.ijantimicag.2014.07.010>
- 92 Green, M.R. and Sambrook, J. (2012) *Molecular cloning : a laboratory manual*, Cold Spring Harbor Laboratory Press
- 93 Darling, A.E., Tritt, A., Eisen, J.A. and Facciotti, M.T. (2011) Mauve assembly metrics. *Bioinformatics* 27 (19), 2756-2757: <https://doi.org/10.1093/bioinformatics/btr451>

- 94 Clinical breakpoints for bacteria, 2019. *EUCAST*. Available from <http://www.eucast.org/>
- 95 Patel, J.B., Clinical and Laboratory Standards, I. (2018) *Performance standards for antimicrobial susceptibility testing*, Clinical and Laboratory Standards Institute
- 96 Baaity, Z., Breunig, S., Önder, K. and Somogyvári, F. (2019) Direct qPCR is a sensitive approach to detect *Mycoplasma* contamination in U937 cell cultures. *BMC Research Notes* 12 (1), 720: <https://doi.org/10.1186/s13104-019-4763-5>
- 97 Weinstein, M.P.C. and Laboratory Standards, I. (2019) *Performance standards for antimicrobial susceptibility testing M100-S29*
- 98 Sárvári, K.P., Sóki, J., Kristóf, K., Juhász, E., Miszt, C., Latkóczy, K., Melegh, S.Z. and Urbán, E. (2018) A multicentre survey of the antibiotic susceptibility of clinical *Bacteroides* species from Hungary. *Infectious Diseases* 50 (5), 372-380: <https://doi.org/10.1080/23744235.2017.1418530>
- 99 Sóki, J., Edwards, R., Hedberg, M., Fang, H., Nagy, E. and Nord, C.E. (2006) Examination of *cfiA*-mediated carbapenem resistance in *Bacteroides fragilis* strains from a European antibiotic susceptibility survey. *International Journal of Antimicrobial Agents* 28 (6), 497-502: <https://doi.org/https://doi.org/10.1016/j.ijantimicag.2006.07.021>
- 100 Rasmussen, B.A., Gluzman, Y. and Tally, F.P. (1990) Cloning and sequencing of the class B beta-lactamase gene (*ccrA*) from *Bacteroides fragilis* TAL3636. *Antimicrobial Agents and Chemotherapy* 34 (8), 1590-1592: <https://doi.org/doi:10.1128/AAC.34.8.1590>
- 101 Leitsch, D., Sóki, J., Kolarich, D., Urbán, E. and Nagy, E. (2014) A study on *Nim* expression in *Bacteroides fragilis*. *Microbiology* 160 (3), 616-622: <https://doi.org/10.1099/mic.0.074807-0>
- 102 Sydenham, T.V., Overballe-Petersen, S., Hasman, H., Wexler, H., Kemp, M. and Justesen, U.S. (2019) Complete hybrid genome assembly of clinical multidrug-resistant *Bacteroides fragilis* isolates enables comprehensive identification of antimicrobial-resistance genes and plasmids. *Microb Genom* 5 (11) <https://doi.org/10.1099/mgen.0.000312>
- 103 Lee, A.S., de Lencastre, H., Garau, J., Kluytmans, J., Malhotra-Kumar, S., Peschel, A. and Harbarth, S. (2018) Methicillin-resistant *Staphylococcus aureus*. *Nature Reviews Disease Primers* 4 (1), 18033: <https://doi.org/10.1038/nrdp.2018.33>
- 104 Stilger, K.L. and Sullivan, W.J., Jr. (2013) Elongator Protein 3 (Elp3) Lysine Acetyltransferase Is a Tail-anchored Mitochondrial Protein in *Toxoplasma gondii*. *Journal of Biological Chemistry* 288 (35), 25318-25329: <https://doi.org/10.1074/jbc.M113.491373>
- 105 Jurénas, D., Garcia-Pino, A. and Van Melder, L. (2017) Novel toxins from type II toxin-antitoxin systems with acetyltransferase activity. *Plasmid* 93, 30-35: <https://doi.org/https://doi.org/10.1016/j.plasmid.2017.08.005>
- 106 Brauner, A., Fridman, O., Gefen, O. and Balaban, N.Q. (2016) Distinguishing between resistance, tolerance and persistence to antibiotic treatment. *Nature Reviews Microbiology* 14 (5), 320-330: <https://doi.org/10.1038/nrmicro.2016.34>
- 107 Sethi, S., Shukla, R., Bala, K., Gautam, V., Angrup, A. and Ray, P. (2019) Emerging metronidazole resistance in *Bacteroides* spp. and its association with the *nim* gene: a study from North India. *Journal of Global Antimicrobial Resistance* 16, 210-214: <https://doi.org/https://doi.org/10.1016/j.jgar.2018.10.015>

- 108 Shafquat, Y., Jabeen, K., Farooqi, J., Mehmood, K., Irfan, S., Hasan, R. and Zafar, A. (2019) Antimicrobial susceptibility against metronidazole and carbapenem in clinical anaerobic isolates from Pakistan. *Antimicrobial Resistance & Infection Control* 8 (1)<https://doi.org/10.1186/s13756-019-0549-8>
- 109 Kouhsari, E., Mohammadzadeh, N., Kashanizadeh, M.G., Saghafi, M.M., Hallajzadeh, M., Fattahi, A., Ahmadi, A., Niknejad, F., Ghafouri, Z., Asadi, A. and Boujary Nasrabadi, M.R. (2019) Antimicrobial resistance, prevalence of resistance genes, and molecular characterization in intestinal *Bacteroides fragilis* group isolates. *Apmis* 127 (6), 454-461: <https://doi.org/10.1111/apm.12943>
- 110 Shenoy, P., Vishwanath, S. and Chawla, K. (2019) Antimicrobial resistance profile and Nim gene detection among *Bacteroides fragilis* group isolates in a university hospital in South India. *Journal of Global Infectious Diseases* 11 (2)https://doi.org/10.4103/jgid.jgid_116_18
- 111 Löfmark, S., Fang, H., Hedberg, M. and Edlund, C. (2005) Inducible Metronidazole Resistance and nim Genes in Clinical *Bacteroides fragilis* Group Isolates. *Antimicrobial Agents and Chemotherapy* 49 (3), 1253-1256: <https://doi.org/10.1128/aac.49.3.1253-1256.2005>
- 112 Sherwood, J.E., Fraser, S., Citron, D.M., Wexler, H., Blakely, G., Jobling, K. and Patrick, S. (2011) Multi-drug resistant *Bacteroides fragilis* recovered from blood and severe leg wounds caused by an improvised explosive device (IED) in Afghanistan. *Anaerobe* 17 (4), 152-155: <https://doi.org/10.1016/j.anaerobe.2011.02.007>
- 113 Sóki, J., Gal, M., Brazier, J.S., Rotimi, V.O., Urbán, E., Nagy, E. and Duerden, B.I. (2005) Molecular investigation of genetic elements contributing to metronidazole resistance in *Bacteroides* strains. *Journal of Antimicrobial Chemotherapy* 57 (2), 212-220: <https://doi.org/10.1093/jac/dki443>
- 114 Wehbe, K., Vezzalini, M. and Cinque, G. (2018) Detection of mycoplasma in contaminated mammalian cell culture using FTIR microspectroscopy. *Analytical and Bioanalytical Chemistry* 410 (12), 3003-3016: <https://doi.org/10.1007/s00216-018-0987-9>
- 115 Soheily, Z., Soleimani, M. and Majidzadeh-Ardebili, K. (2019) Detection of Mycoplasma Contamination of Cell Culture by A Loop-Mediated Isothermal Amplification Method. *Cell J* 21 (1), 43-48: <https://doi.org/10.22074/cellj.2019.5624>
- 116 Kotani, H. and McGarrity, G.J. (1986) Ureaplasma infection of cell cultures. *Infect Immun* 52 (2), 437-444: <https://doi.org/10.1128/iai.52.2.437-444.1986>
- 117 Volokhov, D.V., Graham, L.J., Brorson, K.A. and Chizhikov, V.E. (2011) Mycoplasma testing of cell substrates and biologics: Review of alternative non-microbiological techniques. *Molecular and Cellular Probes* 25 (2), 69-77: <https://doi.org/https://doi.org/10.1016/j.mcp.2011.01.002>
- 118 Molla Kazemiha, V., Amanzadeh, A., Memarnejadian, A., Azari, S., Shokrgozar, M.A., Mahdian, R. and Bonakdar, S. (2014) Sensitivity of biochemical test in comparison with other methods for the detection of mycoplasma contamination in human and animal cell lines stored in the National Cell Bank of Iran. *Cytotechnology* 66 (5), 861-873: <https://doi.org/10.1007/s10616-013-9640-9>
- 119 Molla Kazemiha, V., Bonakdar, S., Amanzadeh, A., Azari, S., Memarnejadian, A., Shahbazi, S., Shokrgozar, M.A. and Mahdian, R. (2016) Real-time PCR assay is superior to other methods for the detection of mycoplasma

- contamination in the cell lines of the National Cell Bank of Iran. *Cytotechnology* 68 (4), 1063-1080: <https://doi.org/10.1007/s10616-015-9862-0>
- 120 Wang, J., Pan, X. and Liang, X. (2016) Assessment for Melting Temperature Measurement of Nucleic Acid by HRM. *J Anal Methods Chem* 2016, 5318935: <https://doi.org/10.1155/2016/5318935>
- 121 Macgillivray, A.D. and McMullen, A.I. (1966) On the influence of ionic strength on the melting temperature of DNA. *Journal of Theoretical Biology* 12 (2), 260-265: [https://doi.org/10.1016/0022-5193\(66\)90117-2](https://doi.org/10.1016/0022-5193(66)90117-2)
- 122 Duguid, J.G., Bloomfield, V.A., Benevides, J.M. and Thomas, G.J. (1995) Raman spectroscopy of DNA-metal complexes. II. The thermal denaturation of DNA in the presence of Sr²⁺, Ba²⁺, Mg²⁺, Ca²⁺, Mn²⁺, Co²⁺, Ni²⁺, and Cd²⁺. *Biophysical Journal* 69 (6), 2623-2641: [https://doi.org/10.1016/S0006-3495\(95\)80133-5](https://doi.org/10.1016/S0006-3495(95)80133-5)
- 123 Walsh, T.R., Bolmström, A., Qwärnström, A., Ho, P., Wootton, M., Howe, R.A., MacGowan, A.P. and Diekema, D. (2001) Evaluation of Current Methods for Detection of Staphylococci with Reduced Susceptibility to Glycopeptides. *Journal of Clinical Microbiology* 39 (7), 2439-2444: <https://doi.org/10.1128/JCM.39.7.2439-2444.2001>
- 124 Brauner, A. and Balaban, N.Q. (2021) Quantitative biology of survival under antibiotic treatments. *Current Opinion in Microbiology* 64, 139-145: <https://doi.org/10.1016/j.mib.2021.10.007>
- 125 Van den Bergh, B., Fauvart, M. and Michiels, J. (2017) Formation, physiology, ecology, evolution and clinical importance of bacterial persisters. *FEMS Microbiology Reviews* 41 (3), 219-251: <https://doi.org/10.1093/femsre/fux001>
- 126 Durán, S.P., Kayser, F.H. and Berger-Bächi, B. (1996) Impact of sar and agr on methicillin resistance in Staphylococcus aureus. *FEMS Microbiology Letters* 141 (2-3), 255-260: <https://doi.org/10.1111/j.1574-6968.1996.tb08394.x>
- 127 Knobloch, J.K.-M., Jäger, S., Huck, J., Horstkotte, M.A. and Mack, D. (2005) mecA Is Not Involved in the B-Dependent Switch of the Expression Phenotype of Methicillin Resistance in Staphylococcus epidermidis. *Antimicrobial Agents and Chemotherapy* 49 (3), 1216-1219: <https://doi.org/10.1128/AAC.49.3.1216-1219.2005>
- 128 Cuirolo, A., Plata, K. and Rosato, A.E. (2009) Development of homogeneous expression of resistance in methicillin-resistant Staphylococcus aureus clinical strains is functionally associated with a β -lactam-mediated SOS response. *Journal of Antimicrobial Chemotherapy* 64 (1), 37-45: <https://doi.org/10.1093/jac/dkp164>
- 129 Medeiros, A.A. (1997) Editorial Response: Relapsing Infection Due to Enterobacter Species: Lessons of Heterogeneity. *Clinical Infectious Diseases* 25 (2), 341-342: <https://doi.org/10.1086/516918>
- 130 Katayama, Y., Murakami-Kuroda, H., Cui, L. and Hiramatsu, K. (2009) Selection of Heterogeneous Vancomycin-Intermediate *Staphylococcus aureus* by Imipenem. *Antimicrobial Agents and Chemotherapy* 53 (8), 3190-3196: <https://doi.org/10.1128/AAC.00834-08>
- 131 Anderson, S.E., Sherman, E.X., Weiss, D.S., Rather, P.N. and Dunman, P. (2018) Aminoglycoside Heteroresistance in Acinetobacter baumannii AB5075. *mSphere* 3 (4), e00271-00218: <https://doi.org/10.1128/mSphere.00271-18>
- 132 Schechter, L.M., Creely, D.P., Garner, C.D., Shortridge, D., Nguyen, H., Chen, L., Hanson, B.M., Sodergren, E., Weinstock, G.M., Dunne, W.M., Belkum, A.v., Leopold, S.R., Onderdonk, A.B., Musser, J. and Ledeboer, N. (2018)

- Extensive Gene Amplification as a Mechanism for Piperacillin-Tazobactam Resistance in *Escherichia coli*. *mBio* 9 (2), e00583-00518: <https://doi.org/doi:10.1128/mBio.00583-18>
- 133** Pournaras, S., Kristo, I., Vrioni, G., Ikonomidis, A., Poulou, A., Petropoulou, D. and Tsakris, A. (2010) Characteristics of Meropenem Heteroresistance in *Klebsiella pneumoniae* Carbapenemase (KPC)-Producing Clinical Isolates of *K. pneumoniae*. *Journal of Clinical Microbiology* 48 (7), 2601-2604: <https://doi.org/doi:10.1128/JCM.02134-09>
- 134** Ikonomidis, A., Tsakris, A., Kantzanou, M., Spanakis, N., Maniatis, A.N. and Pournaras, S. (2008) Efflux system overexpression and decreased OprD contribute to the carbapenem heterogeneity in *Pseudomonas aeruginosa*. *FEMS Microbiology Letters* 279 (1), 36-39: <https://doi.org/10.1111/j.1574-6968.2007.00997.x>
- 135** Engel, H., Mika, M., Denapaite, D., Hakenbeck, R., Mühlemann, K., Heller, M., Hathaway, L.J. and Hilty, M. (2014) A Low-Affinity Penicillin-Binding Protein 2x Variant Is Required for Heteroresistance in *Streptococcus pneumoniae*. *Antimicrobial Agents and Chemotherapy* 58 (7), 3934-3941: <https://doi.org/doi:10.1128/AAC.02547-14>

FINANCIAL SUPPORT

This research was supported by the Tempus Public Foundation- Stipendium Hungaricum Scholarship program 2017-2022, the Albert Szent-Györgyi Research Fund (Albert Szent-Györgyi Medical School, University of Szeged) and the RG Excellence Scholarship 2020-2022.

10. ACKNOWLEDGMENTS

This Ph.D. has been a truly life-changing experience for me, and it would not have been possible without the encouragement and support of many people.

I want to express my gratitude to my supervisors, **Dr. Somogyvári Ferenc** and **Dr. József Sóki**, for their support and guidance throughout my thesis. This thesis would not have been possible without their aid and assistance. Thank you for being my teachers, colleagues, and friends.

I would like to express my gratitude to **Dr. Katalin Burián**, head of the Department of Medical Microbiology, who has always been friendly and supportive since I moved to Hungary in 2017.

I have been privileged to work with some great colleagues; I would like to say thanks to **Prof. Dr. Ildikó Csóka**, **Dr. Dezső Virók**, **Dr. Gabriella Spengler**, **Dr. Tímea Mosolygó**, **Dr. Dávid Kókai**, **Dr. Anita Varga-Bogdanov** and all the other colleagues in the Department of Medical Microbiology.

I'm grateful to my colleagues in the Department of Clinical Microbiology for hosting me and being pleasant and helpful even during the rough days of the COVID-19 pandemic. Special appreciation goes to **Dr. László Orosz**, **Dr. Gabriella Terhes**, **Anikó Salaki**, **Melinda Varján**, and **Tímea Gönczöl**. Many thanks to Professor **Erzsébet Nagy** for offering her scientific experience and support.

I couldn't have accomplished so much without the loving support of my wife, parents, extended family, and friends. They celebrated my progress, gave me a pat on the back, and even cheered me up when I was down.

I'd like to express my gratitude to Hungary for providing me with this scholarship to pursue my doctoral studies. I'd also like to thank the Hungarian people for their kindness and hospitality during those years.

This Ph.D. thesis is dedicated to my lifelong friends Uncle Ali and Senan, who passed away during the period of this Ph.D.

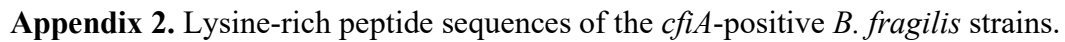
ANNEXES

I. Supplementary Materials

Appendix 1. Cross-correlation values of all strains of examined traits (from **Table 5**).

	X ₀ BHIS	bS PBS	bS BHIS	d PBS	d BHIS	AUC PBS	AUC BHIS	MIC B	MIC WC	HRI	IPase	<i>cfiA</i>	'GNAT'	'XAT'	'GNAT/ XAT'	n K	% K ^a
X ₀ PBS	0.477	-0.613 ^b	-0.477	0.29	0.594	0.916	0.873	0.932	0.924	0.519	0.96	0.669	0.695	0.457	0.227	0.256	0.366
	0.0809	0.0188	0.0809	0.301	0.0235	0.0000002	0.0000002	0.0000002	0.0000002	0.0537	0.0000002	0.00813	0.00507	0.0977	0.484	0.433	0.257
X ₀ BHIS		-0.725	0.125	0.177	0.281	0.625	0.721	0.578	0.523	0.345	0.538	0.143	0.108	0.183	-0.238	-0.081	-0.0931
		0.0018	0.648	0.514	0.3	0.0123	0.00196	0.0231	0.0429	0.199	0.0367	0.602	0.695	0.506	0.442	0.783	0.766
bS PBS			0.0679	-0.173	-0.396	-0.707	-0.779	-0.699	-0.685	-0.283	-0.699	-0.118	-0.47	-0.391	-0.126	0.11	0.0596
			0.802	0.532	0.138	0.00278	0.0000944	0.00326	0.00439	0.3	0.00326	0.667	0.0757	0.146	0.683	0.716	0.834
bS BHIS				-0.392	-0.327	-0.368	-0.382	-0.338	-0.308	-0.401	-0.437	-0.434	-0.652	-0.28	-0.545	-0.0663	-0.134
				0.142	0.23	0.171	0.154	0.209	0.257	0.134	0.101	0.104	0.00785	0.306	0.0623	0.834	0.667
d PBS					0.768	0.346	0.235	0.0807	0.00194	0.535	0.11	0.398	0.558	0.384	0.329	-0.487	-0.511
					0.0003	0.199	0.388	0.763	0.985	0.0382	0.686	0.138	0.0299	0.15	0.284	0.0998	0.0843
d BHIS						0.668	0.519	0.419	0.378	0.408	0.386	0.379	0.7	0.608	0.237	-0.528	-0.474
						0.00614	0.0463	0.117	0.158	0.127	0.15	0.158	0.00326	0.0158	0.442	0.0705	0.111
AUC PBS							0.9	0.804	0.759	0.57	0.824	0.437	0.663	0.43	0.294	-0.0663	0.0112
							0.0000002	0.000000	0.00048	0.0252	0.000000	0.101	0.00654	0.107	0.34	0.834	0.956
AUC BHIS								0.82	0.799	0.412	0.896	0.419	0.616	0.484	0.0559	0.0221	0.104
								0.0000002	0.0000002	0.124	0.0000002	0.117	0.0136	0.0662	0.852	0.939	0.733
MIC B									0.975	0.411	0.892	0.386	0.56	0.412	0.0497	0.247	0.329
									0.0000002	0.124	0.0000002	0.15	0.0287	0.124	0.869	0.429	0.284
MIC WC										0.341	0.908	0.422	0.543	0.412	-0.00352	0.319	0.413
										0.209	0.0000002	0.113	0.0353	0.124	0.974	0.295	0.173
HRI											0.443	0.477	0.591	0.369	0.172	-0.106	-0.166
											0.0946	0.0685	0.0192	0.171	0.572	0.733	0.588
IPase												0.626	0.68	0.532	0.035	0.434	0.521
												0.0123	0.00504	0.0397	0.904	0.15	0.0749
<i>cfiA</i>													0.547	0.493	-0.112	0.67	0.667
													0.0339	0.0597	0.716	0.0154	0.0169
'GNAT'														0.788	0.441	-0.155	-0.0745
														2×10 ⁻⁰⁷	0.143	0.619	0.8
'XAT'															-0.364	-0.125	-0.0968
															0.233	0.683	0.749
'GNAT/XAT'																-0.214	-0.156
																0.484	0.619
n K																	0.988
																	0.0000002

^a Abbreviations are the same as Table 5. ^b Different colors were used depending on the strength of the correlations: blue-green— $|r| \geq 0.85$ and $p = 0.0000002$; light green— $|r| \geq 0.7$ or $p < 0.01$; yellow— $|r| \geq 0.5$, or $p < 0.05$. Boxes marked with A–E indicate common relations and are discussed in the text.



Appendix 5. Etest MIC values of the test strains

<i>B. fragilis</i>	Ref.	MICs ^b											
		<i>AMP</i> ^c	<i>AMC</i>	<i>FOX</i>	<i>IPM</i>	<i>MPM</i>	ERY	CLM	<i>MOX</i>	MTZ	TET	TIG	CHL
Susceptible controls													
NCTC 9343	-	16	0.25	4	0.032	0.064	8	1	0.125	0.125	0.125	0.125	4
638R	-	2	0.25	0.064	0.032	0.032	0.5	0.25	0.25	0.125	0.064	0.032	2
D39		8^d	0.25	4	0.064	0.064	16	0.25	0.25	0.5	16	0.25	8
Silent/HR ^a													
7979	This study	>256	2	32	0.125	2	16	2	0.125	0.25	0.25	0.125	4
3130	This study	2	1	16	0.125	8-(32)	8	0.5	0.064	0.125	0.25	0.064	4
3035		1	1	8	0.125-(4)	2	128	2	0.125	0.25	8	0.25	4
SY69		1	1	16	0.25-(8)	2-(32)	16	2	2	0.125	8	0.125	4
CZE65		32		32	0.25-(1)	2-(8)	4	1	2	0.25	0.125	0.064	4
CZE60		32-(128)^e	8	32	1-(32)	>32	1-(8)	1	4-(16)	0.25	0.125	0.064	16
SLO8		>256	8	128	4-(>32)	>32	2	1	0.125	0.25	0.125	0.25	4
HR-ind ^a													
3130i5	This study	8	2	16	0.5-(16)	>32	16	1	0.064	0.032	0.125	0.064	4
CZE60i	This study	>256	8	64-(256)	>32 (4-(256)^f)	>32	1	1	2	0.25	0.125	0.064	16
With IS ^a													
De248514/19	This study	32	4	32	1-(8)	>32	8-(256)	2	0.125	0.125	16	0.5	4
1672		>256	8	128	>32 (8-(128)^f)	>32	8-(32)	2	0.25	0.5-(2)	16	1	8
TAL3636		>256	4-(16)	128	>32 (256^g)	>32	4	2	0.064	0.125	4	0.125	4

^a Silent/HR – silently or heterogeneously resistant, HR-ind – induced heteroresistant, with IS – IS element in the upstream region of the *cfiA* gene. ^b µg/ml. ^c AMP – ampicillin, AMC – amoxicillin/clavulanic acid, FOX – ceftiofur, IPM – imipenem, MPM – meropenem, ERY – erythromycin, CLM – clindamycin, MOX – moxifloxacin, MTZ – metronidazole, TET – tetracycline, TIG – tigecycline, CHL – chloramphenicol (bactericidal types are bold italic). ^d Resistant values are shown in bold. ^e Heteroresistance is shown by rust colour. ^f The IPM MICs were from MBL Etests. Resistant strains are bold. Strong HR range is in red.

II. OTHER PUBLICATIONS

• PRESENTATIONS AND ABSTRACTS RELATED TO THE TOPIC OF THE THESIS

➤ *Verbal presentations*

- I. Csajbók, D., Nagy, V., **Baaity, Z.**, Ferenc Somogyvári. (2019) ECCMID 29th: Rapid screening for the bacterial pathogens from serum in the case of sepsis., Amsterdam, Netherlands.
- II. **Baaity, Z.**, Somogyvári, F., and Sóki, J. (2020) EUGLOH 1st: (online) Challenging antibiotic resistance mechanisms in the 21st century – the case of *Bacteroides* spp. Szeged, Hungary.
- III. **Baaity, Z.**, Jamal, W., Rotimi, V.O., Burián, K., Leitsch, D., Somogyvári, F., Nagy, E. and Sóki, J. (2020) MMT 2020 (Hungarian Society for Microbiology) Metronidazole-resistant *Bacteroides* strains from Kuwait: a molecular study. Kecskemét, Hungary.

➤ *Poster and abstract presentations*

- I. **Baaity, Z.**, Jamal, W., Rotimi, V.O., Burián, K., Leitsch, D., Somogyvári, F., Nagy, E. and Sóki, J. (2020) ECCMID 30th: (Online) Molecular analysis of metronidazole resistant *Bacteroides* strains from Kuwait. Paris, France.
- II. **Baaity, Z.**, Burián, K., Somogyvári, F., Nagy, E. and Sóki, J. (2020) 15th Biennial Congress of the Anaerobe Society of the Americas (ASA): (Online) Investigations into the phenotypic characteristics and molecular mechanisms of the Heterogeneous carbapenem resistance of *Bacteroides fragilis* strains. Seattle, Washington USA.
- III. **Baaity, Z.**, Jamal, W., Rotimi, V.O., Burián, K., Leitsch, D., Somogyvári, F., Nagy, E. and Sóki, J. (2020) 15th Biennial Congress of the Anaerobe Society of the Americas (ASA): (Online) Molecular characterization of metronidazole resistant *Bacteroides* strains from Kuwait. Seattle, Washington USA.
- IV. **Baaity, Z.**, Nagy, E., Sóki, J. (2020) MMT 2020 (Hungarian Society for Microbiology): Phenotypic and molecular characterization of carbapenem heteroresistant *Bacteroides fragilis* strains. Kecskemét, Hungary.
- V. **Baaity, Z.**, Burián, K., Hamasalih, B., Nagy, E., and Sóki. (2021) ECCMID 31st (Online) Characterization of heteroresistance to imipenem in *Bacteroides fragilis* strains. Vienna, Austria.

• PRESENTATIONS AND ABSTRACTS NOT RELATED TO THE TOPIC OF THE THESIS

- I. Guet-Revillet H., Dumont Y., Justesen U., Boyer P., Morris T., Pranada A., Rompf C., Pierard D., Wybo I., Verdon R., Soki J., Gajdacs M., **Baaity Z.**, Jamal W., Rotimi V, Cordovana M., Foschi C., Assous M., Nurver U., Le Hello S., Parienti J., Join- Lambert O. (2021) ECCMID 31st (Online) and 41st French Convention of Antimicrobial Agents and Infectious Diseases, The burden and epidemiology of anaerobic bacteremia: a retrospective multicenter multinational ESGAI cross-sectional study. Paris, France.
- II. K. Dávid, P. Dóra, **Baaity Z.**, P. V. Dezső, E. Valéria, A. Rita, B. Renáta, and B. Katalin. (2021) 23rd Annual Conference of the European Society for Clinical Virology. Investigation of Antiviral Properties of Hyaluronic Acid. London, United Kingdom.
- III. Á. Visnyovszki, L. Orosz, B. Kintses, T. Stirling, B. M. Vásárhelyi, E. Ari, E. Kiss, B. Papp, G. Apjok, F. Vidovics, L. Lakatos, G. Lengyel, N. Ánosi, J. Sóki, **Baaity Z.**, E. Hajdú, and K. Burián. (2021) Magyar Infektológiai és Klinikai Mikrobiológiai Társaság 48. Kongresszusa. A Covid-19 Pandémiához Társulóan Előfordult Multirezisztens *Acinetobacter Baumannii* Törzsek Molekuláris Jellemzése. Debrecen, Magyarország.
- IV. M. Bakhtiyar, **Baaity Z.**, L. David, B. Katalin, N. Elisabeth, and S. József. (2021) 6th Central European Forum for Microbiology, CEFORM. Investigation of the same *NIM* Gene-Insertion Sequence Configurations on the Expression of the *NIM* Genes and Metronidazole Resistance of *Bacteroides fragilis* Strains. <https://doi.org/10.1556/030.68.2021.002>

RELATED ARTICLES


PUBLICATION I.

RESEARCH NOTE

Open Access



Direct qPCR is a sensitive approach to detect *Mycoplasma* contamination in U937 cell cultures

Zain Baaity¹, Sven Breunig², Kamil Önder² and Ferenc Somogyvári^{1*} 

Abstract

Objective: We aim to directly detect *Mycoplasma* DNA in a U937 suspension cell culture without using DNA purification. In order to make *Mycoplasma* contamination monitoring easier, we optimized a commercially available quantitative PCR (qPCR)-based detection kit. We compared the sensitivity of direct qPCR against qPCR with a purified DNA template.

Results: Our findings indicate that qPCR worked optimally with a 6 µl sample volume and a 52 °C annealing-extension temperature. We were able to decrease the annealing-extension step time from 60 to 20 s without any major decrease in reaction sensitivity. The total cycle time of optimized direct qPCR was 65 min. The optimized qPCR protocol was used to detect *Mycoplasma* DNA before and after DNA purification. Our findings indicate that direct qPCR had a higher sensitivity than regular qPCR. Ct levels produced by direct qPCR with 6 µl templates were almost identical to Ct levels produced by regular qPCR with DNA purified from a 60 µl cell culture sample (23.42 vs 23.49 average Ct levels, respectively). The optimized direct qPCR protocol was successfully applied to monitor the elimination of *Mycoplasma* contamination from U937 cell cultures.

Keywords: *Mycoplasma*, qPCR, PCR, Direct, Elimination

Introduction

Mycoplasma is a small cell-wall free prokaryotic bacterium with a remarkable diversity at the species level. Besides causing human respiratory and urogenital tract infections, *Mycoplasma* contamination of cell cultures is a frequent phenomenon. According to the DSMZ-German Collection of Microorganisms and Cell Cultures survey, the prevalence of *Mycoplasma* contamination of cell lines was 28% including *Mycoplasma* species *M. orale*, *M. hyorhinitis*, *M. arginini*, *M. fermentans*, *M. hominis* and *Acholeplasma laidlawii* [1]. *Mycoplasma* contamination may be introduced by cross-infection with a *Mycoplasma* positive cell line, laboratory personnel (e.g. *M. orale*) or by contaminated cell-culture reagents such as fetal bovine serum. Indeed, bovine *Mycoplasma* species *M. arginini* and *A. laidlawii* are frequent contaminating agents. *Mycoplasma* contamination is hard to

prevent/eradicate since the bacterium is less sensitive to antibiotics commonly applied in cell cultures. Its small size (0.3–1 µm) and non-rigid cell wall makes it also hard to remove by filtration. *Mycoplasma* infection has a pleiotropic effect on cellular physiology including altered metabolism, DNA, RNA and protein synthesis and pro- and anti-inflammatory effects [1–3]. U937 human monocytic cells, the cell-type used in this study, respond to the *Mycoplasma* infection by producing monocyte chemoattractant protein-1, matrix metalloproteinase-12 [4] and interleukin-1β [5].

The high probability of introducing novel *Mycoplasma* infections into cell cultures means it is necessary to monitor cell culture ingredients and cell lines for *Mycoplasma* contamination. There are a wide variety of detection methods available including metabolism detection and *Mycoplasma* genome detection by PCR and qPCR. Regular PCR has high sensitivity and specificity, but in the majority of cases requires nucleic acid purification and gel electrophoresis. qPCR eliminates the gel electrophoresis step, but regular qPCR protocols also include

*Correspondence: somogyvari.ferenc@med.u-szeged.hu

¹ Department of Medical Microbiology and Immunobiology, Faculty of Medicine, University of Szeged, Dóm sq. 10., Szeged 6720, Hungary
Full list of author information is available at the end of the article



nucleic acid purification. DNA purification can be a long and laborious procedure, especially if there are several samples to be purified. Direct PCR and direct qPCR eliminate the purification step, significantly shortening the protocol, but the inhibitory effect of the direct sample can be present. Previously, direct qPCR methods have been successfully applied to monitor *Chlamydia* and herpes simplex virus-2 growth and the antimicrobial effects of various compounds [6–11]. In this study, we want to leave out the DNA purification step and develop a direct qPCR detection method that is suitable to detect *Mycoplasma* contamination within U937 cell cultures.

Main text

Materials and methods

Cell culture

Mycoplasma infected U937 human monocytic cells were grown in an RPMI 1640 medium containing 10% heat-inactivated FBS (Sigma, St. Louis, MO, USA), and 50 µg/mL gentamicin at 37 °C in 5% CO₂, all within a 25 cm² cell culture flask (Greiner Bio-One Hungary, Mosonmagyaróvár, Hungary).

Mycoplasma elimination

Mycoplasma elimination was performed using *Mycoplasma* Elimination Reagent (Bio-Rad, Hercules, CA, USA). The reagent was added to the RPMI 1640 medium at a 0.5 µg/ml final concentration and the U937 cells were then cultured in this medium for 7 days.

DNA extraction and qPCR

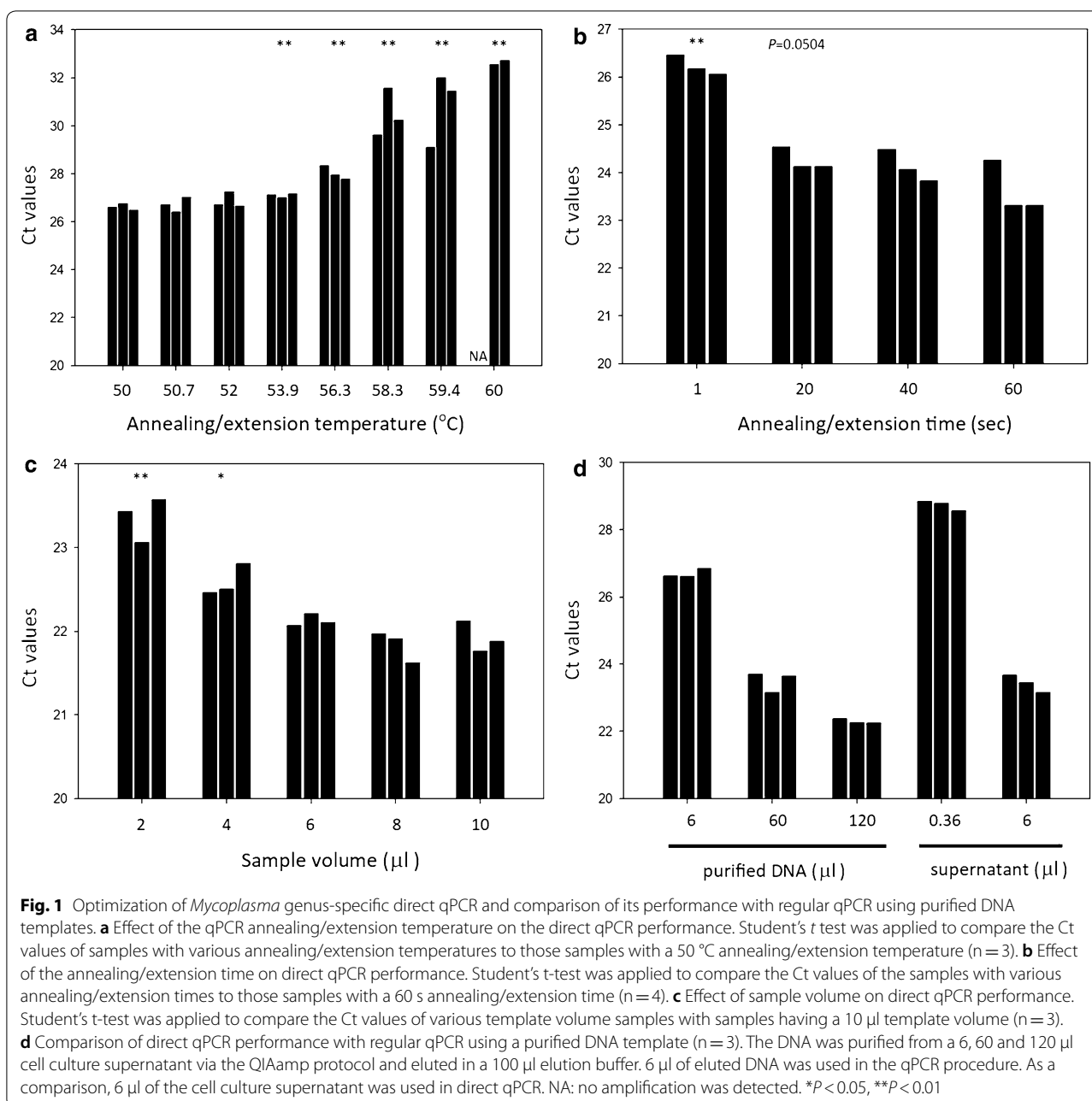
DNA was extracted from *Mycoplasma* infected U937 cell supernatants using the QiaGen QIAamp DNA Mini Kit (QiaGen, Hilden, Germany) according to the manufacturer's instructions. PhoenixDx[®] *Mycoplasma* Mix (Procomcure Biotech, Thalgau, Austria) was used in the qPCR experiments. qPCRs with 20 µl final volume were performed using the Bio-Rad CFX Connect qPCR real-time system. A statistical comparison of qPCR cycle threshold (Ct) values was performed with Student's *t* test, as described previously [12].

Results

To achieve optimal sensitivity and the shortest possible reaction time of direct qPCR, we followed a step-wise optimization of the PhoenixDx *Mycoplasma* Mix (Procomcure Biotech, Thalgau, Austria) protocol that was originally designed to amplify purified DNA samples. First, we tested the optimal annealing/extension temperature for detecting unpurified *Mycoplasma* DNA in *Mycoplasma*-infected U937 cell culture supernatants (Fig. 1a). The results indicated that reactions with 50–52 °C annealing/extension temperature produced

the lowest Ct values (26.84 ± 0.14 – 27.06 ± 0.26). We chose the 52 °C annealing/extension temperature for further tests. Next, we tested to see whether reducing the annealing/extension time might influence qPCR performance (Fig. 1b). Our findings showed that the 60 s annealing/extension time provided the lowest Ct values (23.56 ± 0.47), but the 20 and 40 s annealing/extension times led to only slightly higher Ct values (24.20 ± 0.23 , 24.11 ± 0.27 , respectively), which suggested that reducing the annealing/extension time from 60 to 20 s had a minimal influence on qPCR sensitivity. 20 s annealing/extension time was used for further qPCRs. Next, we tested the effect of sample volume on qPCR performance (Fig. 1c). The Ct levels of samples with 6 µl, 8 µl and 10 µl volumes of supernatants were similar (21.92–22.13 Ct value range), indicating that qPCR sensitivity is influenced by higher *Mycoplasma* DNA content and also by a higher level of qPCR inhibition in the 8 and 10 µl samples. In further experiments, we opted for the 6 µl sample volume. Finally, we compared the performance of direct qPCR and regular qPCR with purified DNA samples (Fig. 1d). The QIAamp DNA purification kit was used to isolate *Mycoplasma* DNA from U937 cell cultures (medium + cells). The elution volume was 100 µl. A comparison of the 6 µl direct sample volume and 6 µl purified sample was not possible as just 6 µl of the 100 µl total elution volume could be used during regular qPCR. Therefore we also decreased the 6 µl direct sample volume by a factor of 6/100 (0.36 µl). In a comparison of these samples we found that the 6 µl purified sample produced lower Ct values (~2 cycles) than the 0.36 µl direct sample, suggesting a low level of qPCR inhibition of the supernatant. However, when we compared the Ct levels of samples with 6 µl supernatant to the Ct levels of samples with purified DNAs we noticed that the Ct values produced with 6 µl supernatants were almost identical to those of the purified 60 µl supernatant (23.42 ± 0.26 , 23.49 ± 0.30 , respectively) indicating an altogether higher sensitivity of the direct qPCR.

As an application of optimized direct qPCR we monitored *Mycoplasma* elimination from the infected U937 cell culture. Our results showed that the supernatants (n=4) containing removal agent or free from removal agent both resulted in nearly the same Ct levels (27.04 ± 0.24 and 26.94 ± 0.45 , respectively) (Fig. 2a). This indicated that the presence of removal agent did not influence qPCR performance. *Mycoplasma* DNA dropped rapidly (by ~80%) after a 24-hour treatment (Fig. 2b). On the fourth day, *Mycoplasma* concentration was 2.3% of the original concentration. By the sixth day of treatment, *Mycoplasma* DNA was no longer detectable (data not shown). Overall, direct qPCR method proved

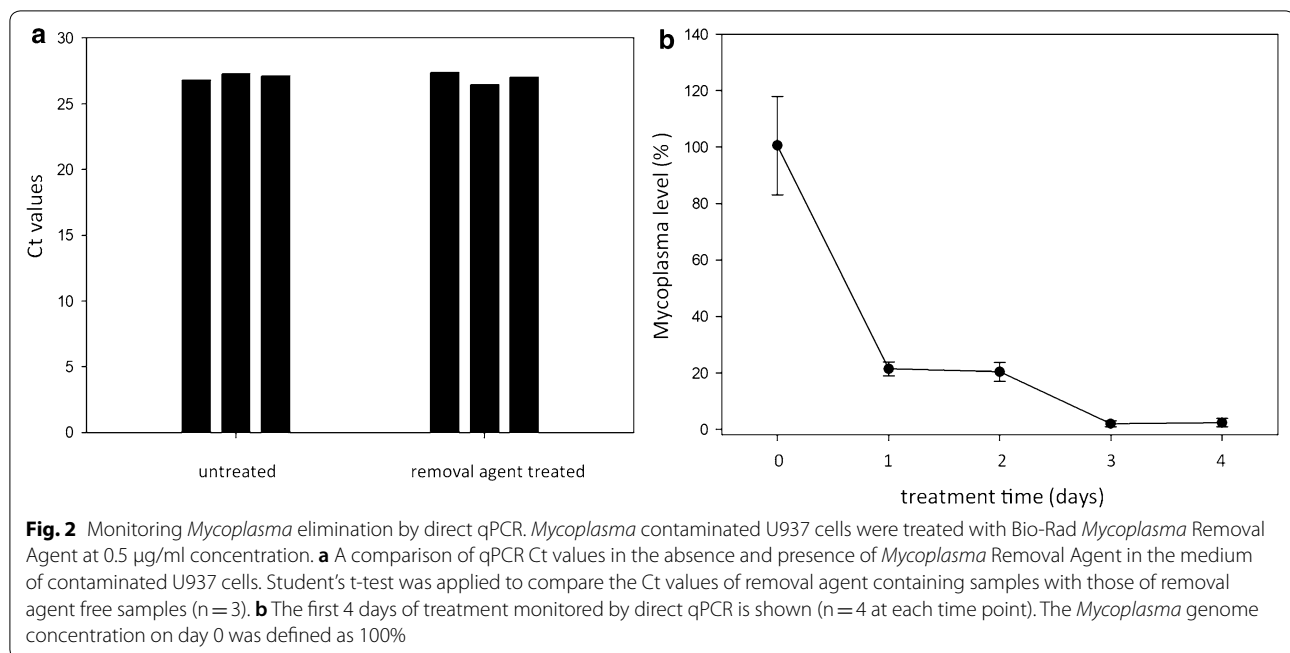


to be a quick and effective method for monitoring the decrease in *Mycoplasma* DNA during the elimination process.

Discussion

While various methods exist for the detection of *Mycoplasma* contamination [13, 14], probably the most frequently used ones are biochemical detection of *Mycoplasma* metabolism and PCR-based detection of *Mycoplasma* DNA. Though the biochemical detection of

mycoplasma ATP generation (Mycoalert (Lonza, Basel, Switzerland)) is a quick protocol, it has certain disadvantages that should be mentioned, including requiring that reagents be reconstituted and brought to 22 °C before each measurement and requiring a luminometer for ATP detection. Aspecificity due to ATP generated by other cells may lead to a high background and eventually false negative measurements. The *Ureaplasma* species which are also a common contaminant in a cell culture [15] cannot be detected by Mycoalert as their own ATP



production relies on the hydrolysis of urea [16]. Finally, the sensitivity of biochemical detection has been shown to be lower than that for PCR or qPCR methods [17, 18].

There are a variety of kits on offer based on regular PCR, followed by gel electrophoresis. The major advantage of these kits is the wide availability of regular PCR and electrophoresis equipment. However, decreased specificity compared to probe-based qPCR, the additional electrophoresis step, and the inability to quantitatively monitor the decrease in *Mycoplasma* genome concentration during treatment are clear drawbacks. Intercalation-based (e.g. SYBR Green) qPCR kits such as MycoSEQ *Mycoplasma* Detection Assay (Thermo Fisher, Waltham, MA, USA) eliminate the electrophoresis step and provide quantitative information about *Mycoplasma* genome concentration. The disadvantages of intercalation-based qPCR kits compared to probe-based kits are a lower specificity, lack of internal control and the potential effect of cell culture composition, ionic composition and ionic strength to change the melting temperature of the qPCR product [19–21]. Since this melting temperature is the basis for evaluating specificity in intercalation based qPCRs, changing it can be problematic. Probe-based qPCRs such as PhoenixDx (Procomcure Biotech, Thalgau, Austria), Microsart RESEARCH *Mycoplasma* (Sartorius, Goettingen, Germany) and qPCR Detection Kit (XpressBio, Frederick, MD, USA) avoid these problems and due the additional requirement of the binding of the probe sequence, these kits provide a higher specificity than regular PCRs and intercalation-based qPCRs.

Noting the advantages of probe-based qPCRs, we optimized the Procomcure PhoenixDx kit to perform a direct qPCR with a *Mycoplasma* infected U937 cell culture. Our results indicates that the optimal temperature was the same as that in the original protocol, so the primer + probe binding was not affected by the presence of the direct template. The fact that the optimal template volume was 6 µl (30% of the total qPCR volume) meant that the direct sample did not have a significant inhibitory effect on the qPCR. A major optimization step that we performed was decreasing the annealing/extension time from 60 s to 20 s, thus saving 40 s in each cycle. Interestingly, this decrease led to only a minor decrease in the sensitivity (~0.6 Ct level increase). In addition, decreasing the number of cycles from 50 to 40, reduced the total qPCR time required to 65 min. When we used the optimized qPCR protocol with direct and purified cell culture templates, we found that Ct levels of a 6 µl direct template was almost identical to that of purified DNA from a 60 µl cell culture. The reason for this is mainly due to a dilution of the original DNA content during the elution step at the end of DNA purification. Overall in our case, direct qPCR sensitivity was higher than qPCR with a purified template, with a saving in the cost/time of DNA purification. We monitored the elimination of *Mycoplasma* contamination from the U937 cell culture using the optimized direct qPCR protocol. One of the concerns using pathogen DNA detection is that the non-viable pathogen's DNA can also be detected and lead to a false positive signal. In our case however, the

Mycoplasma DNA content dropped to ~20% of the original concentration after 1 day of treatment, and though days 1 and 2 contained a similar level of DNA, this decrease continued on day 3. In summary, with direct qPCR we were able to monitor the elimination of *Mycoplasma* over the treatment period.

In conclusion, we optimized a probe-based qPCR to detect *Mycoplasma* contamination in a user-friendly manner. This direct qPCR method does not require a purification step, maintains sensitivity and offers a shorter 65 min protocol.

Limitations

While we did not observe a major qPCR inhibitory effect of U937 cell culture, it cannot be ruled out that components of other cell cultures may have an inhibitory effect. Most probe based qPCR kits, including the kit used here, contain an internal control (e.g. HEX-labelled probe), therefore the detection of qPCR inhibition (no FAM, no HEX signals) is straightforward. In the case of qPCR inhibition, dilution of the direct sample may be a solution for decreasing/eliminating qPCR inhibition.

Abbreviations

qPCR: quantitative PCR; Ct: cycle threshold.

Acknowledgements

Not applicable.

Authors' contributions

ZB: performed optimization experiments, was involved in preparing the manuscript and figures. FS: study design, performed optimization experiments, was involved in preparing the manuscript. SB: performed optimization experiments, was involved in preparing the manuscript. KÖ: involved in the study design, and preparing the manuscript. All authors read and approved the final manuscript.

Funding

This project, design of the study and the analysis was supported by the University of Szeged, Faculty of Medicine (Grant Number: Hetenyi-5S 575 A202). The publication of the article was supported by the University of Szeged Open Access Fund (MPL-USZ-BMCSO-0117).

Availability of data and materials

Not applicable.

Ethics approval and consent to participate

Not applicable.

Consent for publication

Not applicable.

Competing interests

The authors declare the following competing interests: SB and KÖ are employees of Procomure Biotech GmbH, the manufacturer of the PhoenixDx® *Mycoplasma* Mix.

Author details

¹ Department of Medical Microbiology and Immunobiology, Faculty of Medicine, University of Szeged, Dóm sq. 10., Szeged 6720, Hungary. ² Procomure Biotech GmbH, Breitwies 1, 5303 Thalgau, Austria.

Received: 19 September 2019 Accepted: 24 October 2019

Published online: 01 November 2019

References

- Drexler HG, Uphoff CC. Mycoplasma contamination of cell cultures: incidence, sources, effects, detection, elimination, prevention. *Cytotechnology*. 2002;39:75–90.
- Feng N, Huang X, Jia Y. Mycoplasma contamination affects cell characteristics and decreases the sensitivity of BV2 microglia to LPS stimulation. *Cytotechnology*. 2019;71:623–34.
- Hoff FW, Hu CW, Qutub AA, Qiu Y, Graver E, Hoang G, et al. Mycoplasma contamination of leukemic cell lines alters protein expression determined by reverse phase protein arrays. *Cytotechnology*. 2018;70:1529–35.
- Benedetti F, Davinelli S, Krishnan S, Gallo RC, Scapagnini G, Zella D, et al. Sulfur compounds block MCP-1 production by Mycoplasma fermentans-infected macrophages through NF-κB inhibition. *J Transl Med*. 2014;12:145.
- Yang J, Hooper WC, Phillips DJ, Talkington DF. Interleukin-1β responses to Mycoplasma pneumoniae infection are cell-type specific. *Microb Pathog*. 2003;34:17–25.
- Eszik I, Lantos I, Önder K, Somogyvári F, Burián K, Endrész V, et al. High dynamic range detection of Chlamydia trachomatis growth by direct quantitative PCR of the infected cells. *J Microbiol Methods*. 2016;120:15–22.
- Bogdanov A, Janovák L, Lantos I, Endrész V, Sebők D, Szabó T, et al. Nonactivated titanium-dioxide nanoparticles promote the growth of Chlamydia trachomatis and decrease the antimicrobial activity of silver nanoparticles. *J Appl Microbiol*. 2017;123:1335–45.
- Lantos I, Virok DP, Mosolygó T, Rázga Z, Burián K, Endrész V. Growth characteristics of Chlamydia trachomatis in human intestinal epithelial Caco₂ cells. *Pathog Dis*. 2018;76:fty024.
- Párducz L, Eszik I, Wagner G, Burián K, Endrész V, Virok DP. Impact of antiseptics on Chlamydia trachomatis growth. *Lett Appl Microbiol*. 2016;63:260–7.
- Raffai T, Burián K, Janovák L, Bogdanov A, Hegemann JH, Endrész V, et al. Vaginal gel component hydroxyethyl cellulose significantly enhances the infectivity of Chlamydia trachomatis serovars D and E. *Antimicrob Agents Chemother*. 2019;63:e02034–3018.
- Virok DP, Eszik I, Mosolygó T, Önder K, Endrész V, Burián K. A direct quantitative PCR-based measurement of herpes simplex virus susceptibility to antiviral drugs and neutralizing antibodies. *J Virol Methods*. 2017;242:46–52.
- Yuan JS, Reed A, Chen F, Stewart CN. Statistical analysis of real-time PCR data. *BMC Bioinform*. 2006;7:85.
- Wehbe K, Vezzalini M, Cinque G. Detection of mycoplasma in contaminated mammalian cell culture using FTIR microspectroscopy. *Anal Bioanal Chem*. 2018;410:3003–16.
- Soheily Z, Soleimani M, Majidzadeh-Ardebili K. Detection of mycoplasma contamination of cell culture by a loop-mediated isothermal amplification method. *Cell J*. 2019;21:43–8.
- Kotani H, McGarrity GJ. Ureaplasma infection of cell cultures. *Infect Immun*. 1986;52:437–44.
- Volokhov DV, Graham LJ, Brorson KA, Chizhikov VE. Mycoplasma testing of cell substrates and biologics: review of alternative non-microbiological techniques. *Mol Cell Probes*. 2011;25:69–77.
- Molla Kazemiha V, Amanzadeh A, Memarnejadian A, Azari S, Shokrgozar MA, Mahdian R, et al. Sensitivity of biochemical test in comparison with other methods for the detection of mycoplasma contamination in human and animal cell lines stored in the National Cell Bank of Iran. *Cytotechnology*. 2014;66:861–73.
- Molla Kazemiha V, Bonakdar S, Amanzadeh A, Azari S, Memarnejadian A, Shahbazi S, et al. Real-time PCR assay is superior to other methods for the detection of mycoplasma contamination in the cell lines of the National Cell Bank of Iran. *Cytotechnology*. 2016;68:1063–80.
- Duguid JG, Bloomfield VA, Benevides JM, Thomas GJ. Raman spectroscopy of DNA-metal complexes II The thermal denaturation of DNA in the presence of Sr²⁺, Ba²⁺, Mg²⁺, Ca²⁺, Mn²⁺, Co²⁺, Ni²⁺, and Cd²⁺. *Biophys J*. 1995;69:2623–41.

20. Wang J, Pan X, Liang X. Assessment for melting temperature measurement of nucleic acid by HRM. *J Anal Methods Chem*. 2016;2016:5318935.
21. MacGillivray AD, McMullen AI. On the influence of ionic strength on the melting temperature of DNA. *J Theor Biol*. 1966;12:260–5.

Publisher's Note

Springer Nature remains neutral with regard to jurisdictional claims in published maps and institutional affiliations.

Ready to submit your research? Choose BMC and benefit from:

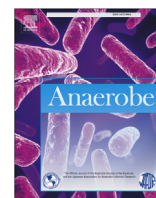
- fast, convenient online submission
- thorough peer review by experienced researchers in your field
- rapid publication on acceptance
- support for research data, including large and complex data types
- gold Open Access which fosters wider collaboration and increased citations
- maximum visibility for your research: over 100M website views per year

At BMC, research is always in progress.

Learn more biomedcentral.com/submissions



PUBLICATION II.



Antimicrobial susceptibility of anaerobic bacteria

Molecular characterization of metronidazole resistant *Bacteroides* strains from Kuwait

Zain Baaity ^{a, b}, Wafaa Jamal ^c, Vincent O. Rotimi ^c, Katalin Burián ^{a, b}, David Leitsch ^d,
Ferenc Somogyvári ^b, Elisabeth Nagy ^a, József Sóki ^{a, *}

^a Institute of Clinical Microbiology, Faculty of Medicine, University of Szeged, Szeged, Hungary

^b Department of Medical Microbiology and Immunobiology, Faculty of Medicine, University of Szeged, Szeged, Hungary

^c Department of Microbiology, Faculty of Medicine, University of Kuwait, Safat, Kuwait

^d Institute for Specific Prophylaxis and Tropical Medicine, Center for Pathophysiology, Infectiology and Immunology, Medical University of Vienna, Vienna, Austria

ARTICLE INFO

Article history:

Received 25 January 2021

Received in revised form

5 March 2021

Accepted 7 March 2021

Available online 11 March 2021

Handling Editor: Professor Boyanova
Lyudmila

Keywords:

Antibiotic resistance

Bacteroides

Kuwait

Metronidazole

nimE

ABSTRACT

Eleven metronidazole resistant *Bacteroides* and one newly classified *Phocaicola dorei* strain from Kuwait were investigated for their resistance mechanisms and the emergence of their resistant plasmids. All but one strain harbored *nimE* genes on differently sized plasmids. Of the 11 *nimE* genes, 9 were preceded by full copies of the prototype ISBf6 insertion sequence element, one carried a truncated ISBf6 and one was activated by an additional copy of IS612B. Nucleotide sequencing results showed that the *nimE* ISBf6 distances were constant and all five different plasmids shared a common region, suggesting that (i) the *nimE*-ISBf6 configuration was inserted into an undisclosed common genetic element, (ii) over time, this common element was mutated by insertions and deletions, spreading the resultant plasmids. Of the 10 *B. fragilis* strains in this collection, 6 were also *cfiA*-positive, one with full imipenem resistance, indicating a tendency for multidrug resistance (MDR) among such isolates. The significant number of metronidazole resistant *Bacteroides* spp. and *P. dorei* strains with the MDR phenotype warns of difficulties in treatment and suggests promoting adherence to antibiotic stewardship recommendations in Kuwait.

© 2021 Elsevier Ltd. All rights reserved.

1. Introduction

Bacteroides species are significant members of the normal human intestinal microbiota. They are also the most frequently isolated opportunistic anaerobic pathogens, causing endogenous soft-tissue infection and sometimes sepsis. By the number of resistance mechanisms and resistance prevalence against different classes of antibiotics, they are also the most antibiotic-resistant among anaerobic pathogens. Carbapenems, 5-nitroimidazoles, beta-lactams with beta-lactamase inhibitors and tigecycline are the most effective drugs in their treatment, together having frequencies of less than 10% resistance [1].

Despite its extensive use in anaerobic infections, metronidazole has shown excellent efficiency against *Bacteroides* spp. in antibiotic resistance surveys in different parts of the world. However, well-

characterized metronidazole resistant *Bacteroides* isolates have reached a significant number too. The best-known and most extensively examined resistance mechanism of *Bacteroides* against metronidazole is mediated by *nim* genes. These were first described between 1980 and 1990 and have since continued to gain more members [2]. Now we have 11 representatives (*nimA-K*) that bear approximately 50–70% amino acid homology among each other [2–6]. They are suspected to act by reducing the nitro moiety of 5-nitroimidazoles into hydroxylamine groups without producing the toxic radical intermediate which mediates the antimicrobial effect of metronidazole [2,7–9]. After more thorough investigation, *nim* genes were found to be preceded by insertion sequence (IS) elements whose function is to drive high expression of those same *nim* genes [2,10]. This is the case for other *Bacteroides* resistance genes, e.g., the carbapenem resistance *cfiA* gene [10]. However, strains with *nim* genes usually do not have high or stable MIC values for metronidazole, and the metronidazole MIC value of some *nimA*-positive strains does not correlate to the expression of *nimA* genes [11]. This latter finding brings the resistance mechanism mentioned

* Corresponding author. Institute of Clinical Microbiology, Faculty of Medicine, University of Szeged, 6725, Semmelweis 6, Szeged, Hungary.

E-mail address: soki.jozsef@med.u-szeged.hu (J. Sóki).

above into question, yet most identified metronidazole resistant *Bacteroides* strains harbor *nim* genes. They can be carried in small plasmids or in the chromosome - the association of chromosomal copies with *cfiA* genes has been described earlier [12]. The chromosomal *nimB* genes were also accompanied by the *cfiA* gene in an international cluster of multidrug-resistant *B. fragilis* strains [13]. Additionally, it is an intriguing and not fully understood phenomenon that *cfiA*-positive *B. fragilis* strains form a genetically well-separated group (Division II), clearly distinguishable with molecular typing methods, from *cfiA*-negative ones (Division I) [14–17]. Some former *Bacteroides* species, like *B. dorei*, *massiliensis*, *salanitronis* and *vulgatus*, were reclassified into the genus *Phocaeicola* (first established for *Phocaeicola abscessus* [18]) based on genomic similarity assessments [19]. Despite the excellent action of metronidazole on clinical *Bacteroides* isolates, overuse can significantly affect resistance rates. Regular antibiotic susceptibility surveys conducted in Europe demonstrated a north-south division in metronidazole resistance, in which the north showed lower resistance rates perhaps due to more prudent use of metronidazole [20,21]. Some reports have also shown some extreme metronidazole resistance values [22]. This study aims to establish a better understanding of the emergence and of the molecular mechanism causing resistance to metronidazole.

To this end, using phenotypic and molecular methods, we characterized the metronidazole resistant *Bacteroides* strains from an antibiotic resistance survey in Kuwait [23].

2. Materials and methods

2.1. Bacterial strains, cultivation, identification and antimicrobial susceptibility tests

Twelve metronidazole resistant strains (Table 1) were selected from the *Bacteroides/Phocaeicola* isolates examined in an antibiotic resistance survey in Kuwait [23]. The long-term storage and transfer of these strains from Kuwait to Hungary was done by lyophilization. The strains were revitalized in chopped-meat bouillon and long-term storage in Hungary was made in a 20%

glycerol-containing Brain-Heart Infusion (BHI) broth at -70°C . The species identification and determination of *B. fragilis* strains' genetic divisions were carried out by MALDI-TOF MS as described earlier [24]. Regular cultivation of the strains involved solid (Columbia agar supplemented with 10% defibrinated and 5% laked sheep blood, 0.3 g/l cysteine and 1 mg/l vitamin K₁) or liquid media (Brain-Heart Infusion broth supplemented with 0.5% yeast extract, 10 mg/l hemin and 1 mg/l vitamin K₁, BHIS) in anaerobiosis (85% N₂, 10% H₂ and 5% CO₂ in an anaerobic cabinet, Concept, Ruskin, UK) at 37°C . In Hungary, antimicrobial susceptibilities for metronidazole and imipenem were recorded by Etests as recommended by the supplier (bioMérieux).

2.2. PCR experiments

PCR template DNA was prepared by the boiling method. The *nim*, *cfiA* PCR reactions and the upstream region examination of both of *nim* and *cfiA* genes were assessed as described previously [13]. The types of *nim* genes were determined by capillary sequencing using the DTCS kit (Beckman Coulter) and the capillary sequencing instrument (GenomeLab GeXP Genetic Analysis System, Beckman Coulter) as recommended by the suppliers. Enterobacterial repetitive intergenic consensus PCR (ERIC-PCR) typing and evaluation were carried out as described earlier [13].

2.3. Plasmid screening, southern blotting and plasmid sequencing

The plasmid profiles of the test *Bacteroides* and *P. doeri* strains were determined by the alkaline-SDS lysis procedure as described earlier [25]. Their analysis was done in 0.7% agarose gels containing 0.5 µg/ml ethidium bromide in 0.5 TBE buffer using a 12 V/cm voltage gradient. For large-scale plasmid isolation, we used the QIAGEN Plasmid Midi Kit (Qiagen, Hilden, Germany). When Southern blotting, we transferred the plasmid DNA by capillary action to Hybond + nylon membranes [25]. The probe labeling, hybridization, and detection were carried out by North2South Labeling and Hybridization kits (Thermo Fisher Scientific). Permanent records of the gels and blots were done by the PXi gel

Table 1
Characterization of the metronidazole resistant strains from Kuwait.

No.	Species	MTZ MIC ₁ ^a (µg/ml)	MTZ MIC ₂ ^a (µg/ml)	<i>nim</i> gene	<i>nim</i> upstream IS ^b - ISBf6	plasmids (kb) ^c	IP MIC ^d (µg/ml)	DivII ^e <i>cfiA</i>	<i>cfiA</i> -up ^f
1	<i>Phocaeicola (Bacteroides) dorei</i>	>256	0.5	<i>nimE</i>	ΔISBf6 26bp	4.1, 5.3 (pPDQ1d), 51	0.25	n.a.	— n.a.
2	<i>Bacteroides thetaiotaomicron</i>	16	0.25	—	n.a.	n.t. ^e	0.125	n.a.	— n.a.
3	<i>Bacteroides fragilis</i>	>256	2	<i>nimE</i>	ISBf6 26bp	5.6, 8.3	0.064	—	— n.a.
4	<i>Bacteroides fragilis</i>	16	2	<i>nimE</i>	ISBf6 26bp	5.6, 8.3 , 66	0.125–(2) ^g	—	— n.a.
5	<i>Bacteroides fragilis</i>	>256	128–(>256) ^g	<i>nimE</i>	ISBf6 26bp	2.7, 4.1, 5.6, 10.7 , 41	0.125	+	+ 282 bp
6	<i>Bacteroides fragilis</i>	>256	128–(>256)	<i>nimE</i>	ISBf6 26bp	2.7, 4.1, 5.6, 10.7 (pBFQ6d), 46	0.5	—	— n.a.
7	<i>Bacteroides fragilis</i>	64	2	<i>nimE</i>	ISBf6 26bp	5.6, 8.3 , ~60	0.25	+	+ 282 bp
8	<i>Bacteroides fragilis</i>	32	2	<i>nimE</i>	ISBf6 26bp	5.6, 8.3 (pBFQ8b), ~60	0.25	+	+ 282 bp
9	<i>Bacteroides fragilis</i>	>256	8	<i>nimE</i>	ISBf6 26bp	4.1, 5.6, 8.3 , 11.0	0.5	+	+ 282 bp
10	<i>Bacteroides fragilis</i>	>256	16	<i>nimE</i>	ISBf6 26bp	2.7, 5.6, 9.3 (pBFQ10c)	> 32	+	+ 1.5 kb (IS613)
11	<i>Bacteroides fragilis</i>	>256	256	<i>nimE</i>	IS612C (ISBf6)	2.6, 5.6, 9.9 (pBFQ11c)	0.25–(8) ^g	+	+ 282 bp
12	<i>Bacteroides fragilis</i>	>256	2	<i>nimE</i>	ISBf6 26bp	5.6, 8.3	0.125	—	— n.a.

^a Metronidazole MICs measured in Kuwait (MTZ MIC₁) and in Hungary (MTZ MIC₂).

^b IS elements detected upstream of the *nimE* genes by PCR mapping or sequencing.

^c Plasmid profiles of the strains. Sizes are in kilobase pairs (kb). Plasmid hybridizing with the *nimE* probes are shown in bold, sequenced plasmid are in brackets.

^d Imipenem MICs.

^e MALDI-TOF MS typing results (n.a. – not applicable, n.t. – not tested).

^f The sizes of the *cfiA* upstream regions (IS613 was detected in *B. fragilis* Q10).

^g When heterogeneous resistance phenotype was experienced, the full inhibition zone is indicated and the disappearance of individual resistance colonies is indicated in parenthesis).

documentation system (Syngene, UK). The nucleotide sequences of the plasmids of *nim*-positive strains were determined on an Illumina platform and de novo assembly of plasmid sequences from preparations was done by the Lasergene 16 suite (DNASTar, Madison, USA). The sequences of *nim* gene-containing plasmids were deposited in GenBank under the following accession numbers: MW388914 (pPDQ1c), MW388913 (pBFQ6d), MW388915 (pBFQ8b), MW448185 (pBFQ10c) and MW448186 (pBFQ11c). The plasmid sequences were aligned using Mauve software [26].

3. Results

The strains were identified by MALDI-TOF MS, metronidazole and imipenem resistance values were determined by Etest (Table 1). The molecular resistance mechanisms and the possible emergence of the strains showed that all but one strain were *nim* gene-positive and nucleotide sequencing revealed that these to be the *nimE* type. Since *nimE* has been described as associated with the ISBf6 insertion sequence element [12,25,28], we carried out PCR detection and PCR mapping of ISBf6 in the *nimE* genes. Among the 11 *nimE*-positive strains, 10 carried ISBf6 that could be mapped to the upstream region of the *nimE* genes. Subsequent sequencing of *nimE*-ISBf6 via PCR-mapping showed that the distance between these elements was a constant 26 bp. We determined the plasmid profiles of the *nimE*-positive strains, and by Southern blotting, the *nimE* carrying plasmids were detected (data not shown). Although only one *nimE* plasmid type has been described to date, in our Southern blots, we detected 5 different *nimE* plasmids. One representative of each of the different sized plasmids was also sequenced by high-throughput sequencing. The exact sizes of these plasmids were: 5364 bp (pPDQ1d), 10711 bp (pBFQ6d), 8331 bp (pBFQ8b), 9322 bp (pBFQ10c), and 9932 bp (pBFQ11c) (see also Table 1). All proved to harbor one copy of the *nimE* gene and using

Mauve alignment, all were shown to be related (Fig. 1), implying a common origin. From the plasmid sequences obtained, we could also deduce that ISBf6 is present in pPDQ1d in truncated form and in pBFQ11c with an internal insertion of IS612B.

A high prevalence of *cfiA* ($n = 6$, 60%), by PCR and MALDI-TOF MS typing, was encountered among the *B. fragilis* strains. Among these, one was resistant to imipenem and in its upstream region of the *cfiA* gene, an insertion sequence element (IS613) was detected. All the other *cfiA*-positive strains were 'silent' (Table 1). Because of the similarities of the 5 *nimE* plasmids with different sizes and the high prevalence of *cfiA*-positive strains among the *nimE*-positives, we also carried out genetic typing of the 10 *nimE*-positive *B. fragilis* strains by ERIC PCR. This showed that the *cfiA*-negative ones belonged to Division I and all the *cfiA*-positives belonged to Division II. However, in this latter case, they were different from the earlier described *nimB*-*cfiA*-positive '*B. fragilis* BF8 MDR cluster' (Fig. S1) [13].

4. Discussion

This study characterized 12 metronidazole resistant *Bacteroides* and *P. doeri* strains from Kuwait, in which the initial antibiotic susceptibility survey detected a 4% prevalence of metronidazole resistance across the country [23]. This figure is high compared to the resistance prevalent in northern countries but is in the described range for countries south of Europe [22,29–31]. Essentially, non-prudent use of metronidazole can be held responsible for this phenomenon.

However, further phenotypic and molecular characterization of these strains at the Szeged laboratory showed that metronidazole MICs were lower than those detected in most strains in Kuwait. In our view, this is not unexpected as it has been experienced before, that in other strains MICs can change through metronidazole induction or withdrawal [32], or the same *nimB* or *nimE* genes with

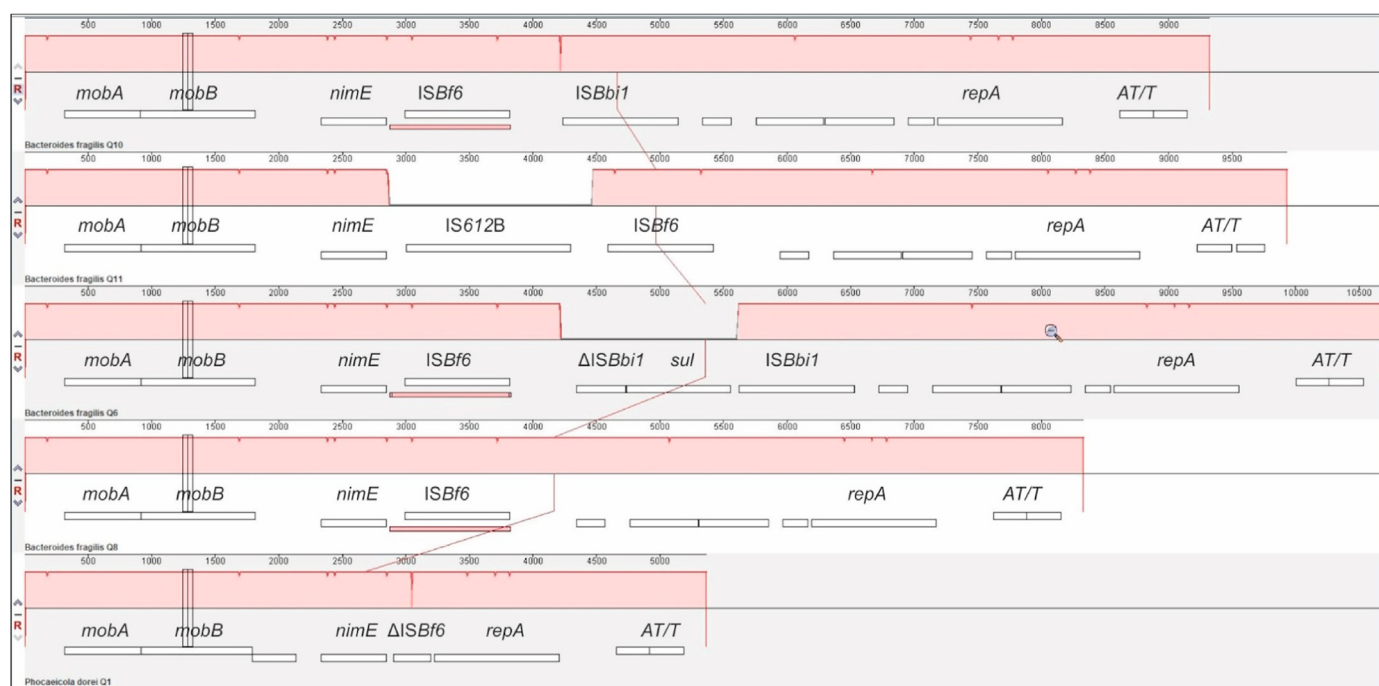


Fig. 1. The full backbone alignment of the five different *nimE* plasmids.

The harboring strains are indicated in the lower-left corners and the homology rates (>0–100%) are marked in pink. Rectangles on the bottoms mark the ORFs of the different plasmids: *mobA* and *mobB* – mobilization protein genes, *nimE* – *nimE* metronidazole resistance gene, Δ ISBf6 – truncated ISBf6, Δ ISBb1 – truncated ISBb1 (*Bifidobacterium bifidum* IS), *sul* – Sulfonamide resistance gene, *repA* – replication initiation protein, *TA/T* – antitoxin-toxin addition system/plasmid stability antitoxin toxin pairs (hypothetical ORFs are not marked with gene names). (For interpretation of the references to colour in this figure legend, the reader is referred to the Web version of this article.)

the same IS elements with constant distances give rise to different metronidazole MICs as it has also been described earlier by SÓki *et al.* [13] or what we encountered in this study. We reported in an earlier study that sometimes the metronidazole MIC of *nim*-positive *Bacteroides* strains does not correlate with *nim* gene expression [11]. This phenomenon is under further investigation in our laboratories. However, since almost all strains that had resistance in Kuwait were *nim* gene-positive, we still expect a functional role for *nim* genes in metronidazole resistance. We also found a highly imipenem resistant strain (*B. fragilis* Q10) for which we have a good explanation – an IS element, IS613, was carried in the upstream region also found for other highly imipenem resistant strains [10]. So for the regulation of *cfiA* and *nim* genes, variations can be suspected.

The *nim* gene typing by sequencing also showed that the 11 *nim* positive strains harbored the *nimE* type, which is also characteristic of strains in southern countries. The *nimE* gene was found predominantly in metronidazole resistant *Bacteroides* strains in India [22,31], Afghanistan [27], and in an earlier report for Kuwait [12].

All these 11 *nimE* genes were located on plasmids, six with the same characteristic size (8.3 kb) described earlier for *nimE* plasmids [12,27,28]. Of the other five, one was much smaller in size (5.3 kb), and the other four (three variants) larger (9.3, 9.9 and 10.7 kb), than the prototypic 8.3 kb. Of the 11 *nimE* genes, 9 harbored ISBf6 in their upstream region, while the other two had a truncated ISBf6 or IS612B in their upstream regions, proving the necessity of an IS for the expression of *nimE* genes. Additionally, the plasmid backbones seemed to share large segments of common DNA sequences (Fig. 1, pink bars). Where we could PCR-map the ISBf6 element to the *nimE* genes (using the PCR mapping or the full plasmid sequences), their distances were constant (26 bp). This implied to us that there was no independent insertion of ISBf6 in the different plasmids, but rather a preformed *nimE*-ISBf6 configuration inserted into a plasmid, and that then mutated and spread later as suggested in SÓki *et al.* [12]. This is also supported by the fact that these *nimE* plasmids had a common backbone despite some variance. Of these, the most notable are pPDQ1c and pBFQ11c where only a sub-segment of ISBf6 and IS612B respectively were in the upstream regions of the *nimE* genes. This origin hypothesis can be discussed together with earlier findings: (i) that chromosomal *nim* gene carrying strains tend to also harbor the *cfiA* gene [12] and (ii) that some such strains (*nimB*, *cfiA*, IS1186 and IS4351 coincidentally positive, '*B. fragilis* BF8 multidrug-resistant cluster') are genetically related [13]. In our case, the *cfiA* positivity was very high (60%) among the *nimE* positive *B. fragilis* strains. ERIC PCR typing confirmed that our *cfiA*-negative strains belonged to Division I and *cfiA*-positive strains belonged to Division II. The strains did not have a common origin to indicate the mobility and horizontal transfer of these plasmids. The *nimE* and *cfiA*-positive strains were different from the '*B. fragilis* BF8 multidrug-resistant cluster' as shown by ERIC typing (Fig. S1), indicating that they emerged from a different background. Additionally, the association between *nim* and *cfiA* genes invites further investigation, crucially in terms of multidrug-resistance phenotypes. One of our *nimE* and *cfiA*-positive strains was highly imipenem resistant and all of our strains can be regarded as multidrug resistant (Table S1) to at least three groups of antibiotics (most β -lactams, clindamycin and metronidazole).

As a summary, we can say that: (i) in Kuwait, similarly other southern countries, there is a considerable resistance rate to metronidazole and the resistance mechanism is plasmid-carried *nimE* genes preceded by IS-provided promoters, (ii) the *nimE* genes are carried on differently sized plasmids of common origin where the *nimE*-ISBf6 configuration emerged first and (iii) the majority of the *nimE*-positive strains also carry the *cfiA* gene together causing severe issues linked to multidrug-resistance.

Financial support

This study was supported by grants from the National Research, Development and Innovation Office of Hungary (ANN_130760), the Gedeon Richter Talent Foundation and gained partial support from GINOP-2.3.2-15-2016-00006, GINOP-2.3.2-15-2016-00011 and GINOP-2.3.2-15-2016-00012. The GINOP grants were funded by the European Regional Development Fund of the European Union and managed in the framework of the Economic Development and Innovation Operational Programme by the Ministry of National Economy, National Research, Development and Innovation Office, Budapest, Hungary.

Declaration of competing interest

We declare no conflict of interests.

Acknowledgments

We gratefully acknowledge the technical assistance rendered by May Shahin, who carried out the susceptibility testing in Kuwait.

Appendix A. Supplementary data

Supplementary data to this article can be found online at <https://doi.org/10.1016/j.anaerobe.2021.102357>.

References

- [1] H.M. Wexler, *Bacteroides: the good, the bad and the nitty-gritty*, Clin. Microbiol. Rev. 20 (4) (2007) 593–621.
- [2] C. Alauzet, A. Lozniewski, H. Marchandin, Metronidazole resistance and *nim* genes in anaerobes: a review, Anaerobe 55 (2019) 40–53.
- [3] C. Alauzet, *et al.*, *nimH*, a novel nitroimidazole resistance gene contributing to metronidazole resistance in *Bacteroides fragilis*, J. Antimicrob. Chemother. 72 (9) (2017) 2673–2675.
- [4] C. Alauzet, *et al.*, Metronidazole resistance in *Prevotella* spp. and description of a new *nim* gene in *Prevotella baroniae*, Antimicrob. Agents Chemother. 54 (1) (2010) 60–64.
- [5] F. Husain, *et al.*, Two multidrug-resistant clinical isolates of *Bacteroides fragilis* carry a novel metronidazole resistance *nim* gene (*nimJ*), Antimicrob. Agents Chemother. 57 (8) (2013) 3767–3774.
- [6] A.C.M. Veloo, *et al.*, Three metronidazole-resistant *Prevotella bivia* strains harbour a mobile element, encoding a novel *nim* gene, *nimK*, and an efflux small MDR transporter, J. Antimicrob. Chemother. 73 (10) (2018) 2687–2690.
- [7] H.K. Leiros, *et al.*, Structural basis of 5-nitroimidazole antibiotic resistance: the crystal structure of NimA from *Deinococcus radiodurans*, J. Biol. Chem. 279 (53) (2004) 55840–55849.
- [8] H.K. Leiros, C. Tedesco, S.M. McSweeney, High-resolution structure of the antibiotic resistance protein NimA from *Deinococcus radiodurans*, Acta Crystallogr. Sect. F Struct. Biol. Cryst. Commun. 64 (Pt 6) (2008) 442–447.
- [9] H.K. Leiros, B.O. Brandsdal, S.M. McSweeney, Biophysical characterization and mutational analysis of the antibiotic resistance protein NimA from *Deinococcus radiodurans*, Biochim. Biophys. Acta 1804 (4) (2010) 967–976.
- [10] J. SÓki, Extended role for insertion sequence elements in the antibiotic resistance of *Bacteroides*, World J. Clin. Infect. Dis. 3 (1) (2013) 1–12.
- [11] D. Leitsch, *et al.*, A study on *Nim* expression in *Bacteroides fragilis*, Microbiology (United Kingdom) 160 (PART 3) (2014) 616–622.
- [12] J. SÓki, *et al.*, Molecular investigation of genetic elements contributing to metronidazole resistance in *Bacteroides* strains, J. Antimicrob. Chemother. 57 (2006) 212–220. Journal Article.
- [13] J. SÓki, *et al.*, Emergence and evolution of an international cluster of MDR *Bacteroides fragilis* isolates, J. Antimicrob. Chemother. 71 (9) (2016) 2441–2448.
- [14] I. Podglajen, J. Breuil, I. Casin, E. Collatz, Genotypic identification of two groups within the species *Bacteroides fragilis* by ribotyping and by analysis of PCR-generated fragment patterns and insertion sequence content, J. Bacteriol. 177 (1995) 5270–5275.
- [15] R. Ruimy, I. Podglajen, J. Breuil, R. Christen, E. Collatz, A recent fixation of *cfiA* genes in a monophyletic cluster of *Bacteroides fragilis* is correlated with the presence of multiple insertion elements, J. Bacteriol. 178 (1996) 1914–1918.
- [16] M. Gutacker, C. Valsangiacome, J.-C. Piffaretti, Identification of two genetic groups in *Bacteroides fragilis* by multilocus enzyme electrophoresis: distribution of antibiotic resistance (*cfiA*, *cepA*) and enterotoxin (*bft*) encoding genes, Microbiology 146 (2000) 1241–1254.
- [17] I. Wybo, *et al.*, Differentiation of *cfiA*-negative and *cfiA*-positive *Bacteroides*

- fragilis isolates by matrix-assisted laser desorption ionization-time of flight mass spectrometry, *J. Clin. Microbiol.* 49 (5) (2011) 1961–1964.
- [18] M. Al Masalma, D. Raoult, V. Roux, *Phocaeicola abscessus* gen. nov., sp. nov., an anaerobic bacterium isolated from a human brain abscess sample, *Int. J. Syst. Evol. Microbiol.* 59 (9) (2009) 2232–2237.
- [19] M. García-López, et al., Analysis of 1,000 type-strain genomes improves taxonomic classification of bacteroidetes, *Front. Microbiol.* 10 (2019) 2083.
- [20] M. Hedberg, et al., Antimicrobial susceptibility of *Bacteroides fragilis* group isolates in Europe, *Clin. Microbiol. Infect.* 9 (6) (2003) 475–488.
- [21] E.U.E. Nagy, C.E. Nord, on behalf of the Escmid Study Group on Antimicrobial Resistance in Anaerobic Bacteria, Antimicrobial susceptibility of *Bacteroides fragilis* group isolates in Europe 20 years of experience, *Clin. Microbiol. Infect.* 17 (3) (2011) 371–379.
- [22] S. Sethi, et al., Emerging metronidazole resistance in *Bacteroides* spp. and its association with the nim gene: a study from North India, *J. Glob. Antimicrob. Resist.* 16 (2019) 210–214.
- [23] W. Jamal, et al., Prevalence and antimicrobial susceptibility of enterotoxigenic extra-intestinal *Bacteroides fragilis* among 13-year collection of isolates in Kuwait, *BMC Microbiol.* 20 (1) (2020) 14.
- [24] V.S. Fenyvesi, et al., Use of MALDI-TOF/MS for routine detection of *cfiA* gene-positive *Bacteroides fragilis* strains, *Int. J. Antimicrob. Agents* 44 (5) (2014) 474–475.
- [25] Sambrook, J., E.F. Fritsch, and T. Maniatis, *Molecular Cloning: A Laboratory Manual*. Cold Spring Harbor, NY: Cold spring Harbor Laboratory Press.
- [26] A.E. Darling, et al., Mauve assembly metrics, *Bioinformatics* 27 (19) (2011) 2756–2757.
- [27] J.E. Sherwood, et al., Multi-drug resistant *Bacteroides fragilis* recovered from blood and severe leg wounds caused by an improvised explosive device (IED) in Afghanistan, *Anaerobe* 17 (4) (2011) 152–155.
- [28] T.V. Sydenham, et al., Complete hybrid genome assembly of clinical multidrug-resistant *Bacteroides fragilis* isolates enables comprehensive identification of antimicrobial-resistance genes and plasmids, *Microb. Genom.* 5 (11) (2019).
- [29] Y. Shafquat, et al., Antimicrobial susceptibility against metronidazole and carbapenem in clinical anaerobic isolates from Pakistan, *Antimicrob. Resist. Infect. Contr.* 8 (2019) 99.
- [30] E. Kouhsari, et al., Antimicrobial resistance, prevalence of resistance genes, and molecular characterization in intestinal *Bacteroides fragilis* group isolates, *Apmis* 127 (6) (2019) 454–461.
- [31] S. Vishwanath, P.A. Shenoy, K. Chawla, Antimicrobial resistance profile and nim gene detection among *Bacteroides fragilis* group isolates in a university hospital in south India, *J. Global Infect. Dis.* 11 (2) (2019) 59–62.
- [32] S. Löfmark, et al., Inducible metronidazole resistance and nim genes in clinical *Bacteroides fragilis* group isolates, *Antimicrob. Agents Chemother.* 49 (3) (2005) 1253–1256.

Supplementary material

Table S1. Antibigrams and isolation of the test strains.

No.	Organism	SPECIMEN	XL	CM	MP	MZ	PG	PP	PTC	FOX	TGC	HOSPITAL
1	<i>P. dorei</i>	Wound swab	> 256	> 256	1	> 256	> 256	> 256	32	16	-	MAK
2	<i>B. thetaiotaomicron</i>	Wound swab	> 256	> 256	0.125	16	64	> 256	16	32	-	MAK
3	<i>B. fragilis</i>	Wound swab	0.5	0.5	0.5	> 256	> 256	> 256	-	128	-	MAK
4	<i>B. fragilis</i>	Pus swab	0.25	> 256	0.25	16	32	32	-	4	-	MAK
5	<i>B. fragilis</i>	Swab	32	2	8	> 256	> 256	> 256	-	64	-	AMIRI
6	<i>B. fragilis</i>	Pus swab	8	> 256	1	> 256	> 256	> 256	-	8	8	MAK
7	<i>B. fragilis</i>	Perianal tissue	32	> 256	8	64	> 256	> 256	-	32	4	AMIRI
8	<i>B. fragilis</i>	Pus swab	16	> 256	8	32	> 256	> 256	-	32	4	AMIRI
9	<i>B. fragilis</i>	Peritoneal fluid	2	> 256	4	> 256	> 256	> 256	-	64	16	MAK
10	<i>B. fragilis</i>	Pus swab	> 256	> 256	> 32	> 256	> 256	> 256	-	> 256	2	MAK
11	<i>B. fragilis</i>	Pus fluid	> 256	> 256	> 32	> 256	> 256	> 256	-	32	8	MAK
12	<i>B. fragilis</i>	Blood	16	> 256	0.5	> 256	> 256	> 256	-	8	4	AMIRI

XL amoxicillin/clavulanic acid

CM clindamycin

MP meropenem

MZ metronidazole

pp piperacillin

PTC piperacillin/tazobactam

FOX cefoxitin

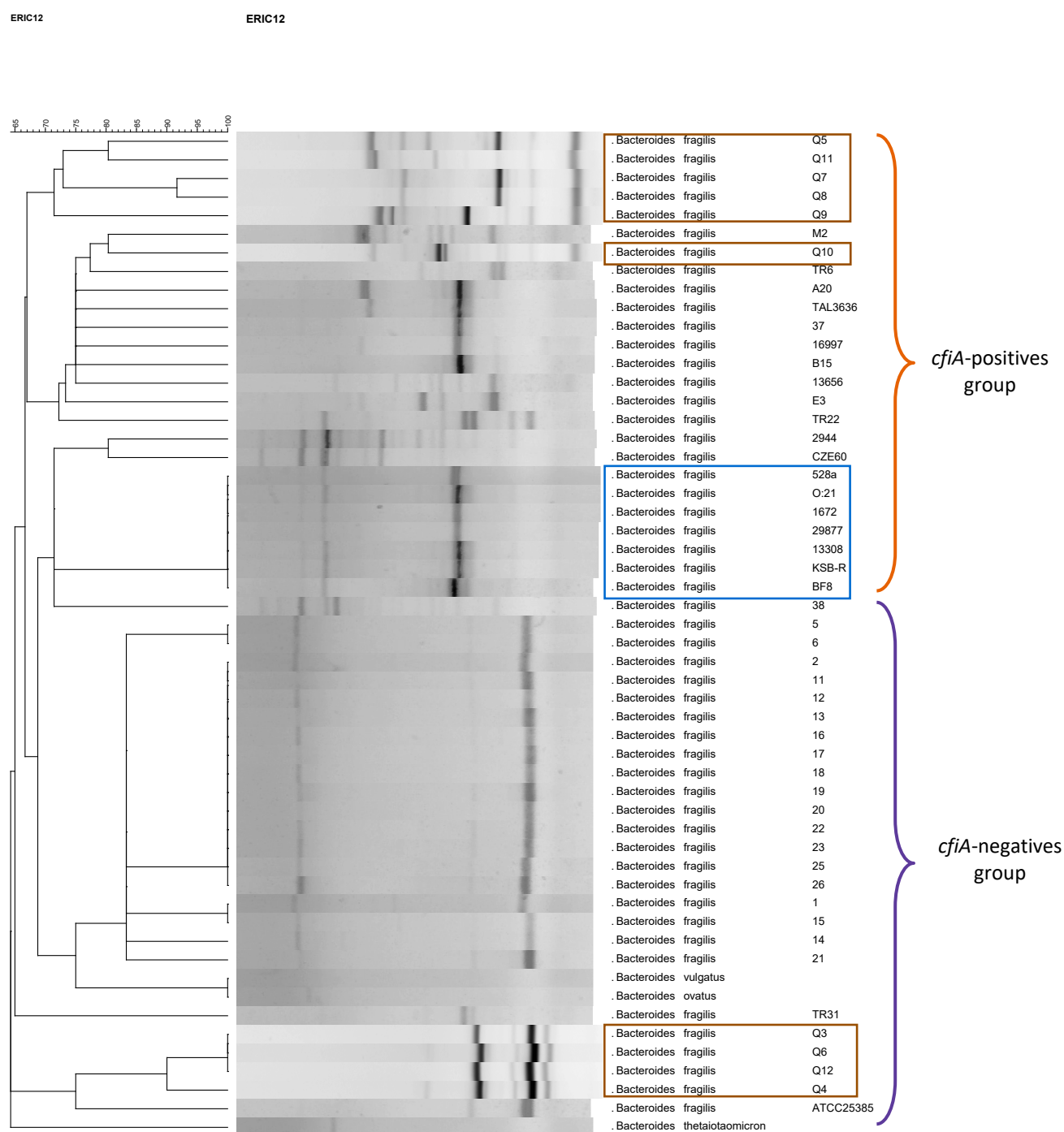
TGC tigecycline

MAK Mubarak hospital

AMIRI Amiri Hospital

- Resistant values, according to EUCAST [1] or CLSI [2], are in bold.

Fig. S1. ERIC PCR typing of *B. fragilis* strains from different sources.



The *cfiA*-negative and positive *B. fragilis* groups are indicated on the right. The strains from Kuwait are shown in brown boxes and the '*B. fragilis* BF8 multidrug-resistant cluster' is boxed in blue.

References

- [1] *Clinical breakpoints for bacteria*. 2019; Available from <http://www.eucast.org/>.
- [2] *Performance Standards for Antimicrobial Susceptibility Testing; Twenty-First Informational Supplement M100-S29*. 2018, Clinical Laboratory Standards Institute: CLSI, Wayne, PA, USA.

PUBLICATION III.



Article

Phenotypic and Molecular Characterization of Carbapenem-Heteroresistant *Bacteroides fragilis* Strains

Zain Baaity ¹, Friederike D. von Loewenich ^{2,†}, Elisabeth Nagy ¹, László Orosz ¹, Katalin Burián ¹, Ferenc Somogyvári ¹ and József Sóki ^{1,*}

¹ Institute of Medical Microbiology, Albert Szent-Györgyi Health Centre and School of Medicine, University of Szeged, H-6725 Szeged, Hungary; baaity.zain@med.u-szeged.hu (Z.B.); nagy.erzsebet@med.u-szeged.hu (E.N.); orosz.laszlo@med.u-szeged.hu (L.O.); burian.katalin@med.u-szeged.hu (K.B.); somogyvari.ferenc@med.u-szeged.hu (F.S.)

² Department for Medical Microbiology and Hygiene, University of Mainz, D-55131 Mainz, Germany; friederike.loewenich@unimedizin-mainz.de

* Correspondence: author: soki.jozsef@med.u-szeged.hu

† Current address: Institute of Virology, University of Mainz, D-55131 Mainz, Germany.

Abstract: Carbapenem-resistant *Bacteroides fragilis* strains usually emerge by an insertion sequence (IS) jump into the upstream region of the *cfiA* carbapenemase gene. However, intermediate or fully resistant *cfiA*-positive strains also exist. These do not have such IS element activations, but usually have heterogeneous resistance (HR) phenotypes, as detected by a disc diffusion or gradient tests. Heteroresistance is a serious antibiotic resistance problem, whose molecular mechanisms are not fully understood. We aim to characterize HR and investigate diagnostic issues in the set of *cfiA*-positive *B. fragilis* strains using phenotypic and molecular methods. Of the phenotypic methods used, the population analysis profile (PAP) and area under curve (AUC) measurements were the best prognostic markers for HR. PAP AUC, imipenem agar dilution and imipenemase production corresponded well with each other. We also identified a saturation curve parameter (quasi-PAP curves), which correlated well with these phenotypic traits, implying that HR is a stochastic process. The genes, on a previously defined ‘*cfiA* element’, act in a complex manner to produce the HR phenotype, including a lysine-acetylating toxin and a lysine-rich peptide. Furthermore, imipenem HR is triggered by imipenem. The two parameters that most correlate with the others are imipenemase production and ‘GNAT’ expression, which prompted us to suspect that carbapenem heteroresistance of the *B. fragilis* strains is stochastically regulated and is mediated by the altered imipenemase production.

Keywords: *Bacteroides fragilis*; carbapenem resistance; imipenem; heterogeneous resistance; toxin-antitoxin pair; GNAT acetyltransferase toxin



Citation: Baaity, Z.; von Loewenich, F.D.; Nagy, E.; Orosz, L.; Burián, K.; Somogyvári, F.; Sóki, J. Phenotypic and Molecular Characterization of Carbapenem-Heteroresistant *Bacteroides fragilis* Strains. *Antibiotics* **2022**, *11*, 590. <https://doi.org/10.3390/antibiotics11050590>

Academic Editor: Marc Maresca

Received: 31 March 2022

Accepted: 20 April 2022

Published: 27 April 2022

Publisher’s Note: MDPI stays neutral with regard to jurisdictional claims in published maps and institutional affiliations.



Copyright: © 2022 by the authors. Licensee MDPI, Basel, Switzerland. This article is an open access article distributed under the terms and conditions of the Creative Commons Attribution (CC BY) license (<https://creativecommons.org/licenses/by/4.0/>).

1. Introduction

Bacteroides fragilis is the most significant anaerobic pathogen in terms of both its pathogenicity and our knowledge of its biology [1]. It resides in the normal intestinal microbiota of mammals, exerting important physiological activities there. It is also an opportunistic pathogen, being the most common species isolated from endogenous anaerobic infections such as intra-abdominal abscesses, pelvic abscesses, soft-tissue infections, wound infections and sepsis. Its parent genus, *Bacteroides*, with more than 60 described species, belongs to the Bacteroidetes phylum [1]. Regarding the number of antibiotic resistance mechanisms and resistance to various antimicrobials, members of the *Bacteroides* genus are the most antibiotic-resistant species among anaerobic pathogens. Of the pathogenicity factors of *B. fragilis*, its capsular polysaccharide (CPS) molecules, adhesins, oxygen tolerance and its enterotoxin are the most important [1]. The prevalence of *B. fragilis* in the intestinal microbiota varies person to person, but can range from 0% to 30% [2]. Its main interactions with hosts are mediated mainly by CPS types, which have immunomodulatory effects. This

is important for physiologically shaping immune tolerance to *B. fragilis* in the intestine [3] and pathogenically in inducing abscesses [4]. Carbohydrate utilization is an additional characteristic common to *B. fragilis* and other *Bacteroides* species [5].

Antibiotic resistance can be categorized into the following prevalence classes: high (>60% for penicillins, cephalosporins and tetracyclines), moderate (10–60% for cephamycins, clindamycin, moxifloxacin and sometimes β -lactam/ β -lactamase inhibitor combinations) and low (<5–10% for carbapenems, 5-nitroimidazoles and tigecycline) [2]. For carbapenems, the resistance rate is usually approximately 1–5% depending on the geographical location. It is mediated by a metallo- β -lactamase enzyme encoded by the *cfiA* gene. A well-known, but less well-characterized, property of *B. fragilis* strains is that they form two genetic divisions separable either by the presence of *cepA* penicillinase/cephalosporinase (Division I) or *cfiA* carbapenemase (Division II) genes, or by typing methods (genomic DNA homologies, ribotyping, multi-locus enzyme electrophoresis, multi-locus sequence typing, arbitrary primed polymerase chain reaction (AP-PCR) and matrix-assisted laser desorption ionization-time of flight mass spectrometry (MALDI-TOF MS)) [6]. In highly carbapenem-resistant *cfiA*-positive *B. fragilis* strains, the *cfiA* gene is usually activated by an insertion sequence (IS) element, which serves as a strong promoter for the expression of these resistance genes [6]. Several studies have already examined and described this configuration. However, the carbapenem resistance of *B. fragilis* is more complicated: (i) strains without an IS element have a silent *cfiA* gene and have low carbapenem MIC (<1 $\mu\text{g/mL}$), (ii) IS-activated *cfiA*-positive strains have high carbapenem minimal inhibitory concentrations (MICs, $\geq 16 \mu\text{g/mL}$) and (iii) *cfiA*-positive strains with an inactive IS element have elevated carbapenem MICs (>2 $\mu\text{g/mL}$) [7–11]. These latter strains also show heterogeneous carbapenem resistance phenotypes usually identified through Etest antimicrobial susceptibility test (AST) experiments [7,9–11].

Heterogeneous resistance (or hetero-resistance, HR) has been well examined in aerobic pathogens and some metronidazole-resistant *Clostridioides difficile* cases [12], but has been rarely reported on for other anaerobes. Although sometimes other phenomena are described as HR, true, ‘monoclonal’ or *bona fide* HR means that the subpopulations of cells with a higher resistance level exist in a bacterial culture or, equally, that the distribution of antibiotic susceptibilities of cells in the strain is wider than for normal bacterial populations [13]. HR is often noticed in routinely performed disc diffusion or gradient ASTs. However, the gold standard for detecting HR is recording its population analysis profile (PAP), whereby the proportion of surviving cells of a population is determined along with increasing antibiotic concentrations. PAP curves usually plot the logarithmic antibiotic concentration (x-axis) against the logarithm of the proportion of resistant cells (y-axis). HR is determined when the difference of MICs between the least and the most resistant population is ≥ 8 (\geq three steps in two-fold dilutions) [13]. HR can also be observed in susceptible, intermediate (susceptible with increased exposure) and fully resistant categories of antibiotic resistance phenotypes [13]. As previously stated, HR for aerobic pathogens has been well described, with methicillin-resistant *Staphylococcus aureus* (MRSA) being the most well-known example [14]. Most ‘in the field’ MRSA strains exhibit HR, but the exact mechanism of HR in these and other aerobic species has not yet been well characterized [13]. For MRSA, experimental alterations in the expression of peptidoglycan synthesis genes and proteins often yielded HR phenotypes whose PAP profiles could be differentiated as (i) susceptible and homogeneous, (ii) some types of HR or (iii) highly resistant but also homogeneous [15]. The importance of HR and bacterial persistence is that it greatly increases the risk of developing full resistance during the use of antibiotics for ongoing infections [16].

The *cfiA* gene of *B. fragilis* also resides on a proposed genetic element (Figure 1), which, besides *cfiA*, codes for two acetyltransferase genes, ‘GNAT’ and ‘XAT’. The former shows homology to toxin–antitoxin (TA) system toxins [17]. TA gene pairs, with their toxic and labile neutralizing antitoxin activities, can kill post-segregational plasmid-less daughter cells (if harbored by plasmids) or halt cell division by stopping vital cellular functions (in

the case of chromosomal localization). In this latter case, antibiotic persistence can emerge, meaning that during the replication stop, a small fraction of bacterial cells withstand the action of bactericidal antibiotics and, after their removal, the cells start dividing again [18].

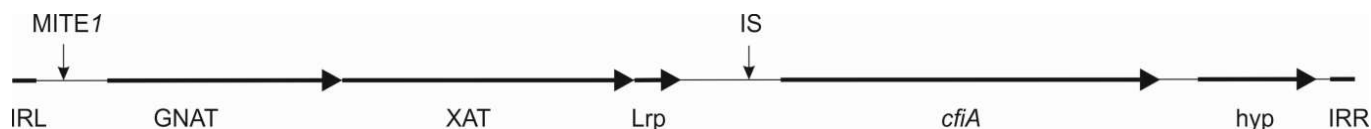


Figure 1. An updated scheme of the *cfiA* 'element'. IRL and IRR inverted repeats bordering the element; 'GNAT'—ORF coding a Gcn5-like acetylase protein; 'XAT'—another acetylase protein; Lrp—a short ORF coding for a lysine-rich peptide; hyp—an ORF coding for a hypothetical protein; MITE1 with arrow—possible insertion of miniature transposable element 1; IS with arrow—possible insertion of a *cfiA*-activating IS element.

Using some *B. fragilis* strains selected after carbapenem Etest ASTs, our aim is to prove the HR phenotype by using differently plotted survival curves. We also examine the phenotypic traits underlying these phenomena by performing calculations on optimal HR detection methods and study the gene expression of the '*cfiA* element' to approximate how HR develops.

2. Results

2.1. Phenotypic Characterization and PAP Experiments

As our main aim was to further characterize imipenem HR, we chose the following test strains: three imipenem-susceptible *cfiA*-negative, nine *cfiA*-positive but 'silent' or heterogeneously imipenem-resistant in gradient tests and three imipenem-resistant, *cfiA*-positive, IS element-activated *B. fragilis* strains (Table 1). A typical imipenem gradient test example showing HR is displayed in Figure 2A, marking the start of the inhibition zone to the total disappearance of resistant colonies. The expression of imipenem HR phenotypes, as determined by gradient tests, varied from low to high (Table 1). We analyzed the HR behavior of colonies in the partial inhibition zone. For strains displaying low-grade HR phenotypes, the direct use of the cells in further gradient tests did not result in partial inhibition. However, if we allowed a 'recovery' period for those cells, incubating them on supplemented Columbia blood agar, the original HR phenotype recovered (without increased HR; Figure 2B–D), which demonstrated a monoclonal HR [14]. However, for strains showing a highly expressed HR phenotype, such as *B. fragilis* CZE60, some induction was observed as HR increased in these cases (data not shown).

2.2. PAP Curves, Assessment and Correlation of the Phenotypic Heteroresistance Parameters

In addition to PAP plots, plots without logarithmic axes (x- and y-axis direct—hyperbolic curves, x-axis logarithmic and y-axis direct—saturation curves) were also examined (Figure 3A–F), allowing more insight into the nature of HR. The saturation curves displayed some meaningful properties: it was interesting that, sometimes, at the lowest imipenem concentrations, we obtained fewer colony-forming units (CFU) than on the next higher-concentration plate (Figure 3B,E). We explained this by presuming that some dormant cells were present in the inoculating cell preparations (cultures suspended in PBS or BHIS) and that the higher, but non-selective, imipenem concentration, induced the cells to exit dormancy. The starting imipenem concentrations caused a smoothly decreasing curve, validating our sigmoid hypothesis, and the decrease in CFUs caused by increasing imipenem concentrations also tended to be somewhat continuous (Figure 3B,E). The saturation curves widened as the HR increased (Table 1, bS PBS and BHIS) and also produced the x_0 value (Equation (1)), which was the inflection point or the maximum value of their derivative, the density function. In addition to these parameters, the PAP curves widened (the maximum being ≥ 3 times the minimum values, dil PBS and BHIS; Table 1).

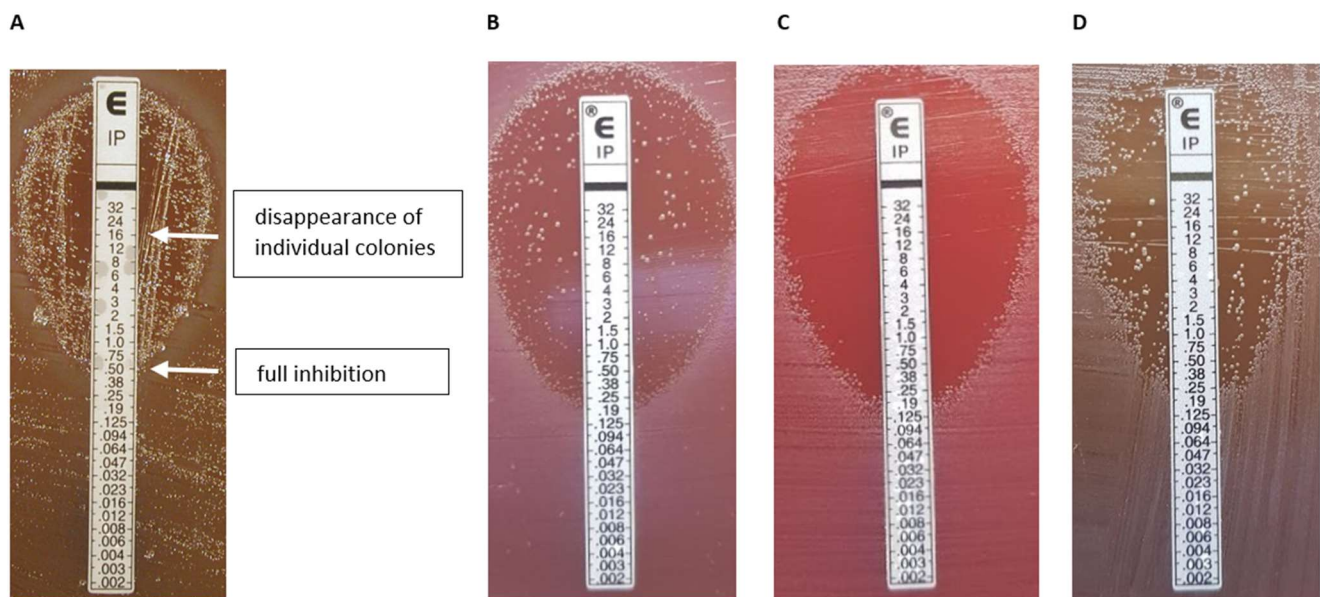


Figure 2. Etest HR phenotypes. A typical Etest phenotype (*B. fragilis* 16997) [8] showing the reading annotation; in this example 0.5–(16), the first value expresses the inhibition of full growth, then after a dash, the value indicates in parenthesis where the inside colonies disappeared. (A). The ‘inheritance’ of the Etest HR phenotype (B–D). Original appearance (B); an inner colony direct Etest (C); an Etest result of an inner colony after an intermediate cultivation on a Columbia blood agar (D).

To evaluate this curve’s widening in conjunction with other possible HR parameters, agar dilution MICs, HRI and imipenemase production were measured and compared for all strains (Table 1). We also recorded imipenem MICs on WC agar plates, since the latter was also used for PAP measurements. The PAP AUC ratios were also calculated, curves for which can be seen in Figure 4 and values in Table 1. All the phenotypic parameters are summarized and shown in Table 1. To analyze the data, the first variance analysis was performed according to HR categorization values (as PAP dilution increased by ≥ 3 or HRI was >0 , Table 2). Almost all test parameters showed some potential for HR (Table 2). These parameters were also cross-correlated to see the connections between them, which was a cumulative assessment of relatedness (Table 3, where cells marked with different colors show differing degrees of correlation). Instead of examining the connection of only two parameters, it was a much more complete analysis. Through the cross-correlations, we also wanted to assess which had the best predictive and explanatory values for HR. We obtained a quite good rate of relatedness between the following parameters: (i) the x_0 PBS and BHIS values correlated well with almost all the phenotypic parameters, (ii) the AUC PBS and BHIS and MIC Brucella and MIC WC also demonstrated a very high correlation and (iii) imipenemase production also correlated well with the other phenotypic parameters. This implied that (i) the AUC calculation best predicted HR, (ii) agar dilution predicted the resistance level quite well and (iii) an increased imipenemase production could be a cause of the HR phenotype.

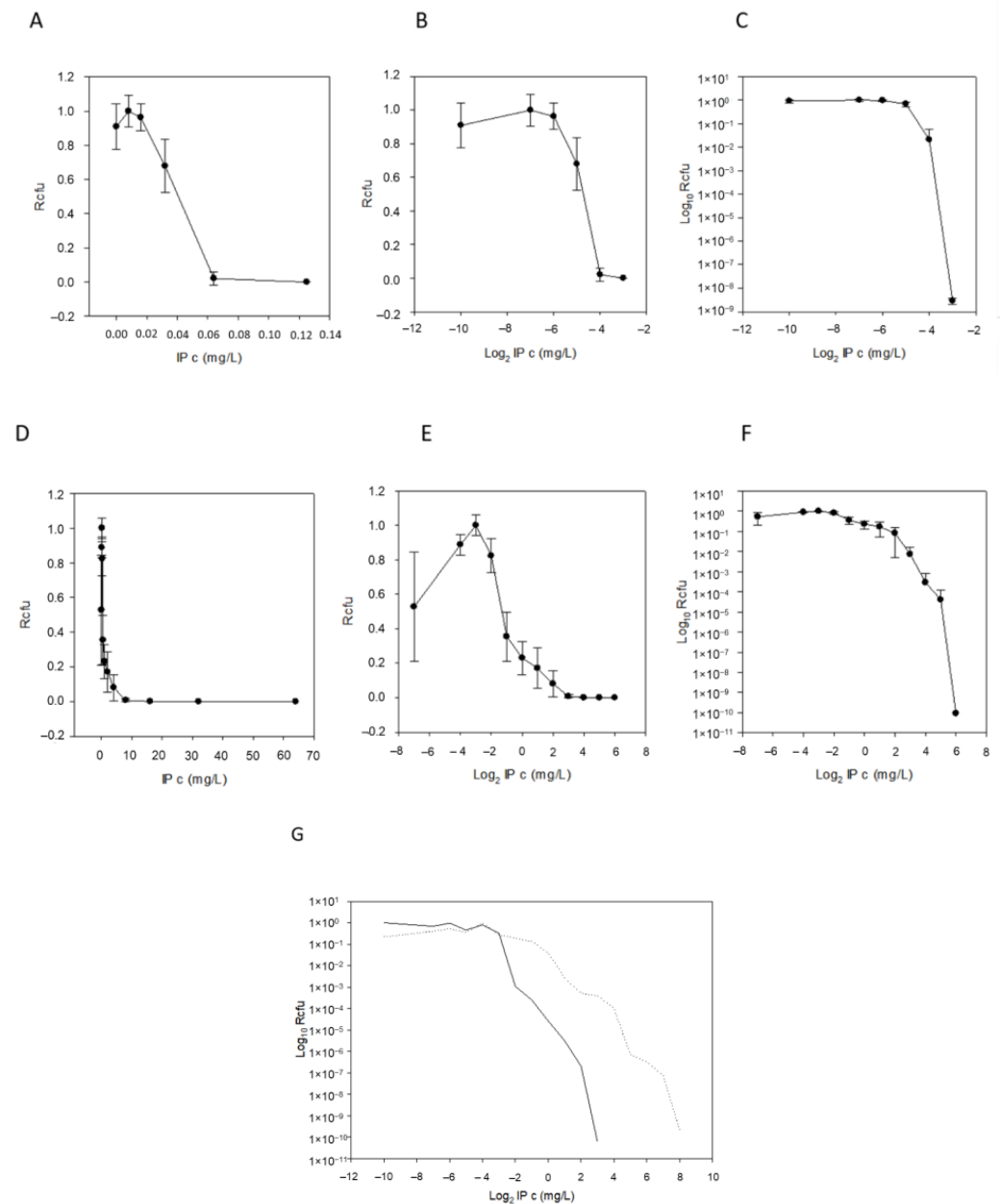


Figure 3. Demonstration of PAP curves. Imipenem concentration vs. growing colony number plots with different scale axes and with error bars for the imipenem susceptible and *cfiA*-negative *B. fragilis* NCTC 9342 (A–C) and for HR and *cfiA*-positive *B. fragilis* CZE60 (D–F). Direct plots (hyperbola-like curves, (A,D)), logarithmic IP concentration (saturation-like curves, (B,E)) and both axes logarithmic (classic PAP curves, (C,F)). (To be able to logarithmize zero concentration of imipenem, we used an 8-fold smaller value, such as 0.004 mg/L, instead of 0.032 mg/L). Comparison of the PAP curves of imipenem uninduced (solid line) and imipenem-induced (dashed line) *B. fragilis* 3130 (G).

2.3. Imipenem Induction of HR and Correlating the Molecular Characteristics of HR

A chromosomal segment ('*cfiA* element') containing the *cfiA* gene and a proposed TA gene pair with some insertional elements (MITE1, IS elements) were identified earlier as being characteristic of Division II *B. fragilis* strains (Figure 1). Additionally, during examination of the upstream regions of *cfiA* genes in *B. fragilis* strains, we identified a lysine-rich peptide (Lrp) in the '*cfiA* element' (Figure 1). The 'GNAT' toxin gene showed a high homology to the elongation protein 3 ($e = 1.03 \times 10^{-40}$) [19] or to the AtaT-TacT-ItaT TA toxins ($e = 3.4 \times 10^{-5}$, classical members of acetylating toxin members of bacterial TA systems) [20] in protein BLAST conserved domain searches (Figure S1). Since a proposed

TA gene pair resided on the '*cfiA* element' and imipenem stirred the HR strain cells from dormancy, we attempted to induce or increase HR by imipenem treatment. The same phenotypic parameters for two strains (*B. fragilis* 3130i5 and CZE60i2) after serial imipenem inductions (five steps for 3130i5 and two steps for CZE60i2) were also recorded (Table 1). The detailed data for the *B. fragilis* 3130i5 HR induction process are shown in Figure 5. It can be seen that as imipenem concentration increased, HR, measured by E-tests and *cfiA* expression, 'GNAT' and 'XAT' genes and the 'GNAT-XAT' expression ratio, also showed increases. The increased HR in *B. fragilis* 3130i5 through induction with imipenem could also be clearly seen (Figure 3G), where the detected PAP curve widened and showed an increased resistance span. No growth was obtained when we exposed *B. fragilis* 3130 to a 128 mg/L imipenem concentration directly.

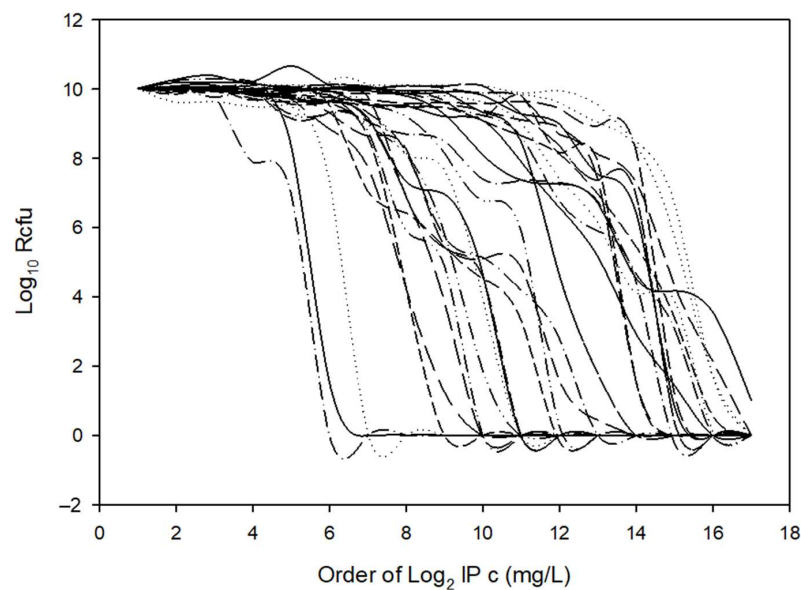


Figure 4. Cumulative PAP plots used in AUC calculations of our 15 *B. fragilis* test strains (Table 1) cultured on solid (supplemented Columbia blood agar) or in liquid (BHIS) media.

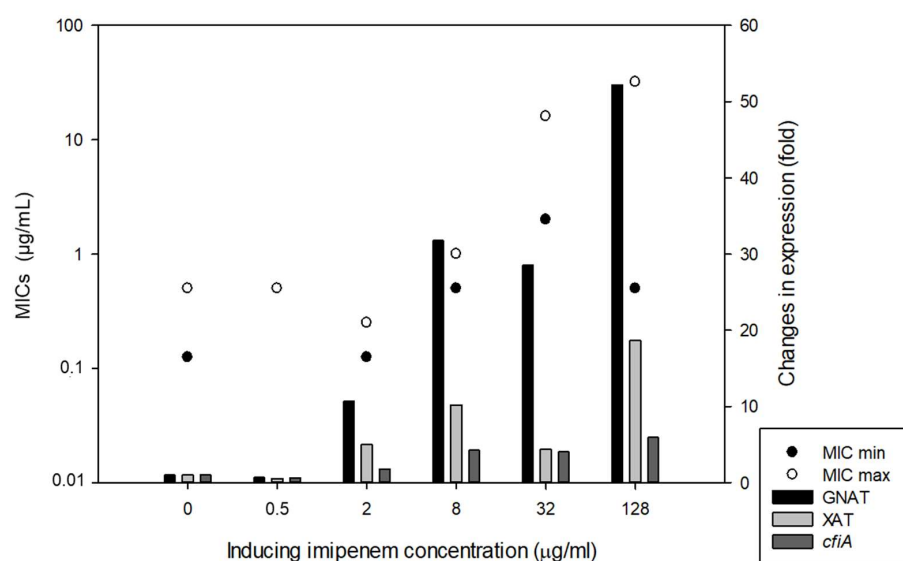


Figure 5. Induction of HR in *B. fragilis* 3130 with increasing imipenem concentration in the culture media (BHIS). The left-hand y-axis denotes the Etest AST values (full and partial inhibition marked as minimal and maximal MICs) and right-hand y-axis shows the gene expression changes for the strains in the induction experiments, respectively.

Induction experiments suggested that other ORFs on the '*cfiA* element' ('GNAT', 'XAT' and Lrp) may also play a role in HR. Their contribution could be assessed based on their correlation with phenotypic traits. The cross-correlation of molecular traits also provided some insights into the possible action mechanism. The expression of 'GNAT' correlated with almost all the phenotypic traits, and imipenemase production correlated with the expressions of *cfiA* and 'XAT' (Table 3). 'GNAT' and 'XAT' showed significant correlation with each other (Table 3). *cfiA* gene expression showed a strong correlation with the composition of Lrp, as detected by the sequencing of its fragments by PCR amplification. Surprisingly, it also demonstrated a high degree of heterogeneity (Table S3, Figure S2).

2.4. Time–Kill Curves

Since we hypothesized that 'GNAT-XAT' formed a TA pair that may also cause persister phenotypes, we performed some time–kill experiments to obtain further data (Figure 6). However, the curves were straight, reminiscent of antibiotic tolerance [21] even for the *B. fragilis* 638R control strain. Additionally, if a strain is tolerant to one antibiotic, it can also display tolerance to others through slow growth [21]. This was not the case for our strains, as shown in Table S2. Nonetheless, we assumed that the tolerance to imipenem was mediated by other mechanisms in *B. fragilis* 638R and our other *cfiA*-positive test strains. This was reinforced, as imipenem induction did not cause alterations in the curves of imipenem-induced and non-induced strains (Figure 6).

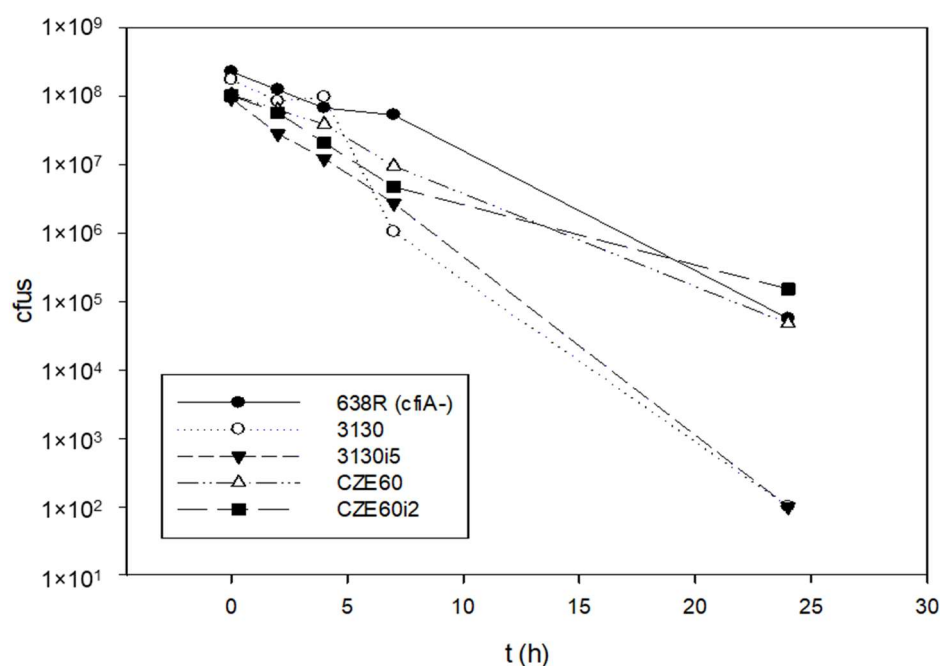


Figure 6. Time–kill curves of *B. fragilis* strains with or without *cfiA* gene. *B. fragilis* 638R was *cfiA*-negative, all the other strains were *cfiA*-positive. The imipenem non-induced and induced variants of *B. fragilis* 3130 and CZE60 did not show much difference in their killing curves.

Table 1. List of strains, recorded data on imipenem susceptibilities, PAP profiles, imipenemase production and molecular data.

<i>B. fragilis</i>	Ref.	Phenotypic Parameters ^a										Molecular Parameters								
												<i>cfiA</i> and IS		qRT-PCR ^b			Lrp ^c			
		x ₀ PBS	x ₀ BHIS	bS PBS	bS HIS	d PBS	d BHIS	AUC PBS	AUC BHIS	MIC B	MIC WC	IP HRI	Ipase	<i>cfiA</i>	<i>cfiA</i> -IS	<i>cfiA</i>	‘GNAT’	‘XAT’	‘GNAT/XATK no.	K%
Susceptible controls																				
NCTC 9343	-	-4.8142	-4.3392	-0.2092	-0.3902	2	2	1	1	0.125	0.064	0	0	-	n.a.	0	0	0	n.a.	n.a.
638R	-	-4.4449	-4.9148	-0.2721	-1.0111	2	2	1.4757	1.4046	0.125	0.064	0	0	-	n.a.	0	0	0	n.a.	n.a.
D39	[22]	-4.4350	-5.7965	-0.1012	-0.2192	2	2	1.4886	0.7642	0.5	0.064	0	0	-	n.a.	0	0	0	n.a.	n.a.
Silent/HR ^d																				
7979	This study	-3.0103	-3.5941	-0.4000	-0.8885	3	4	1.8045	1.5884	0.125	0.032	0	5.1	+	-	16.35	6.91	5.56	1.2428	7
3130	This study	-2.7685	-3.0168	-0.6269	-0.0451	3	6	1.8785	1.5532	8	8	0	2.6	+	-	1	1	1	1	5
3035	[7]	-2.8450	-2.7613	-0.3141	-0.3887	3	3	1.7810	1.4387	1	2	5	9.7	+	-	166.3	0.02	0.993	0.0201	9
SY69	[22]	-2.2774	-3.4300	-0.2062	-1.5269	5	6	2.0114	1.7008	4	4	5	10.1	+	-	92.0	17.7	32.6	0.5429	5
CZE65	[10]	-2.6235	0.9301	-0.9546	-1.1148	5	5	2.6027	2.3992	16	8	2	25.5	+	-	2.46	1.93	0.16	12.0625	7
CZE60	[10]	0.0886	-0.7637	-1.4586	-0.6320	3	4	2.7013	1.8329	16	16	5	33.3	+	-	12.91	7.78	0.49	15.8775	7
SLO8	[9]	1.8171	-4.0275	-0.6387	-1.1367	3	8	2.7294	2.2562	128	128	3	133	+	-	76.06	182.94	255.47	0.7161	8
HR-ind ^d																				
3130i5	This study	-0.3129	-2.1373	-1.2807	-0.5161	4	8	2.9720	2.4650	4	4	5	28	+	-	5.91	52.18	18.67	2.80	5
CZE60i2	This study	3.1618	-2.7092	-0.4220	-2.0045	3	5	3.0608	2.4110	128	64	6	36.8	+	-	22.93	8.78	0.33	26.6061	7
With IS ^d																				
De248514/19	This study	0.2977		-0.5716	-3.9655	3	4	2.4364	2.1085	16	64	3	134	+	IS614B	509.8	460.1	3.7	124.3514	8
1672	[8]		2.1815	-7.1023	-0.8173	2	3	2.6174	2.5047	256	256	4	189	+	IS1168	2.02	10.49	185.59	0.0565	7
TAL3636	[23]	3.5263	3.3190	-0.6621	-0.4304	2	4	2.8433	2.7366	128	256	0	354	+	IS942	97.5	0.024	0.697	0.0343	8

^a Abbreviations as follows: bS PBS—b parameter from PBS suspensions; bS BHIS—b parameter from BHIS broth cultures; d PBS—fold/dilution increase in PBS PAPs; d BHIS—fold/dilution increase in BHIS PAPs; Ipase—specific imipenemase production (u/mg cell extract). ^b Q-RT-PCR expressions and the relative expression (ratio of expressions) of ‘GNAT-XAT’. ^c K no.—number of lysines in Lrp; K %—the lysine content in Lrp in percentages. ^d Types of *cfiA*-positive strains: silent without IS elements but showing some HR, induced HR and strains with IS activated *cfiA* genes.

Table 2. Variance analysis of the examined traits of the test *B. fragilis* strains.

Grouping Category	Trait														
	x ₀ PBS	x ₀ BHIS	bS PBS ^a	bS BHIS	d PBS	d BHIS	AUC PBS	AUC BHIS	MIC B	MIC WC	IP HRI	Ipase	cfiA	‘GNAT’	‘XAT’
Dilution change in PBS (p) ^b	0.003	0.018	0.031	n.s. ^c	p.d. ^d (0.004)	0.015	0.005	0.002	0.017	0.017	n.s.	0.007	0.033	0.029	0.031
Differences between groups ^e	1–2, 1–3	1–3	1–3			1–2	1–2, 1–3	1–2, 1–3, 2–3	1–3	1–3		1–3	1–2	1–2	
Dilution change in BHIS (p)	0.01	0.03	0.021	n.s.	0.02	p.d. (0.011)	0.002	0.002	0.019	0.029	0.031	0.009	0.009	0.009	0.009
HRI (p)	0.001	n.s.	n.s.	n.s.	n.s.	n.s.	<0.001	<0.001	0.019	0.017	p.d. (<0.001)	0.005	0.028	0.024	n.s.
Differences between groups	1–2, 1–3						1–2, 1–3	1–2, 1–3			1–2, 2–3	1–3, 1–2		1–2	

^a Abbreviations are the same as Table 1. ^b p—significance values; ^c n.s.—non-significant; ^d Classifier traits (in bold, p.d.—per definition). ^e Numbers mean the following groups: 1—homogeneously susceptible; 2—heterogeneous resistance; 3—homogeneously resistant.

Table 3. Cross-correlation values of all strains of the traits examined (from Table 1).

	X ₀ BHIS	bS PBS	bS BHIS	d PBS	d BHIS	AUC PBS	AUC BHIS	MIC B	MIC WC	HRI	IPase	cfiA	'GNAT'	'XAT'	'GNAT/XAT'	n K	% K ^a
X ₀ PBS	0.477	−0.613 ^b	−0.477	0.29	0.594	0.916	0.873	0.932	0.924	0.519	0.96	0.669	0.695	0.457	0.227	0.256	0.366
	0.0809	0.0188	0.0809	0.301	0.0235	0.0000002	0.0000002	0.0000002	0.0000002	0.0537	0.0000002	0.00813	0.00507	0.0977	0.484	0.433	0.257
X ₀ BHIS		−0.725	0.125	0.177	0.281	0.625	0.721	0.578	0.523	0.345	0.538	0.143	0.108	0.183	−0.238	−0.081	−0.0931
		0.0018	0.648	0.514	0.3	0.0123	0.00196	0.0231	0.0429	0.199	0.0367	0.602	0.695	0.506	0.442	0.783	0.766
bS PBS			0.0679	−0.173	−0.396	−0.707	−0.779	−0.699	−0.685	−0.283	−0.699	−0.118	−0.47	−0.391	−0.126	0.11	0.0596
			0.802	0.532	0.138	0.00278	0.0000944	0.00326	0.00439	0.3	0.00326	0.667	0.0757	0.146	0.683	0.716	0.834
bS BHIS				−0.392	−0.327	−0.368	−0.382	−0.338	−0.308	−0.401	−0.437	−0.434	−0.652	−0.28	−0.545	−0.0663	−0.134
				0.142	0.23	0.171	0.154	0.209	0.257	0.134	0.101	0.104	0.00785	0.306	0.0623	0.834	0.667
d PBS					0.768	0.346	0.235	0.0807	0.00194	0.535	0.11	0.398	0.558	0.384	0.329	−0.487	−0.511
					0.0003	0.199	0.388	0.763	0.985	0.0382	0.686	0.138	0.0299	0.15	0.284	0.0998	0.0843
d BHIS						0.668	0.519	0.419	0.378	0.408	0.386	0.379	0.7	0.608	0.237	−0.528	−0.474
						0.00614	0.0463	0.117	0.158	0.127	0.15	0.158	0.00326	0.0158	0.442	0.0705	0.111
AUC PBS							0.9	0.804	0.759	0.57	0.824	0.437	0.663	0.43	0.294	−0.0663	0.0112
							0.0000002	0.0000002	0.00048	0.0252	0.0000002	0.101	0.00654	0.107	0.34	0.834	0.956
AUC BHIS								0.82	0.799	0.412	0.896	0.419	0.616	0.484	0.0559	0.0221	0.104
								0.0000002	0.0000002	0.124	0.0000002	0.117	0.0136	0.0662	0.852	0.939	0.733
MIC B									0.975	0.411	0.892	0.386	0.56	0.412	0.0497	0.247	0.329
									0.0000002	0.124	0.0000002	0.15	0.0287	0.124	0.869	0.429	0.284
MIC WC										0.341	0.908	0.422	0.543	0.412	−0.00352	0.319	0.413
										0.209	0.0000002	0.113	0.0353	0.124	0.974	0.295	0.173
HRI											0.443	0.477	0.591	0.369	0.172	−0.106	−0.166
											0.0946	0.0685	0.0192	0.171	0.572	0.733	0.588
IPase												0.626	0.68	0.532	0.035	0.434	0.521
												0.0123	0.00504	0.0397	0.904	0.15	0.0749
cfiA													0.547	0.493	−0.112	0.67	0.667
													0.0339	0.0597	0.716	0.0154	0.0169
'GNAT'														0.788	0.441	−0.155	−0.0745
														2 × 10 ^{−7}	0.143	0.619	0.8
'XAT'															−0.364	−0.125	−0.0968
															0.233	0.683	0.749
'GNAT/XAT'																−0.214	−0.156
																0.484	0.619
n K																	0.988
																	0.0000002

^a Abbreviations are the same as Table 1. ^b Different colors were used depending on the strength of the correlations: blue— $\text{IrI} \geq 0.85$ and $p = 0.0000002$; light green— $\text{IrI} \geq 0.7$ or $p < 0.01$; yellow— $\text{IrI} \geq 0.5$, or $p < 0.05$. Boxes marked with A–E indicate common relations and are discussed in the text.

3. Discussion

This study revealed that carbapenem heteroresistance is a characteristic phenotype of some *cfiA*-positive *B. fragilis* strains. The phenotypic parameters studied as the saturation curve x_0 and b , the PAP curve dilution and AUC, the imipenem MIC and HRI values and the specific imipenemase activities of the strains were interconnected and predicted HR well. The most important and central parameter was the imipenemase production, which could mediate the resistance and affect the other phenotypic parameters as it was proportional to the other parameters observed: agar dilution MICs, PAP AUC ratios and the saturation curve (simpler PAP curve) extension in PAPs of agar plate-grown cells. In our opinion, all the studied parameters could predict HR, but PAP AUC was the best. However, since most of these parameters were continuous in form from low to high imipenem MICs and HR parameters, continuing to use PAP curve extensions could also be regarded as a very good method. The PAP AUC method was also suggested as a good prediction parameter for the reduced glycopeptide susceptibility of staphylococci [24].

We related the HR phenotype to stochastic processes. According to our hypothesis, this was due to the action of a proposed toxin ('GNAT') that may stop growth, but also allows viability under antibiotic-exposed circumstances. The primary finding supporting this was the widening of the PAP saturation curve parameter, b , which could be regarded as a standard deviation parameter. To improve the discussion of HR and persistence, Brauner and Balaban suggested the term heterotolerance for HR [25]. In more thoroughly investigated tolerance and persistence mechanisms, it has also been suggested that wider distributions, and those above a certain persistence factor threshold, yield more persisters [24]. We believe this is true for the carbapenem heteroresistance of *B. fragilis*, as we also detected a widening of our saturation curves. Imipenemase activity values, as an effector mechanism, also correlated with most of the phenotypic parameters of HR [26].

We propose an HR mechanism of *cfiA*-positive *B. fragilis* strains as follows: (i) *cfiA* is expressed proportionally to HR, and (ii) the parallel expression of 'GNAT-XAT' allows reduced cellular activities. We conclude the same from experiments in which we induced imipenem HR by imipenem; however, to obtain a more detailed picture about this, experiments are under way in our laboratory to determine the promoters of *cfiA* and 'GNAT-XAT', how they act individually and in conjunction with other promoters, what is the biochemical nature of 'GNAT' and 'XAT', do they form a TA pair and what is the role of the lysine-rich peptide in the '*cfiA* element'. It is conceivable through the above that 'GNAT' acts through the acetylation of a lysine in a ribosomal protein or in tRNA^{Lys} molecules and Lrp may modify these actions.

At present, no particular common mechanism was found to explain HR in other bacteria. However, in some cases, regulatory proteins were involved as well [27–31], which we believe may also produce stochastic regulation. Additionally, monoclonal heteroresistance could also emerge by the tandem duplication of DNA segments of the effector genes of *Acinetobacter baumannii* [32], *Escherichia coli* [33], *Klebsiella pneumoniae* [34], *Pseudomonas aeruginosa* [35], *Salmonella typhimurium* [36] or *Streptococcus pneumoniae* [37]. However, this latter mechanism can result in a variable number of repeats in the cells of a given population, which can be both stochastic and difficult to detect. Recently, for the aminoglycoside HR of *A. baumannii* in a *recA*-negative background, a modest copy number variation of the *aadB* gene-containing integron was linked to HR. The step causing the copy number increase was hypothesized as a stochastic process [32]. In earlier experiments, we did not observe that *cfiA* or the '*cfiA* element' had copy number variations or that the *cfiA* promoter was invertible (data not shown), as CPS promoters usually are in *B. fragilis*. The role of global regulatory systems ((p)ppGpp, *relA*, *spoT*) in bacterial persistence was proven, something which we would like to examine regarding the HR of *B. fragilis* [26].

For TA systems, the prominent role of governing persistence was attributed, but some parallels between HR and persister phenotypes could also be drawn: HR can be regarded as concentration-dependent, while persistence can be regarded as a time-dependent survival

phenomenon. In our opinion, the stochastic hypothesis of carbapenem HR of *B. fragilis* may facilitate research into this being the case in other HR systems as well.

In this study, we analyzed extensively the phenotypic parameters of control and HR *B. fragilis* strains, which yielded scattered but statistically evaluable data enabling novel description by saturation curves. In summary, these investigations into the various HR traits revealed that while the AUC PAP method was the best predictor/classifier for HR, other traits could also be considered suitable. Among the phenotypic traits examined, the saturation curve, PAP AUC, agar dilution and imipenemase activities correlated well. This indicated that they were also good predictors and were linked to the HR mechanism, for which imipenemase production could be the primary contributor. The calculation of the widening of the saturation and PAP curves, for the PBS suspensions, showed a good correlation with the PAP AUCs, agar dilution MICs and imipenemase production. Therefore, we saw our stochastic explanation of the nature of HR as compelling. This latter point was also supported by the fact that imipenem HR could be induced by imipenem and that the expression of the '*cfiA* element' genes ('GNAT', 'XAT', and *cfiA*) correlated. 'GNAT' can act as a toxin causing dormancy, and these genes may form a complex interaction.

4. Materials and Methods

4.1. Bacterial Strains and Cultivation

The test strains used in this study are listed in Table 1. The strains were selected from our collection stored at $-70\text{ }^{\circ}\text{C}$ in brain–heart infusion broth (BHI) containing 20% glycerol. Their cultivation was performed on anaerobic Columbia blood agar plates (Columbia agar supplemented with 2.5% defibrinated sheep blood, 1.25% laked sheep blood, 300 mg/L L-cysteine and 1 mg/L vitamin K₁), on Wilkins–Chalgren (WC) agar or in supplemented BHI broth (BHIS, with the addition of 0.5% yeast extract, 5 mg/L hemin and 1 mg/L vitamin K₁) at $37\text{ }^{\circ}\text{C}$ under anaerobiosis (85% N₂, 10% H₂ and 5% CO₂) in an anaerobic cabinet (Concept400, Ruskinn, UK).

4.2. MIC Determinations, Recording of Population Analysis Profiles and Time–Kill Curves

Gradient tests (E-test, bioMérieux, France) were conducted on supplemented Columbia blood agar plates. Agar dilution was carried out as recommended by CLSI [38] on supplemented Columbia blood agar plates. Agar dilution was also performed on WC plates as the PAP records were also determined on this media.

In PAP experiments, we used the following cell suspensions/cultures: (1) 0.5 McFarland phosphate-buffered saline (PBS, 137 mM NaCl/2.7 mM KCl/1.8 mM KH₂PO₄/10 Na₂HPO₄ pH 7.2) cell suspensions taken after 48 h cultivations on Columbia blood agar plates or (2) overnight incubated BHIS broth culture. Optical density (at 600 nm) was measured by spectrophotometer (Thermo Scientific, Budapest, Hungary) for later normalization. Ten-fold dilutions were composed in PBS and 100 μL inocula were spread on Wilkins–Chalgren agar plates with an appropriate concentration of imipenem (from the 0.008–1024 $\mu\text{g}/\text{mL}$ range), which was determined by trials to yield 50–500 countable colonies per plate. Two independent experiments (biological replicates) were carried out using two–three parallels (technical replicates) for each concentration. The inoculated WC plates were then incubated anaerobically for 48 h and, afterwards, colony counts were determined by a gel documentation system (PXi, SYNGENE, Oxford, UK).

Time–kill curves were recorded by plating after 0 h, 2 h, 4 h, 10 h and 24 h of incubation on antibiotic-free WC agar plates, 100 μL aliquots of serial 10-fold dilutions of PBS suspensions with a turbidity of 0.5 McFarland. These also contained 32-fold higher imipenem concentrations than the original imipenem MICs. The WC plates were incubated in anaerobiosis for 48 h. Colonies were counted as described above.

4.3. Imipenemase Activity Measurement and Induction of HR by Imipenem Treatment

In total, 8 mL of overnight BHIS cultures was centrifuged (at $4\text{ }^{\circ}\text{C}$, 8000 rpm, 10 min), washed 3 times with cold PBS and sonicated. The crude cell extracts were then used for

imipenemase activity determination in 1 mL UV-transparent plastic cuvettes in an Assay buffer (50 mM HEPES, 25 μ M ZnSO₄, pH 7) using 0.1 mM imipenem concentration and an adjusted enzyme volume to obtain a linear decay of imipenem followed at 299 nm. The results were expressed by 1 pmole imipenem hydrolyzed per 1 min (U) and standardized by the protein content of the extracts (U/mg). Protein concentrations were determined by the Qubit Protein Assay Kit (Thermo Fisher Scientific, Budapest, Hungary).

Imipenem and imipenem heteroresistance were increased through 10 mL anaerobic BHIS cultures of *B. fragilis* 3130 and CZE60 being exposed to stepwise increments (0, 2, 8, 32 and 128 μ g/mL for *B. fragilis* 33130 and 0, 32 and 128 μ g/mL for *B. fragilis* CZE60) of imipenem concentrations. This was achieved by subculturing the lower imipenem concentration, containing stationary phase cultures, to the next level of imipenem-concentrated BHIS broth, to obtain an OD₆₀₀ of 0.05–0.1. We let it propagate to a stationary phase (OD₆₀₀ of 0.7–1.5) which took more time, from 1 to 4 days, as the imipenem concentrations increased.

4.4. Conventional PCR, Nucleotide Sequencing and qRT-PCR Experiments

Conventional PCRs and the nucleotide sequencing of some of its PCR products were carried out as described previously. PCR primer sequences and cycling conditions are contained in Supplementary Materials Table S1.

To examine the '*cfiA* element' constant gene ('GNAT', 'XAT' and *cfiA*) expression levels, total RNA was isolated (HighPure RNA Isolation Kit, Roche) from the *cfiA*-positive test strains and we performed subsequent qRT-PCR in an RT-PCR instrument (StepOne, Life Technologies). The 10 μ L final volume PCR reactions contained 5 μ L SYBR Green mastermix (Verso 1-Step RT-PCR Mastermix with ROX, Thermo Fisher Scientific, Budapest, Hungary), 0.7 μ M primers and 1 μ L RNA sample.

4.5. Curve Plotting, Curve Parameter Calculation, Statistical Evaluation and Bioinformatics

Means and standard deviations were calculated after normalization of the OD₆₀₀ values in MS Excel. The highest colony counts for each type of measurement were then regarded as 1, and smaller colony counts were expressed as a fraction of that. The values of growth fraction for each imipenem concentration obtained this way were then plotted (Sigmaplot 12) by direct axes (quasi hyperbolic curves), logarithmic x-axis of imipenem concentrations and direct y-axis of growth fraction ('saturation curves') and with both axes logarithmic (classical PAP curves). For the saturation curves, the following Equation (1) (3-parameter sigmoid models) was used to assess the slope (b parameters) of the HR growth:

$$y = a / (1 + \exp(-(x - x_0)/b)) \quad (1)$$

In estimating HR by calculating the ≥ 3 dilution decreases (dilution change) in the PAP curves, we started to count once the difference in the number of colonies was in the ten-fold range (since there were minimal differences in colony counts in the low-concentration ranges). For PAP curves, the extensions in imipenem concentrations and area under curve (AUC) ratios were calculated after all cell content was normalized to 10¹⁰ CFU. PAP AUCs were calculated by Sigmaplot 12 and divided by the value of *B. fragilis* NCTC 9343 PAPs (from PBS suspensions and BHIS cultures). We also included the HR index of gradient tests (HRI), which expressed the number of step differences in 2-fold increments between the full growth and full inhibition values (Table 1).

To estimate the congruence between the test strains various phenotypic and molecular parameters, 1-way ANOVA with different HR grouping parameters ((i) ≥ 3 -fold changes in PBS PAP dilutions, (ii) ≥ 3 -fold changes in BHIS PAP dilutions and (iii) HRI > 0) was used. The Holm–Sidak method (normal distributions) or Dunn's methods were used (Sigmaplot 12) between group differentiations. In addition, Spearman rank correlation calculations were performed to estimate congruences between recorded parameters (Sigmaplot 12).

Alignments of nucleotide and amino acid sequences were performed by Lasergene 17 (DNASTar Inc., Madison, WI, USA) using the Clustal Ω algorithm.

Supplementary Materials: The following supporting information can be downloaded at: <https://www.mdpi.com/article/10.3390/antibiotics11050590/s1>, Figure S1: Alignment of amino acid sequences of GNAT acetylating toxin homologs, Figure S2: Showing the variations in the alignment of lysine-rich peptide nucleotide sequences in case of each sequence types, Table S1: PCR experiment parameters, Table S2: Etest MIC values of the test strains, Table S3: Lysine-rich peptide sequences of the *cfiA*-positive *B. fragilis* strains.

Author Contributions: Z.B. did all the phenotypic HR tests and the RT-qPCRs; F.D.v.L. isolated *B. fragilis* De248514/19 and participated in the manuscript preparation and final editing; E.N. checked the manuscript versions and provided suggestions; L.O. checked the manuscript versions and provided suggestions; K.B. checked the manuscript versions and allowed institutional financial background; F.S. checked the manuscript versions and provided suggestions; J.S. conceptualized the study, applied for support and wrote the manuscript. All authors have read and agreed to the published version of the manuscript.

Funding: This study was supported by the Albert Szent-Györgyi Research Fund from the Albert Szent-Györgyi School of Medicine, University of Szeged, and the Gedeon Richter Talent Fund.

Institutional Review Board Statement: Not applicable.

Informed Consent Statement: Not applicable.

Data Availability Statement: Not applicable.

Acknowledgments: We thank Gergely Röst for consultation on the topic of stochasticity.

Conflicts of Interest: The authors declare that there are no conflict of interest.

References

- Wexler, H.M. *Bacteroides*: The good, the bad and the nitty-gritty. *Clin. Microbiol. Rev.* **2007**, *20*, 593–621. [\[CrossRef\]](#) [\[PubMed\]](#)
- Sóki, J.; Wybo, I.; Wirth, R.; Hajdú, E.; Matuz, M.; Burián, K. A comparison of the antimicrobial resistance of fecal *Bacteroides* isolates and assessment of the composition of the intestinal microbiotas of carbapenem-treated and non-treated persons from Belgium and Hungary. *Anaerobe* **2021**, *73*, 102480. [\[CrossRef\]](#) [\[PubMed\]](#)
- Mazmanian, S.K.; Liu, C.H.; Tzianabos, A.O.; Kasper, D.L. An immunomodulatory molecule of symbiotic bacteria directs maturation of the host immune system. *Cell* **2005**, *122*, 107–118. [\[CrossRef\]](#) [\[PubMed\]](#)
- Kalka-Moll, W.M.; Wang, Y.; Comstock, L.E.; Gonzalez, S.E.; Tzianabos, A.O.; Kasper, D.L. Immunochemical and biological characterization of three capsular polysaccharides from a single *Bacteroides fragilis* strain. *Infect. Immun.* **2001**, *69*, 2339–2344. [\[CrossRef\]](#) [\[PubMed\]](#)
- Rakoff-Nahoum, S.; Foster, K.R.; Comstock, L.E. The evolution of cooperation within the gut microbiota. *Nature* **2016**, *533*, 255–259. [\[CrossRef\]](#) [\[PubMed\]](#)
- Sóki, J. Extended role for insertion sequence elements in the antibiotic resistance of *Bacteroides*. *World J. Clin. Infect. Dis.* **2013**, *3*, 1–12. [\[CrossRef\]](#)
- Sóki, J.; Edwards, R.; Urbán, E.; Fodor, E.; Beer, Z.; Nagy, E. Screening of isolates from faeces for carbapenem-resistant *Bacteroides* strains; existence of strains with novel types of resistance mechanisms. *Int. J. Antimicrob. Agents* **2004**, *24*, 450–454. [\[CrossRef\]](#)
- Sóki, J.; Fodor, E.; Hecht, D.W.; Edwards, R.; Rotimi, V.O.; Kerekes, I.; Urbán, E.; Nagy, E. Molecular characterization of imipenem-resistant, *cfiA*-positive *Bacteroides fragilis* isolates from the USA, Hungary and Kuwait. *J. Med. Microbiol.* **2004**, *53*, 413–419. [\[CrossRef\]](#)
- Jeverica, S.; Sóki, J.; Premru, M.M.; Nagy, E.; Papst, L. High prevalence of division II (*cfiA* positive) isolates among blood stream *Bacteroides fragilis* in Slovenia as determined by MALDI-TOF MS. *Anaerobe* **2019**, *58*, 30–34. [\[CrossRef\]](#)
- Sóki, J.; Edwards, R.; Hedberg, M.; Fang, H.; Nagy, E.; Nord, C.E. Examination of *cfiA*-mediated carbapenem resistance in *Bacteroides fragilis* strains from a European antibiotic susceptibility survey. *Int. J. Antimicrob. Agents* **2006**, *28*, 497–502. [\[CrossRef\]](#)
- Sóki, J.; Eitel, Z.; Urbán, E.; Nagy, E. Molecular analysis of the carbapenem and metronidazole resistance mechanisms of *Bacteroides* strains reported in a Europe-wide antibiotic resistance survey. *Int. J. Antimicrob. Agents* **2013**, *41*, 122–125. [\[CrossRef\]](#) [\[PubMed\]](#)
- Wickramage, I.; Spigaglia, P.; Sun, X. Mechanisms of antibiotic resistance of *Clostridioides difficile*. *J. Antimicrob. Chemother.* **2021**, *76*, 3077–3090. [\[CrossRef\]](#) [\[PubMed\]](#)
- El-Halfawy, O.M.; Valvano, M.A. Antimicrobial heteroresistance: An emerging field in need of clarity. *Clin. Microbiol. Rev.* **2015**, *28*, 191–207. [\[CrossRef\]](#) [\[PubMed\]](#)
- Lee, A.S.; de Lencastre, H.; Garau, J.; Kluytmans, J.; Malhotra-Kumar, S.; Peschel, A.; Harbarth, S. Methicillin-resistant *Staphylococcus aureus*. *Nat. Rev. Dis. Primers* **2018**, *4*, 18033. [\[CrossRef\]](#)
- Ryffel, C.; Strässle, A.; Kayser, F.H.; Berger-Bächi, B. Mechanisms of heteroresistance in methicillin-resistant *Staphylococcus aureus*. *Antimicrob. Agents Chemother.* **1994**, *38*, 724–728. [\[CrossRef\]](#)

16. Andersson, D.I.; Nicoloff, H.; Hjort, K. Mechanisms and clinical relevance of bacterial heteroresistance. *Nat. Rev. Microbiol.* **2019**, *17*, 479–496. [\[CrossRef\]](#)
17. Söki, J.; Hedberg, M.; Patrick, S.; Bálint, B.; Herczeg, R.; Nagy, I.; Hecht, D.W.; Nagy, E.; Urbán, E. Emergence and evolution of an international cluster of MDR *Bacteroides fragilis* isolates. *J. Antimicrob. Chemother.* **2016**, *71*, 2441–2448. [\[CrossRef\]](#)
18. Unterholzner, S.J.; Poppenberger, B.; Rozhon, W. Toxin-antitoxin systems: Biology, identification, and application. *Mob. Genet. Elem.* **2013**, *3*, e26219. [\[CrossRef\]](#)
19. Stilger, K.L.; Sullivan, W.J., Jr. Elongator protein 3 (Elp3) lysine acetyltransferase is a tail-anchored mitochondrial protein in *Toxoplasma gondii*. *J. Biol. Chem.* **2013**, *288*, 25318–25329. [\[CrossRef\]](#)
20. Jurėnas, D.; Garcia-Pino, A.; Van Melder, L. Novel toxins from type II toxin-antitoxin systems with acetyltransferase activity. *Plasmid* **2017**, *93*, 30–35. [\[CrossRef\]](#)
21. Brauner, A.; Fridman, O.; Gefen, O.; Balaban, N.Q. Distinguishing between resistance, tolerance and persistence to antibiotic treatment. *Nat. Rev. Microbiol.* **2016**, *14*, 320–330. [\[CrossRef\]](#) [\[PubMed\]](#)
22. Sárvari, K.P.; Söki, J.; Kristóf, K.; Juhász, E.; Miszt, C.; Latkóczy, K.; Meleg, S.Z.; Urbán, E. A multicentre survey of the antibiotic susceptibility of clinical *Bacteroides* species from Hungary. *Infect. Dis.* **2018**, *50*, 372–380. [\[CrossRef\]](#) [\[PubMed\]](#)
23. Rasmussen, B.A.; Gluzman, Y.; Tally, F.P. Cloning and sequencing of the class B beta-lactamase gene (*ccrA*) from *Bacteroides fragilis* TAL3636. *Antimicrob. Agents Chemother.* **1990**, *34*, 1590–1592. [\[CrossRef\]](#) [\[PubMed\]](#)
24. Walsh, T.R.; Bolmström, A.; Qwärnström, A.; Ho, P.; Wootton, M.; Howe, R.A.; MacGowan, A.P.; Diekema, D. Evaluation of current methods for detection of staphylococci with reduced susceptibility to glycopeptides. *J. Clin. Microbiol.* **2001**, *39*, 2439–2444. [\[CrossRef\]](#)
25. Brauner, A.; Balaban, N.Q. Quantitative biology of survival under antibiotic treatments. *Curr. Opin. Microbiol.* **2021**, *64*, 139–145. [\[CrossRef\]](#)
26. Van den Bergh, B.; Fauvart, M.; Michiels, J. Formation, physiology, ecology, evolution and clinical importance of bacterial persisters. *FEMS Microbiol. Rev.* **2017**, *41*, 219–251. [\[CrossRef\]](#)
27. Piriz Durán, S.; Kayser, F.H.; Berger-Bächi, B. Impact of *sar* and *agr* on methicillin resistance in *Staphylococcus aureus*. *FEMS Microbiol. Lett.* **1996**, *141*, 255–260. [\[CrossRef\]](#)
28. Knobloch, J.K.; Jäger, S.; Huck, J.; Horstkotte, M.A.; Mack, D. *mecA* is not involved in the sigmaB-dependent switch of the expression phenotype of methicillin resistance in *Staphylococcus epidermidis*. *Antimicrob. Agents Chemother.* **2005**, *49*, 1216–1219. [\[CrossRef\]](#)
29. Cuirolo, A.; Plata, K.; Rosato, A.E. Development of homogeneous expression of resistance in methicillin-resistant *Staphylococcus aureus* clinical strains is functionally associated with a beta-lactam-mediated SOS response. *J. Antimicrob. Chemother.* **2009**, *64*, 37–45. [\[CrossRef\]](#)
30. Medeiros, A.A. Relapsing infection due to *Enterobacter* species: Lessons of heterogeneity. *Clin. Infect. Dis.* **1997**, *25*, 341–342. [\[CrossRef\]](#)
31. Katayama, Y.; Murakami-Kuroda, H.; Cui, L.; Hiramatsu, K. Selection of heterogeneous vancomycin-intermediate *Staphylococcus aureus* by imipenem. *Antimicrob. Agents Chemother.* **2009**, *53*, 3190–3196. [\[CrossRef\]](#) [\[PubMed\]](#)
32. Anderson, S.E.; Sherman, E.X.; Weiss, D.S.; Rather, P.N. Aminoglycoside Heteroresistance in *Acinetobacter baumannii* AB5075. *mSphere* **2018**, *3*, e00271-18. [\[CrossRef\]](#)
33. Schechter, L.M.; Creely, D.P.; Garner, C.D.; Shortridge, D.; Nguyen, H.; Chen, L.; Hanson, B.M.; Sodergren, E.; Weinstock, G.M.; Dunne, W.M., Jr.; et al. Extensive Gene Amplification as a Mechanism for Piperacillin-Tazobactam Resistance in *Escherichia coli*. *mBio* **2018**, *9*, e00583-18. [\[CrossRef\]](#) [\[PubMed\]](#)
34. Pournaras, S.; Kristo, I.; Vrioni, G.; Ikonomidis, A.; Poulou, A.; Petropoulou, D.; Tsakris, A. Characteristics of meropenem heteroresistance in *Klebsiella pneumoniae* carbapenemase (KPC)-producing clinical isolates of *K. pneumoniae*. *J. Clin. Microbiol.* **2010**, *48*, 2601–2604. [\[CrossRef\]](#) [\[PubMed\]](#)
35. Ikonomidis, A.; Tsakris, A.; Kantzanou, M.; Spanakis, N.; Maniatis, A.N.; Pournaras, S. Efflux system overexpression and decreased OprD contribute to the carbapenem heterogeneity in *Pseudomonas aeruginosa*. *FEMS Microbiol. Lett.* **2008**, *279*, 36–39. [\[CrossRef\]](#)
36. Hjort, K.; Nicoloff, H.; Andersson, D.I. Unstable tandem gene amplification generates heteroresistance (variation in resistance within a population) to colistin in *Salmonella enterica*. *Mol. Microbiol.* **2016**, *102*, 274–289. [\[CrossRef\]](#)
37. Engel, H.; Mika, M.; Denapaite, D.; Hakenbeck, R.; Mühlemann, K.; Heller, M.; Hathaway, L.J.; Hilty, M. A low-affinity penicillin-binding protein 2x variant is required for heteroresistance in *Streptococcus pneumoniae*. *Antimicrob. Agents Chemother.* **2014**, *58*, 3934–3941. [\[CrossRef\]](#)
38. Clinical Laboratory Standards Institute. *Performance Standards for Antimicrobial Susceptibility Testing*; Twenty-First Informational Supplement M100-S29; Clinical Laboratory Standards Institute (CLSI): Wayne, PA, USA, 2018.

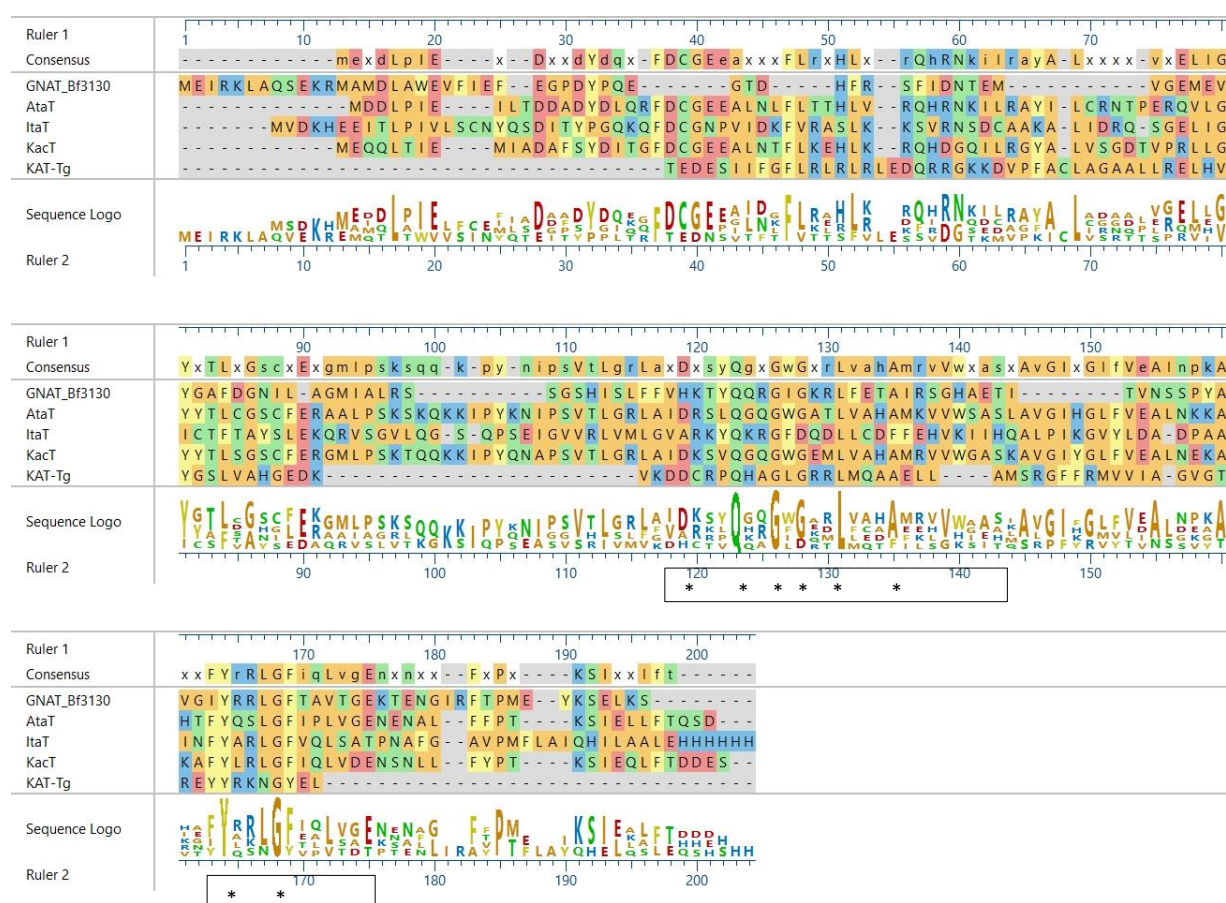
Supplementary Materials

Table S1. PCR experiment parameters

Primer	PCR type	Sequence 5'-3'	PCR cycling ^a	Ref.
cfiA1	conv. ^b	TCCATGCTTTTCCCTGTGCGCAGTTAT	94 °C 30 s, 50 °C 1 min, 72 °C 1 min, 35x	This study
cfiA2		GGGCTATGGCTTTGAAGTGC		
Up2	conv.	TACGCTTTTCTGTGCCATAACTGC	94 °C 30 s, 52 °C 1 min, 72 °C 3 min,35x	
G		CGCCAAGCTTTGCCTGCCATTA		
gap-F	qRT-PCR	AGCCATTGTAGCAGCTTTTT	94 °C 15 s, 55 °C 30 s, 72°C 30s, 35x	
gap-R		GAAGACGGGATGATGTTTTTC		
cfiA-RT1	qRT-PCR	AATCGAAGGATGGGGTATGG		
cfiA-RT2		CGGTCAGTGAATCGGTGAAT		
GNAT-F	qRT-PCR	ACAGAAATGGTGGAAAGAAAT	94 °C 15 s, 55 °C 30 s, 72°C 30s, 35x	
GNAT-R		GTTGACGGTAATCGTCTCTG		
XAT-F	qRT-PCR	CTGATAATCGGCAAGTTTTG		
XAT-R		CTTCGTAACCGATCCATACA		
Lrp-F	conv.	GAGGGGCTTGCGGCTGTG	94°C 30 s, 50°C 30 s, 72°C 30 s, 35x	This study
Lrp-R		ATCTTATGGTTGTTTTTCCG		

^a For conventional PCR, we used starting denaturation and final elongation with the following parameters 94 °C 5 min and 72 °C 10 min, respectively. For qRT-PCR the values recommended by the supplier were used. ^b Conventional PCR.

Figure S1. Alignment of amino acid sequences of GNAT acetylating toxin homologs.



GNAT_Bf3130 – the ‘GNAT’ protein of the ‘*cfiA* element’ in *B. fragilis* 3130; AtaT – TA toxin of *Escherichia coli* (acc. no. WP_142447164); ItaT – TA toxin of *Escherichia coli* (acc. no. 7BY_D); KacT – TA toxin of *Klebsiella pneumoniae* (acc. no. QXW56992); KAT-Tg – the lysine acetylase domain in *Toxoplasma gondii* Elongation protein 3 (acc. no. PUA86011, residues 617-721)

Conserved active centre residues are marked with asterisks.

Table S2. Etest MIC values of the test strains

<i>B. fragilis</i>	Ref.	MICs ^b											
		AMP^c	AMC	FOX	IPM	MPM	ERY	CLM	MOX	MTZ	TET	TIG	CHL
Susceptible controls													
NCTC 9343	-	16	0.25	4	0.032	0.064	8	1	0.125	0.125	0.125	0.125	4
638R	-	2	0.25	0.064	0.032	0.032	0.5	0.25	0.25	0.125	0.064	0.032	2
D39		8^d	0.25	4	0.064	0.064	16	0.25	0.25	0.5	16	0.25	8
Silent/HR ^a													
7979	This study	>256	2	32	0.125	2	16	2	0.125	0.25	0.25	0.125	4
3130	This study	2	1	16	0.125	8-(32)	8	0.5	0.064	0.125	0.25	0.064	4
3035		1	1	8	0.125-(4)	2	128	2	0.125	0.25	8	0.25	4
SY69		1	1	16	0.25-(8)	2-(32)	16	2	2	0.125	8	0.125	4
CZE65		32		32	0.25-(1)	2-(8)	4	1	2	0.25	0.125	0.064	4
CZE60		32-(128)^e	8	32	1-(32)	>32	1-(8)	1	4-(16)	0.25	0.125	0.064	16
SLO8		>256	8	128	4-(>32)	>32	2	1	0.125	0.25	0.125	0.25	4
HR-ind ^a													
3130i5	This study	8	2	16	0.5-(16)	>32	16	1	0.064	0.032	0.125	0.064	4
CZE60i	This study	>256	8	64-(256)	>32 (4-(256)^f)	>32	1	1	2	0.25	0.125	0.064	16
With IS ^a													
De248514/19	This study	32	4	32	1-(8)	>32	8-(256)	2	0.125	0.125	16	0.5	4
1672		>256	8	128	>32 (8-(128)^f)	>32	8-(32)	2	0.25	0.5-(2)	16	1	8
TAL3636		>256	4-(16)	128	>32 (256^f)	>32	4	2	0.064	0.125	4	0.125	4

^a Silent/HR – silently or heterogeneously resistant, HR-ind – induced heteroresistant, with IS – IS element in the upstream region of the *cfiA* gene. ^b µg/ml. ^c AMP – ampicillin, AMC – amoxicillin/clavulanic acid, FOX – ceftioxin, IPM – imipenem, MPM – meropenem, ERY – erythromycin, CLM – clindamycin, MOX – moxifloxacin, MTZ – metronidazole, TET – tetracycline, TIG – tigecycline, CHL – chloramphenicol (bactericidal types are bold italic). ^d Resistant values are shown in bold. ^e Heteroresistance is shown by rust colour. ^f The IPM MICs were from MBL Etests.

Table S3. Lysine-rich peptide sequences of the *cfiA*-positive *B. fragilis* strains

Strain	Amino acid and nucleotide sequence ^a	Number of lysines and (ratio)	
<i>B. fragilis</i>			
7979	M L R D H K R K K N K Q D I D G T R T Y K K K Y H Y atgcttagagatcataaaaagaaagaaaaacaaacaggatatagacggcacacgaacttataaaaagaagtatcattactaa	7	(26.9 %)
3130	M L G N H K R E A N S I Q T A H E L I K R S I I T K L S Q H R K N N H K I atgcttgggaatcataaaagagaggcaaacagtatccagacggcacacgaacttataaaaagaagtatcattactaaactttcccaacatcggaaaaaacaaccataagatataa	5	(13.5 %)
3035	M L R D H K R K K K K Q Y P D G T R T Y K K K Y H Y Q T F P P S E K Q P atgcttagagatcataaaaagaaagaaaaagaaacagtatccagacggcacacgaacttataaaaagaagtatcattaccaaaactttcccaccatcggaaaaaacaaccataa	9	(25.0%)
SY69	M L G N H K R E A N S I Q T A H E L I K R S I I T K L S Q H R K N N H K I atgcttgggaatcataaaagagaggcaaacagtatccagacggcacacgaacttataaaaagaagtatcattactaaactttcccaacatcggaaaaaacaaccataagatataa	5	(13.5 %)
CZE65	M L R D H K R K K N K Q D I D G T R T Y K K K Y H Y atgcttagagatcataaaaagaaagaaaaacaaacaggatatagacggcacacgaacttataaaaagaagtatcattactaa	7	(26.9 %)
CZE60	M L R D H K R K K N K Q D I D G T R T Y K K K Y H Y atgcttagagatcataaaaagaaagaaaaacaaacaggatatagacggcacacgaacttataaaaagaagtatcattactaa	7	(26.9 %)
SLO8	M L R D H K R K K K K Q Y P D G T R T Y K K K Y H Y Q T F P P S E K Q P atgcttagagatcataaaaagaaagaaaaagaaacagtatccagacggcacacgaacttataaaaagaagtatcattaccaaaactttcccaccatcggaaaaaacaaccataa	9	(25.0 %)
3130i5	M L G N H K R E A N S I Q T A H E L I K R S I I T K L S Q H R K N N H K I atgcttgggaatcataaaagagaggcaaacagtatccagacggcacacgaacttataaaaagaagtatcattactaaactttcccaacatcggaaaaaacaaccataagatataa	5	(13.5 %)
CZE60i	M L R D H K R K K N K Q D I D G T R T Y K K K Y H Y atgcttagagatcataaaaagaaagaaaaacaaacaggatatagacggcacacgaacttataaaaagaagtatcattactaa	7	(26.9 %)
De248514	M L R D H K R K K K K Q Y P D G T R T Y K K K Y H Y Q T F P P S E K Q P atgcttagagatcataaaaagaaagaaaaagaaacagtatccagacggcacacgaacttataaaaagaagtatcattaccaaaactttcccaccatcggaaaaaacaaccataa	9	(25.0 %)
1672	M L R D H K R K K N K Q D I D G T R T Y K K K Y H Y atgcttagagatcataaaaagaaagaaaaacaaacaggatatagacggcacacgaacttataaaaagaagtatcattactaa	7	(26.9 %)
TAL3636	M L R D H K R K K K Q Y P D G T R T Y K K K Y H Y Q T F P P S E K Q P atgcttagagatcataaaaagaaagaaaaagaaacagtatccagacggcacacgaacttataaaaagaagtatcattaccaaaactttcccaccatcggaaaaaacaaccataa	9	(25.0 %)

^a Lysines (K) are shown in bold.

Figure S2. Showing the variations in the alignment of lysine-rich peptide nucleotide sequences in case of each sequence types

Lrp_3130	<u>atg</u> ctttggg----aatcataaaagagaggcaaacagtatccagacgggcacacgaacttat	56
Lrp_CZE60	<u>atg</u> cttagagatcataaaagaaagaaaaacaaacaggatatagacgggcacacgaacttat	60
Lrp_De248514	<u>atg</u> cttagagatcataaaagaaagaaaaagaaacagtatccagacgggcacacgaacttat	60
	***** * * * ***** * ***** ** *****	
Lrp_3130	aaaaagaagtatcattactaaacttttcccaacatcggaaaaaacaaccataagat-a <u>taa</u>	114
Lrp_CZE60	aaaaagaagtatcattact <u>taa</u> acttttcccaacatcggaaaaaacaaccataagat-atag	118
Lrp_De248514	aaaaagaagtatcattaccaaactttccaccatcggaaaaaacaacca <u>taag</u> atcctaa	119

Start codons are underlined, stop codons are bold underlined. Aligning nucleotides are marked with asterics

∞

∞ *To my father, who has always worked hard, encouraged me to do the same and been a role model for how to be a good man.*

∞ *To my mother, who has always been the most supportive, loving and enduring person I know.*

∞ *To my brother and sister, my eternal friends and companions.*

∞ *To my loving and caring companion who lights up my day, Ruby.*

∞ *To my family and friends, with whom I have shared the most joys and sorrows, and to everyone we unconditionally love.*

∞ *To the ones who left this world but live rent-free in my heart and soul.*

∞